HELICAL MOVEMENTS OF FLAGELLATED PROPELLING MICROORGANISMS

Thesis by
Allen Tse-Yung Chwang

In Partial Fulfillment of the Requirements

for the Degree of

Doctor of Philosophy

California Institute of Technology
Pasadena, California
1971

(Submitted March 25, 1971)

"There cannot be the slightest doubt that on the borderlines of physics, engineering and biology lie some of the most fascinating and challenging aspects of animal locomotion."

Sir James Gray (1968)

Acknowledgments

The author wishes to express his sincere gratitude and deep appreciation to Professor Theodore Yao-Tsu Wu for his excellent supervision on this work and his great assistance in the preparation of this thesis. His inspiration and warm personality have won the author's highest respect and love.

Sincere thanks are due to Dr. Howard Winet for some interesting discussions and Mr. Lang-Wah Lee for assisting in performing the experiments. Thanks are also due to Mrs. Barbara Hawk for typing the manuscript and Miss Cecilia Lin for making the drawings.

The author is grateful to the California Institute of Technology for the award of Earle C. Anthony Fellowship and teaching assistantships during the years of his graduate studies. Part of this research was sponsored by the National Science Foundation, under Grant GK 10216, and by the Office of Naval Research, under Contract N00014-67-A-0094-0012.

Abstract

The helical motion of an infinitely long flagellum with a cross-sectional radius b, along which a helical wave of amplitude h, wavelength λ and phase velocity c is propagated, has been analyzed by using Stokes' equations in a helical coordinate system (r, ξ, x). In order to satisfy all the boundary conditions, namely the no-slip condition on the flagellum surface and zero perturbation velocity at infinity, the flagellum must propel itself with a propulsion velocity U in the opposite direction to the phase velocity c. For small values of kb (where $k = 2\pi/\lambda$ is the wave number), by a single-harmonic approximation for the outer region $(r > h)$, the ratio of the propulsion velocity U to the phase velocity c is found to be

$$\frac{U}{c} = k^3 h^3 \frac{2 + \frac{1}{2} k^2 h^2 - kh \frac{K_1(kh)}{K_0(kh)} - \frac{1}{2} k^2 h^2 \frac{K_0(kh)}{K_2(kh)}}{3kh + 2 \frac{K_1(kh)}{K_0(kh)} + kh \frac{K_0(kh)}{K_2(kh)}} + O(b/h)^2 \quad ,$$

where $K_n(kh)$ is the modified Bessel function of the second kind.

A modified and improved version of the Gray and Hancock method has been developed and applied to evaluate helical movements of a freely swimming microorganism with a spherical head of radius a and a tail of finite length and cross-sectional radius b. The propulsion velocity U and the induced angular velocity Ω of the organism are derived. In order that this type of motion can be realized, it is necessary for the head of the organism to exceed a certain critical size, and some amount of body rotation is inevitable. For fixed kb and kh, an optimum head-tail ratio a/b, at which the propulsion velocity U

reaches a maximum, has been discovered. The power required for propulsion by means of helical waves is determined, based on which a hydromechanical efficiency η is defined. This η reaches a maximum at $kh \simeq 0.9$ for microorganisms with optimum head-tail ratios. In the neighborhood of $kh = 0.9$, the optimum head-tail ratio varies in the range $15 < a/b < 40$, the propulsion velocity in $0.08 < U/c < 0.2$, and the efficiency in $0.14 < \eta < 0.24$, as kb varies over $0.03 < kb < 0.2$.

The modified version of the Gray and Hancock method has also been utilized to describe the locomotion of spirochetes. It is found that although a spirochete has no head to resist the induced viscous torque, it can still propel by means of helical waves provided that the spirochete spins with an induced angular velocity Ω. Thus the 'Spirochete paradox' is resolved. In order to achieve a maximum propulsion velocity, it is discovered that a spirochete should keep its amplitude-wavelength ratio h/λ around 1:6 (or $kh \simeq 1$). At $kh = 1$, the propulsion velocity varies in the range $0 < U/c < 0.2$, and the induced angular velocity in $0.4 < \Omega/\omega < 1$ (where $\omega = kc$ is the circular frequency of the helical wave), as the radius-amplitude ratio varies over $0 < b/h < 1$.

A series of experiments have been carried out to determine by simulation the relative importance of the so-called 'neighboring' effect and 'end' effect, and results for the case of uniform helical waves are presented.

TABLE OF CONTENTS

I. INTRODUCTION

The study of flagellated-propulsion of microscopic organisms opens up a new field in hydrodynamics. As various kinds of bacteria and spermatozoa are extremely minute in size, the Reynolds number based on the body length or certain characteristic dimension, ℓ, and its mean forward velocity U is very small, i.e. $Re = \frac{U\ell}{\nu} \ll 1$, ν being the kinematic viscosity coefficient. For the motion of spermatozoa, the Reynolds number is generally of order 10^{-3} or less, and for bacteria it is 10^{-6} or less. Hence the predominant forces acting on microorganisms are entirely of a viscous origin, the inertia forces can be neglected and Stokes' equations be used. Taylor (1952) applied Stokes' equations in a cylindrical polar coordinate system to analyze the motion of an infinitely long cylindrical tail which makes progressive helical waves of small amplitude i.e. $h \ll b$ (where h is the amplitude of the helical wave and b the radius of the cylindrical tail). He was able to find that the propulsion velocity U of this cylindrical tail is in the opposite direction to the phase velocity c of the helical wave and the magnitude of U for small values of kb is

$$\lim_{kh \ll kb \to 0} \frac{U}{c} = k^2 h^2 \frac{K_o(kb) - \frac{1}{2}}{K_o(kb) + \frac{1}{2}} ,$$

where $k = 2\pi/\lambda$ is the wave number, λ being the wavelength, and $K_o(kb)$ is the modified Bessel function of the second kind with argument kb. Meanwhile, Taylor found that a constant couple (or torque) must be applied to the tail about its length in order that it may not rotate. Unfortunately, he incorrectly used w_1' instead of v_1' in his equations

(3.10) and (3.12). For small values of kb, the correct expression for the torque M exerted on the cylinder in a wavelength by the surrounding fluid should be (Drummond, 1966)

$$\lim_{kh \ll kb \to 0} M = -4\pi\mu\, kh^2 c\lambda \Big/ \left[K_o(kb) + \frac{1}{2}\right] \quad ,$$

where μ is the viscosity coefficient.

The assumption made in Taylor's work that the amplitude of the helical wave, h, is small in comparison with the radius of the tail, b, is not generally met in nature, since even though kh may be small, h is usually greater than b. For a great variety of motions employed by microorganisms the kh value is generally of order O(1), as was found experimentally by the biologists. Hancock (1953) suggested an alternative approach. He analyzed the movement of a long thin cylindrical filament along which helical waves of lateral displacement are propagated. The flow around the filament is determined by distributing a system of 'doublets' and 'Stokeslets' inside the surface of the filament whose strengths are determined by the no-slip boundary condition on the filament surface together with the condition that the total energy of the induced velocity field remains finite. In Hancock's theory, the amplitude of propagating helical waves, h, need not be small as compared with the wavelength λ, yet the radius of the filament, b, shrinks to zero. Under these conditions, he was able to find that the propulsion velocity U is

$$\frac{U}{c} = \frac{k^2 h^2}{1+2k^2 h^2} \quad .$$

However, he did not obtain an expression for the torque exerted on the

filament by the surrounding fluid because of his 'zero radius' assumption.

In this past decade, many biologists (e.g. Rikmenspoel, 1962) reported that the velocities predicted by Taylor (1952) or Hancock (1953) are too high, by a factor of 10 for the model of Taylor or a factor of 5 for that of Hancock. In order to gain a deeper understanding of the nature of helical waves, a new approach is developed here, as will be presented in Chapter II of this thesis. By this new approach, it is possible, at least in principle, to find the propulsion velocity U, the torque acting on the flagellum in a wavelength and the energy required per wavelength of flagellum for helical waves of arbitrary amplitude h produced by an infinitely long flagellum of arbitrary circular cross-sectional radius b with $b < h$.

In reality, the flagellum of a microorganism is not infinitely long nor can it swim by making helical waves without some means to counter-balance the induced torque. To analyze the helical motion of a freely swimming microorganism with a head and a finitely long tail, a modified and improved version of the Gray and Hancock method (1955), the original version of which was devised to investigate the planar wave motion of minute creatures, has been developed and presented in Chapter III. By this simple but powerful method, the locomotion of microorganisms employing helical waves is studied with particular emphasis on their optimum performances. Some new concepts, such as the optimum head-tail ratio and the optimum amplitude-wavelength ratio, are introduced. The value of $kh \simeq 1$ is found to be very significant, and it is a characteristic of all microorganisms employing

helical waves whether the organism has an inertial head or not.

In Chapter IV, a series of experiments on rigid, uniform, helical wires moving through a viscous fluid is discussed and the results are analyzed as a first step to investigate the so-called 'neighboring' effect and 'end' effect on the helical movements of flagellated-propelling microorganisms.

II. THEORETICAL ANALYSIS OF HELICAL WAVES PRODUCED BY AN INFINITELY LONG FLAGELLUM

2.1 Governing equations and boundary conditions

For most microscopic organisms employing the flagellated propulsion, such as spermatozoa and certain bacteria, the organism's tail (or flagellum) is very long in comparison with its cross-sectional radius, also with the size of its head (or body). Hence, as a first approximation, the flagellum can be idealized as a long section of an infinitely long one. This implies that the end effects of the long flagellum may be neglected, and the locomotion of this microorganism may be comprehended by analyzing the movement of the infinitely long flagellum.

The Reynolds number of the motion of spermatozoa and bacteria is very small, generally of the order 10^{-3} or less for spermatozoa and may be as small as 10^{-6} for bacteria. In this range of small Reynolds numbers, the predominant forces acting on microorganisms are viscous forces, the inertia forces can be neglected and Stokes' equations be used. For an incompressible viscous fluid, the Stokes' equations are

$$\nabla \cdot \vec{u} = 0 \quad , \tag{2.1a}$$

$$0 = \nabla P + \mu \nabla \times (\nabla \times \vec{u}) \quad , \tag{2.2}$$

where μ is the coefficient of viscosity, P is the pressure and $\vec{u}$ is the velocity vector.

As a specific model of the actual motion, suppose that an infinitely long flagellum, of circular cross-section with radius b,

makes a helical wave of amplitude h, wavelength λ, phase velocity c in the negative x direction, and in the meantime it propels itself with a constant velocity U in the positive x direction. The position of the centerline of this flagellum, in a cylindrical polar coordinate system (r,θ,x) moving with the same constant velocity U in the positive x direction as the flagellum does, is given by

$$r = h \quad , \qquad \theta = k(x+ct) = kx + \omega t \quad , \tag{2.3a}$$

where $k = 2\pi/\lambda$ is the wave number (see Fig. 1a). It is convenient to introduce a helical coordinate system (r,ξ,x) defined by

$$\xi = \theta - (kx+\omega t) \quad . \tag{2.4}$$

In this new coordinate system, Eq. (2.3a) becomes

$$r = h \quad , \qquad \xi = 0 \quad , \tag{2.4a}$$

which exhibits a simple symmetry of the flagellum motion. It is assumed that no stretching of the flagellum takes place throughout motion, and that the circular cross-section which moves in a plane perpendicular to the x direction remains circular. The boundary surface of this flagellum is then given by

$$r = h\cos\xi \pm \sqrt{b^2 - h^2\sin^2\xi} \quad ,$$

and

$$|\xi| \leqslant \sin^{-1}\left(\frac{b}{h}\right) \quad . \tag{2.5a}$$

Alternatively, the boundary surface can be expressed as

$$r(\alpha) = \sqrt{h^2 - b^2\sin^2\alpha} \quad + b\cos\alpha \quad ,$$

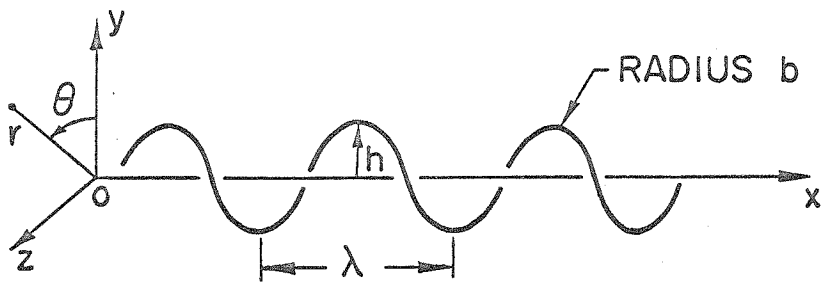

(a)

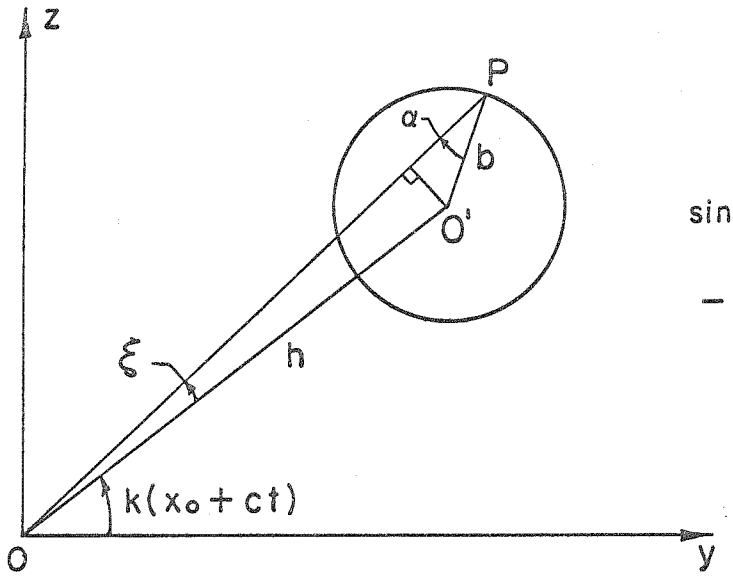

$b < h$

$$\sin\xi = \frac{b \sin\alpha}{h}$$

$$-\pi < \alpha < \pi$$

(b) at $x = x_o$ plane

Fig. 1

and

$$\xi(\alpha) = \sin^{-1}\left(\frac{b \sin\alpha}{h}\right) \quad , \tag{2.5b}$$

where α is a parameter ranging from $-\pi$ to π (see Fig. 1b). The use of (2.5b) instead of (2.5a) has two main advantages. Firstly, since α spans the full range, from $-\pi$ to π, the set $\{1, \sin n\alpha, \cos n\alpha\}$ $(n = 1, 2, 3, \ldots)$ is orthogonal and complete. Thus we can express the velocity boundary conditions on the flagellum surface in Fourier series in terms of the parameter α. In contrast, the use of ξ as a running variable on the flagellum surface does not have the same property, for ξ only varies from $-\sin^{-1}\left(\frac{b}{h}\right)$ to $+\sin^{-1}\left(\frac{b}{h}\right)$ provided, of course, $b < h$. Secondly, when the radius-amplitude ratio b/h becomes small, which is the case for practically all flagellated propulsion of microorganisms, it is desirable to expand all quantities in ascending power series of b/h, the superiority of (2.5b) over (2.5a) is thus obvious.

Taking the divergence of (2.2) and making use of (2.1a), we have

$$\nabla^2 P = 0 \quad . \tag{2.6a}$$

Hence the pressure P is a harmonic function. In the helical coordinate system (r, ξ, x), the Laplacian operator ∇^2 takes the form

$$\nabla^2 = \frac{\partial^2}{\partial r^2} + \frac{1}{r}\frac{\partial}{\partial r} + \left(\frac{1}{r^2} + k^2\right)\frac{\partial^2}{\partial \xi^2} - 2k\,\frac{\partial^2}{\partial \xi \partial x} + \frac{\partial^2}{\partial x^2} \quad . \tag{2.7}$$

Since the flagellum is assumed to be infinitely long, we have, in this helical coordinate system, $\frac{\partial}{\partial x} = 0$.

By (2.6a) and (2.7),

$$\left[\frac{\partial^2}{\partial r^2} + \frac{1}{r}\frac{\partial}{\partial r} + \left(\frac{1}{r^2} + k^2\right)\frac{\partial^2}{\partial \xi^2}\right] P = 0 \quad . \tag{2.6b}$$

Let the velocity components in the r, θ, x directions (note that they are not the r, ξ, x-components) be u, v, and w respectively. They may depend on r and ξ, but not on x. Then (2.2) becomes

$$\frac{1}{\mu}\frac{\partial P}{\partial r} = \left[\frac{\partial^2}{\partial r^2} + \frac{1}{r}\frac{\partial}{\partial r} + \left(\frac{1}{r^2} + k^2\right)\frac{\partial^2}{\partial \xi^2} - \frac{1}{r^2}\right]u - \frac{2}{r^2}\frac{\partial v}{\partial \xi} \quad , \tag{2.8}$$

$$\frac{1}{\mu}\frac{\partial P}{r\,\partial \xi} = \left[\frac{\partial^2}{\partial r^2} + \frac{1}{r}\frac{\partial}{\partial r} + \left(\frac{1}{r^2} + k^2\right)\frac{\partial^2}{\partial \xi^2} - \frac{1}{r^2}\right]v + \frac{2}{r^2}\frac{\partial u}{\partial \xi} \quad , \tag{2.9}$$

$$-\frac{k}{\mu}\frac{\partial P}{\partial \xi} = \left[\frac{\partial^2}{\partial r^2} + \frac{1}{r}\frac{\partial}{\partial r} + \left(\frac{1}{r^2} + k^2\right)\frac{\partial^2}{\partial \xi^2}\right]w \quad . \tag{2.10}$$

Equations (2.6b), (2.8), (2.9), and (2.10) are the governing differential equations for the pressure $P(r, \xi)$ and three velocity components $u(r, \xi)$, $v(r, \xi)$ and $w(r, \xi)$. The boundary conditions on the flagellum surface are no-slip conditions (see Fig. 2). Thus

$$u(r(\alpha), \xi(\alpha)) = \omega h \sin \xi(\alpha) = \omega b \sin \alpha \quad , \tag{2.11}$$

$$v(r(\alpha), \xi(\alpha)) = \omega h \cos \xi(\alpha) = \omega h \sqrt{1 - \frac{b^2}{h^2}\sin^2 \alpha} \quad , \tag{2.12}$$

$$w(r(\alpha), \xi(\alpha)) = 0 \quad . \tag{2.13}$$

Since the fluid at infinity is otherwise at rest, and the helical coordinates (r, ξ, x) is moving with velocity U in the positive x direction, we have the boundary conditions at infinity as

$$\lim_{r \to \infty} u(r, \xi) = 0 \quad , \quad \lim_{r \to \infty} v(r, \xi) = 0 \quad , \quad \lim_{r \to \infty} w(r, \xi) = -U \quad , \tag{2.14}$$

and

$$\lim_{r \to \infty} P(r, \xi) = 0 \quad . \tag{2.15}$$

It should be noted here that if the pressure P at infinity is P_∞, a constant other than zero, we can always define a new pressure by $P_{new} = P - P_\infty$ so that P_{new} is zero at infinity.

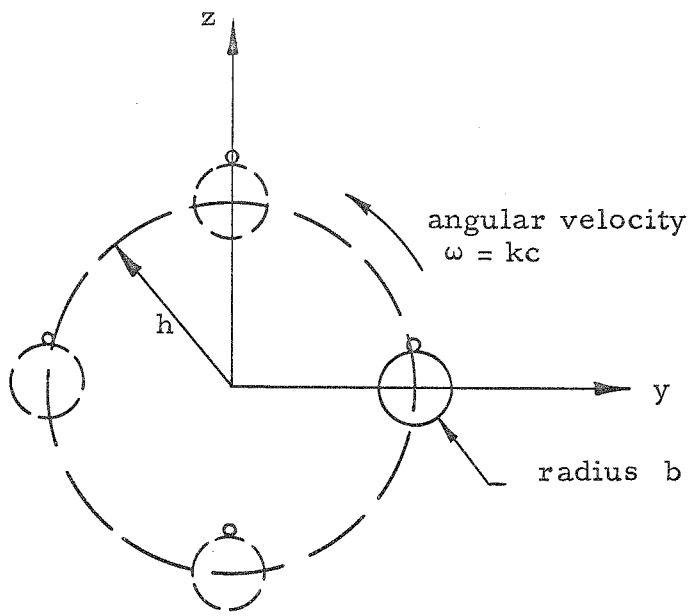

Fig. 2

2.2 Pressure and velocity distributions

Since $\xi(\alpha)$ is an odd function of α whereas $r(\alpha)$ is even in α, as indicated by (2.5b), $\sin n\xi(\alpha)$ (n=1, 2, 3, . . .) is odd, and $\cos n\xi(\alpha)$ (n=1, 2, 3, . . .) is even in α. Hence, by Eqs. (2.8) - (2.13),

the pressure P and the velocity component in the r-direction, u, must be odd functions of α, whereas the velocity components in the θ- and x-directions, i.e. v and w, must be even in α. Let the pressure P and the velocity components u, v, and w be of the form

$$P(r,\xi) = k\mu \sum_{n=1}^{\infty} P_n(r)\sin n\xi \quad , \tag{2.16}$$

$$u(r,\xi) = \sum_{n=1}^{\infty} u_n(r)\sin n\xi \quad , \tag{2.17}$$

$$v(r,\xi) = \frac{1}{2} v_o(r) + \sum_{n=1}^{\infty} v_n(r)\cos n\xi \quad , \tag{2.18}$$

$$w(r,\xi) = \frac{1}{2} w_o(r) + \sum_{n=1}^{\infty} w_n(r)\cos n\xi \quad . \tag{2.19}$$

Substituting (2.16) into (2.6b) and collecting the coefficients of like terms of $\sin n\xi$, we have

$$\frac{d^2P_n}{dr^2} + \frac{1}{r}\frac{dP_n}{dr} - \left(\frac{n^2}{r^2} + n^2k^2\right) P_n = 0 \quad , \quad (n=1,2,3, \ . \ . \ .) \ . \tag{2.20}$$

Since the pressure must be finite throughout the unbounded fluid region $(0 \leqslant r < \infty)$, we obtain from (2.20) that

$$P_n(r) = \begin{cases} A_n \dfrac{K_n(nkr)}{K_n(nkh)} \quad , & (r > h) \\ \\ B_n \dfrac{I_n(nkr)}{I_n(nkh)} \quad , & (0 \leqslant r < h) \end{cases} \qquad (n=1,2,3, \ . \ . \ .) \tag{2.21}$$

where $I_n(nkr)$ and $K_n(nkr)$ are the modified Bessel functions of the first and second kind, respectively, of order n and argument nkr, A_n and B_n are arbitrary constants which will be determined later to guarantee the necessary smoothness of the function $P(r,\xi)$ at $r = h$. In fact, $P(r,\xi)$ must be continuous and its derivatives of any order should also be continuous in the entire fluid region $(D - D_o)$, where D represents the whole space, $D = D[(r,\xi,x) \mid 0 \leqslant r < \infty, -\pi \leqslant \xi \leqslant \pi, -\infty < x < \infty]$, and D_o is the part of the space which is occupied by the flagellum. Thus,

$$P \in c^{\infty}(D - D_o) \quad .$$

It should be noted that at $r = h$, the variable ξ for the fluid region spans only a subinterval of $[-\pi, \pi]$, i.e. $\pi \geqslant |\xi| \geqslant \xi_o = 2 \sin^{-1}\left(\frac{b}{2h}\right)$.

Substituting (2.16) - (2.18), and (2.21) into (2.8) and collecting the coefficients of like terms of $\sin n\xi$, we have

$$nk^2 \begin{Bmatrix} A_n \\ B_n \end{Bmatrix} \frac{C_n'(nkr)}{C_n(nkh)} = \left[\frac{d^2}{dr^2} + \frac{1}{r}\frac{d}{dr} - \left(\frac{n^2+1}{r^2} + n^2k^2\right)\right] u_n(r) + \frac{2n}{r^2} v_n(r) \quad ,$$

$$(n = 1, 2, 3, \ldots) \qquad (2.22)$$

where the circular function $C_n(z)$ is defined as

$$C_n(z) = \begin{cases} K_n(z) & , \quad (r > h) \\ I_n(z) & , \quad (0 \leqslant r < h) \end{cases} \qquad (2.23)$$

and $C_n'(z)$ denotes $\frac{d}{dz}[C_n(z)]$. The expression involving two quantities placed at two different levels inside a curly bracket means that the upper one should be taken when $r > h$ and the lower one for $0 \leqslant r < h$.

This notation will be adopted throughout the remaining part of this chapter.

Similarly, by substituting (2.16) - (2.18), and (2.21) into (2.9), we obtain the following

$$\left[\frac{d^2}{dr^2} + \frac{1}{r}\frac{d}{dr} - \frac{1}{r^2}\right] v_o(r) = 0 \quad , \qquad (2.24)$$

$$\frac{nk}{r}\left\{\begin{matrix} A_n \\ B_n \end{matrix}\right\} \frac{C_n(nkr)}{C_n(nkh)} = \left[\frac{d^2}{dr^2} + \frac{1}{r}\frac{d}{dr} - \left(\frac{n^2+1}{r^2} + n^2k^2\right)\right] v_n(r) + \frac{2n}{r^2} u_n(r) \quad ,$$

$$(n=1,2,3, \ . \ . \ .) \ . \qquad (2.25)$$

By (2.24), it follows that

$$v_o(r) = \left\{\begin{matrix} c_3 \dfrac{h}{r} \\ \\ c_4 \dfrac{r}{h} \end{matrix}\right\} \quad , \qquad (2.26a)$$

where c_3 and c_4 are arbitrary constants. Making use of the well-known identities for the modified Bessel functions that

$$C_{n-1}(z) - C_{n+1}(z) = \left\{\begin{matrix} -1 \\ +1 \end{matrix}\right\} \frac{2n}{z} C_n(z) \quad ,$$

$$C_{n-1}(z) + C_{n+1}(z) = \left\{\begin{matrix} -1 \\ +1 \end{matrix}\right\} 2 C_n'(z) \quad ,$$

where $C_n(z)$ is defined by (2.23), the differential equations for $[u_n(r) + v_n(r)]$ and $[u_n(r) - v_n(r)]$ can be obtained, by adding and subtracting (2.22) and (2.25), as

$$\left[\frac{d^2}{dr^2} + \frac{1}{r}\frac{d}{dr} - \frac{(n-1)^2}{r^2} - n^2k^2\right] [u_n(r) + v_n(r)] = \left\{\begin{matrix} -A_n \\ +B_n \end{matrix}\right\} nk^2 \frac{C_{n-1}(nkr)}{C_n(nkh)} \quad ,$$

$$\left[\frac{d^2}{dr^2} + \frac{1}{r}\frac{d}{dr} - \frac{(n+1)^2}{r^2} - n^2k^2\right][u_n(r) - v_n(r)] = \begin{Bmatrix} -A_n \\ +B_n \end{Bmatrix} nk^2 \frac{C_{n+1}(nkr)}{C_n(nkh)} \quad .$$

The solution of the above two equations consisting of complementary functions and particular integrals can be found, for $n = 1, 2, 3, \ldots$, as

$$u_n(r) + v_n(r) = \begin{Bmatrix} G_n \\ D_n \end{Bmatrix} \frac{C_{n-1}(nkr)}{C_{n-1}(nkh)} + \begin{Bmatrix} A_n \\ B_n \end{Bmatrix} \frac{kr}{2} \frac{C_n(nkr)}{C_n(nkh)} \quad ,$$

$$u_n(r) - v_n(r) = \begin{Bmatrix} H_n \\ E_n \end{Bmatrix} \frac{C_{n+1}(nkr)}{C_{n+1}(nkh)} + \begin{Bmatrix} A_n \\ B_n \end{Bmatrix} \frac{kr}{2} \frac{C_n(nkr)}{C_n(nkh)} \quad ,$$

where G_n, D_n, H_n and E_n are arbitrary constants. Therefore, it follows immediately that, for $n = 1, 2, 3, \ldots$,

$$u_n(r) = \frac{1}{2}\begin{Bmatrix} G_n \\ D_n \end{Bmatrix} \frac{C_{n-1}(nkr)}{C_{n-1}(nkh)} + \frac{kr}{2}\begin{Bmatrix} A_n \\ B_n \end{Bmatrix} \frac{C_n(nkr)}{C_n(nkh)} + \frac{1}{2}\begin{Bmatrix} H_n \\ E_n \end{Bmatrix} \frac{C_{n+1}(nkr)}{C_{n+1}(nkh)} \quad , \tag{2.27}$$

and

$$v_n(r) = \frac{1}{2}\begin{Bmatrix} G_n \\ D_n \end{Bmatrix} \frac{C_{n-1}(nkr)}{C_{n-1}(nkh)} - \frac{1}{2}\begin{Bmatrix} H_n \\ E_n \end{Bmatrix} \frac{C_{n+1}(nkr)}{C_{n+1}(nkh)} \quad . \tag{2.26b}$$

The continuity equation (2.1a) expressed in terms of the helical coordinates (r, ξ, x), while keeping the velocity components in the cylindrical polar coordinates (r, θ, x), is

$$\frac{\partial u}{\partial r} + \frac{u}{r} + \frac{1}{r}\frac{\partial v}{\partial \xi} - k\frac{\partial w}{\partial \xi} = 0 \quad . \tag{2.1b}$$

Therefore, from Eqs. (2.1b), (2.10), (2.16) - (2.19), (2.21), (2.26) and (2.27) we can derive that

$$w_o(r) = \begin{Bmatrix} c_5 \\ c_6 \end{Bmatrix} \quad , \tag{2.28a}$$

$$w_n(r) = \frac{1}{2}\begin{Bmatrix} G_n \\ -D_n \end{Bmatrix} \frac{C_n(nkr)}{C_{n-1}(nkh)} + \frac{1}{2}\begin{Bmatrix} H_n \\ -E_n \end{Bmatrix} \frac{C_n(nkr)}{C_{n+1}(nkh)} + \frac{kr}{2}\begin{Bmatrix} A_n \\ -B_n \end{Bmatrix} \frac{C_{n-1}(nkr)}{C_n(nkh)}$$

$$+ \frac{n-2}{2n}\begin{Bmatrix} A_n \\ B_n \end{Bmatrix} \frac{C_n(nkr)}{C_n(nkh)} \quad , \qquad (n=1,2,3, \ . \ . \ .) \ . \tag{2.28b}$$

In (2.28a), c_5 and c_6 are arbitrary constants, and the term $\log r$ is discarded.

So far, the solutions of Eqs. (2.1b), (2.8) - (2.10) are found separately for the fluid regions $(D - D_o) \cap (r > h)$ and $(D - D_o) \cap (r < h)$, nothing has been mentioned about how these two separate solutions should match across $r = h$, and how smooth these solutions will be at $r = h$. To ensure that the solutions given by (2.16) - (2.19) together with (2.21), (2.26) - (2.28) behave properly at $r = h$, we first prove the following theorem.

Theorem. If the pressure $P(r,\xi)$ and the velocity components $u(r,\xi)$, $v(r,\xi)$, $w(r,\xi)$ given by (2.16) - (2.19) together with (2.21), (2.26) - (2.28) have the following properties that in the region $(D - D_o) \cap (r = h)$

(1) P is continuous,

(2) u is continuous,

(3) v is continuous and has continuous first derivative w. r. t. r and

(4) w is continuous and has continuous first derivative w.r.t. r, then the solutions P, u, v, and w are infinitely smooth in the entire fluid region $(D - D_o)$; in other words,

$$P \in c^{\infty}(D - D_o) \quad , \quad u \in c^{\infty}(D - D_o) \quad , \quad v \in c^{\infty}(D - D_o) \quad ,$$
$$w \in c^{\infty}(D - D_o) \quad .$$

Proof. The proof of the above theorem is done by induction. First, we note that modified Bessel functions $I_m(z)$ and $K_m(z)$ are regular functions of z throughout the z-plane cut along the negative real axis, and for fixed $z(\neq 0)$ each is an entire function of m. For $m = 0, \pm 1, \pm 2, \ldots, I_m(z)$ is an entire function of z. Since n is a positive integer, the wave number k is real and positive, r is real and non-negative, therefore $K_m(nkr)$ $(m = 0, \pm 1, \pm 2, \ldots;$ $n = 1, 2, 3, \ldots)$ is regular in $(D - D_o) \cap (r > h)$, and $I_m(nkr)$ $(m = 0, \pm 1, \pm 2, \ldots ; n = 1, 2, 3, \ldots)$ is regular in $(D - D_o) \cap (r < h)$. Moreover, the trigonometric functions $\sin n\xi$ and $\cos n\xi$ $(n = 1, 2, 3, \ldots)$ are regular functions for real ξ, $-\pi \leqslant \xi \leqslant \pi$. By the recurrence relations

$$\frac{dK_m(z)}{dz} = -\frac{1}{2}\left(K_{m-1}(z) + K_{m+1}(z)\right) \quad , \quad \frac{dI_m(z)}{dz} = \frac{1}{2}\left(I_{m-1}(z) + I_{m+1}(z)\right),$$

$$\frac{d \sin nz}{dz} = n \cos nz \quad , \quad \frac{d \cos nz}{dz} = -n \sin nz \quad ,$$

we may conclude that the pressure $P(r, \xi)$ and the velocity components $u(r, \xi)$, $v(r, \xi)$, $w(r, \xi)$ given by (2.16) - (2.19) are continuous and have continuous derivatives of any order in $(D - D_o) \cap (r > h)$ and $(D - D_o) \cap (r < h)$ separately. Now, in the region $(D - D_o) \cap (r = h)$, if

(i) $P(r, \xi)$ is continuous and has continuous derivatives $w, r, t,$ r up to and including order q, $\frac{\partial^m P(r, \xi)}{\partial r^m}$ $(m = 0, 1, 2, \ldots, q)$,

(ii) $u(r,\xi)$ is continuous and has continuous derivatives w. r. t. r up to and including order q, $\frac{\partial^m u(r,\xi)}{\partial r^m}$ $(m = 0, 1, 2, \ldots, q)$,

(iii) $v(r,\xi)$ is continuous and has continuous derivatives w. r. t. r up to and including order $(q+1)$, $\frac{\partial^m v(r,\xi)}{\partial r^m}$ $(m = 0, 1, 2, \ldots, q, q+1)$,

and

(iv) $w(r,\xi)$ is continuous and has continuous derivatives w. r. t. r up to and including order $(q+1)$, $\frac{\partial^m w(r,\xi)}{\partial r^m}$ $(m=0, 1, 2, \ldots, q, q+1)$,

then we will prove that in $(D - D_o)\cap(r = h)$ the following are true,

(v) $\frac{\partial^{q+1} P(r,\xi)}{\partial r^i \partial \xi^j}$ $(i,j=0, 1, 2, \ldots, q+1;\ i+j = q+1)$ exists and is continuous,

(vi) $\frac{\partial^{q+1} u(r,\xi)}{\partial r^i \partial \xi^j}$ $(i,j=0, 1, 2, \ldots, q+1;\ i+j = q+1)$ exists and is continuous,

(vii) $\frac{\partial^{q+2} v(r,\xi)}{\partial r^i \partial \xi^j}$ $(i,j=0, 1, 2, \ldots, q+2;\ i+j = q+2)$ exists and is continuous,

(viii) $\frac{\partial^{q+2} w(r,\xi)}{\partial r^i \partial \xi^j}$ $(i,j = 0, 1, 2, \ldots, q+2;\ i+j = q+2)$ exists and is continuous.

For $j \geqslant 1$, the proof is trivial. For instance, let us prove (v) is true in the case $j \geqslant 1$. Since $P(r,\xi) \in c^\infty((D - D_o)\cap(r > h))$, $\frac{\partial^{q+1} P(r,\xi)}{\partial r^i \partial \xi^j}$ does exist and is continuous in $(D - D_o)\cap(r > h)$. Similarly, $\frac{\partial^{q+1} P(r,\xi)}{\partial r^i \partial \xi^j}$ also exists and is continuous in $(D - D_o)\cap(r < h)$. As r approaches to h from above and from below, the jump of the quantity $\frac{\partial^{q+1} P(r,\xi)}{\partial r^i \partial \xi^j}$ across $r = h$ is

$$\left[\frac{\partial^{q+1}P(r,\xi)}{\partial r^i\partial\xi^j}\right]_-^+ \equiv \lim_{0<(r-h)\to 0}\frac{\partial^{q+1}P(r,\xi)}{\partial r^i\partial\xi^j} - \lim_{0>(r-h)\to 0}\frac{\partial^{q+1}P(r,\xi)}{\partial r^i\partial\xi^j}$$

$$= \frac{\partial^j}{\partial\xi^j}\left[\frac{\partial^i P(r,\xi)}{\partial r^i}\right]_-^+ \quad (i+j = q+1;\ j \geqslant 1 \text{ or } i \leqslant q) \ .$$

By assumption (i),

$$\left[\frac{\partial^i P(r,\xi)}{\partial r^i}\right]_-^+ = 0 \qquad (i \leqslant q) \ .$$

Hence,

$$\left[\frac{\partial^{q+1}P(r,\xi)}{\partial r^i\partial\xi^j}\right]_-^+ = 0 \qquad (i+j = q+1;\ \ j \geqslant 1 \text{ or } i \leqslant q) \ .$$

Therefore statement (v) is true for $j \geqslant 1$. Similarly, we can prove (vi), (vii) and (viii) hold for $j \geqslant 1$.

When $j = 0$, since $P(r,\xi)$, $u(r,\xi)$, $v(r,\xi)$ and $w(r,\xi)$ are infinitely smooth in $(D - D_o)\cap(r > h)$ and in $(D - D_o)\cap(r < h)$, $\frac{\partial^{q+1}P(r,\xi)}{\partial r^{q+1}}$, $\frac{\partial^{q+1}u(r,\xi)}{\partial r^{q+1}}$, $\frac{\partial^{q+2}u(r,\xi)}{\partial r^{q+2}}$, $\frac{\partial^{q+2}v(r,\xi)}{\partial r^{q+2}}$ and $\frac{\partial^{q+2}w(r,\xi)}{\partial r^{q+2}}$ exist and are continuous in $(D - D_o)\cap(r > h)$ and in $(D - D_o)\cap(r < h)$. Differentiating (2.1b) w. r. t. r q-times and taking the limit as r approaches h from above and from below, then subtracting, we have

$$\left[\frac{\partial^{q+1}u(r,\xi)}{\partial r^{q+1}}\right]_-^+ + \left[\frac{\partial^q(u/r)}{\partial r^q}\right]_-^+ + \left[\frac{\partial^q}{\partial r^q}\left(\frac{1}{r}\frac{\partial v}{\partial\xi}\right)\right]_-^+ - k\frac{\partial}{\partial\xi}\left[\frac{\partial^q w}{\partial r^q}\right]_-^+ = 0 \ .$$

By (ii), (iii) and (iv)

$$\left[\frac{\partial^q(u/r)}{\partial r^q}\right]_-^+ = \left[\frac{\partial^q}{\partial r^q}\left(\frac{1}{r}\frac{\partial v}{\partial\xi}\right)\right]_-^+ = \left[\frac{\partial^q w}{\partial r^q}\right]_-^+ = 0 \ .$$

Therefore

$$\left[\frac{\partial^{q+1} u(r,\xi)}{\partial r^{q+1}}\right]_-^+ = 0 \quad . \tag{ix}$$

If we differentiate (2.1b) w. r. t. r (q+1)-times, take the limit as r approaches h from above and from below, subtract, and make use of (ii), (iii), (iv) and (ix), we have

$$\left[\frac{\partial^{q+2} u(r,\xi)}{\partial r^{q+2}}\right]_-^+ = 0 \quad . \tag{x}$$

Hence $\frac{\partial^{q+1} u}{\partial r^{q+1}}$ and $\frac{\partial^{q+2} u}{\partial r^{q+2}}$ are continuous in $(D - D_o)\cap(r = h)$. By differentiating (2.8) w. r. t. r q-times, taking the limit as r approaches h from above and from below, subtracting and making use of (ii), (iii), (ix) and (x), it follows immediately that

$$\left[\frac{\partial^{q+1} P(r,\xi)}{\partial r^{q+1}}\right]_-^+ = 0 \quad .$$

Similarly, by differentiating (2.9) and (2.10) w. r. t. r q-times and applying the same technique as before, we will find that

$$\left[\frac{\partial^{q+2} v(r,\xi)}{\partial r^{q+2}}\right]_-^+ = 0 \quad \text{and} \quad \left[\frac{\partial^{q+2} w(r,\xi)}{\partial r^{q+2}}\right]_-^+ = 0 \quad .$$

Thus, if (i), (ii), (iii) and (iv) are true, (v), (vi), (vii) and (viii) follow likewise. By our assumptions (1), (2), (3) and (4), they are true for $q = 0$, hence they are true for any integer q by induction. Therefore, $P(r,\xi)$, $u(r,\xi)$, $v(r,\xi)$ and $w(r,\xi)$ are infinitely smooth in $(D - D_o)\cap(r=h)$. But P, u, v, and w are infinitely smooth in $(D-D_o)\cap(r>h)$ and in $(D-D_o)\cap(r<h)$ by arguments in the beginning of this proof, hence

$$P \in c^{\infty}(D - D_o) \quad , \quad u \in c^{\infty}(D - D_o) \quad , \quad v \in c^{\infty}(D - D_o) \quad , \quad w \in c^{\infty}(D - D_o) \; .$$

(Q.E.D.)

From the above theorem, we know that if we make conditions (1), (2), (3) and (4) hold, the solutions will be infinitely smooth in the entire fluid region. By (1), (2.16), (2.21), it follows that

$$\sum_{n=1}^{\infty} (A_n - B_n) \sin n\xi = 0 \quad \text{in} \quad (D - D_o) \cap (r = h) \; . \tag{2.30}$$

Equation (2.30) does <u>not</u> imply that $A_n = B_n$, because in $(D - D_o) \cap (r = h)$, ξ only varies over a subinterval, $\pi \geqslant |\xi| \geqslant \xi_o = 2 \sin^{-1} \left| \frac{b}{2h} \right|$, and in this subinterval, the set $\{1, \sin n\xi, \cos n\xi\}$ $(n=1,2,3, \ldots)$ is no longer a completely orthogonal set. Although

$$\int_{\xi_o \leqslant |\xi| \leqslant \pi} \sin n\xi \cos m\xi \, d\xi = 0 \quad , \tag{2.31a}$$

yet

$$\int_{\xi_o \leqslant |\xi| \leqslant \pi} \sin n\xi \sin m\xi \, d\xi = \frac{\sin(m+n)\xi_o}{m+n} - \frac{\sin(m-n)\xi_o}{m-n} \neq 0 \quad , \quad (m \neq n)$$

$$= \pi - \xi_o + \frac{\sin(2n\xi_o)}{2n} \quad , \quad (m=n) \quad , \tag{2.31b}$$

and

$$\int_{\xi_o \leqslant |\xi| \leqslant \pi} \cos n\xi \cos m\xi \, d\xi = - \frac{\sin(m+n)\xi_o}{m+n} - \frac{\sin(m-n)\xi_o}{m-n} \neq 0 \quad , \quad (m \neq n)$$

$$= \pi - \xi_o - \frac{\sin(2n\xi_o)}{2n} \quad , \quad (m=n) \quad . \tag{2.31c}$$

Similarly, by (2), (3), (4), (2.17) - (2.19) and (2.26) - (2.28), we require that for $\xi_o \leqslant |\xi| \leqslant \pi$,

$$\sum_{n=1}^{\infty} [(G_n - D_n) + kh(A_n - B_n) + (H_n - E_n)] \sin n\xi = 0 \quad , \tag{2.32}$$

$$c_3 - c_4 + \sum_{n=1}^{\infty} [(G_n - D_n) - (H_n - E_n)] \cos n\xi = 0 \quad , \tag{2.33}$$

$$\frac{c_3 + c_4}{h} + \sum_{n=1}^{\infty} \left[G_n \frac{K_{n-2}(nkh) + K_n(nkh)}{K_{n-1}(nkh)} + D_n \frac{I_{n-2}(nkh) + I_n(nkh)}{I_{n-1}(nkh)} \right.$$
$$\left. - H_n \frac{K_n(nkh) + K_{n+2}(nkh)}{K_{n+1}(nkh)} - E_n \frac{I_n(nkh) + I_{n+2}(nkh)}{I_{n+1}(nkh)} \right] \frac{nk}{2} \cos n\xi = 0 \quad , \tag{2.34}$$

$$c_5 - c_6 + \sum_{n=1}^{\infty} \left[G_n \frac{K_n(nkh)}{K_{n-1}(nkh)} + D_n \frac{I_n(nkh)}{I_{n-1}(nkh)} + H_n \frac{K_n(nkh)}{K_{n+1}(nkh)} \right.$$
$$\left. + E_n \frac{I_n(nkh)}{I_{n+1}(nkh)} + \left(1 - \frac{2}{n}\right)(A_n - B_n) + khA_n \frac{K_{n-1}(nkh)}{K_n(nkh)} + khB_n \frac{I_{n-1}(nkh)}{I_n(nkh)} \right] \cos n\xi = 0 \quad , \tag{2.35}$$

$$\sum_{n=1}^{\infty} \left[G_n \left(1 + \frac{K_{n+1}(nkh)}{K_{n-1}(nkh)}\right) - D_n \left(1 + \frac{I_{n+1}(nkh)}{I_{n-1}(nkh)}\right) + H_n \left(1 + \frac{K_{n-1}(nkh)}{K_{n+1}(nkh)}\right) \right.$$
$$- E_n \left(1 + \frac{I_{n-1}(nkh)}{I_{n+1}(nkh)}\right)$$
$$+ A_n \frac{khK_{n-2}(nkh) + \left(1 - \frac{4}{n}\right)K_{n-1}(nkh) + \left(1 - \frac{2}{n}\right)K_{n+1}(nkh)}{K_n(nkh)} + khA_n - khB_n$$
$$\left. + B_n \frac{-khI_{n-2}(nkh) + \left(1 - \frac{4}{n}\right)I_{n-1}(nkh) + \left(1 - \frac{2}{n}\right)I_{n+1}(nkh)}{I_n(nkh)} \right] n \cos n\xi = 0 \quad . \tag{2.36}$$

The above equations, namely (2.30), (2.32) - (2.36), are the complete matching conditions for $P(r,\xi)$, $u(r,\xi)$, $v(r,\xi)$ and $w(r,\xi)$ at $r = h$, $\xi_o \leqslant |\xi| \leqslant \pi$.

On the flagellum surface, the velocity components can be expanded in Fourier series with α as an independent variable. Thus

$$u(r(\alpha),\xi(\alpha)) = \sum_{\ell=1}^{\infty} \sigma_\ell \sin \ell\alpha \quad , \tag{2.37a}$$

$$v(r(\alpha),\xi(\alpha)) = \frac{1}{2}\tau_o + \sum_{\ell=1}^{\infty} \tau_\ell \cos \ell\alpha \quad , \tag{2.38a}$$

$$w(r(\alpha),\xi(\alpha)) = \frac{1}{2}\varphi_o + \sum_{\ell=1}^{\infty} \varphi_\ell \cos \ell\alpha \quad , \tag{2.39a}$$

where the coefficients are determined from (2.11) - (2.13) as

$$\sigma_1 = \omega b \quad , \quad \sigma_\ell = 0 \quad (\ell = 2,3,4, \ldots) \tag{2.37b}$$

$$\tau_o = \frac{4\omega h}{\pi}\, \mathbb{E}\left(\frac{b}{h}\right) \quad , \quad \tau_1 = 0 \quad , \quad \tau_\ell = \frac{2\omega h}{\pi} \int_o^{\pi} \sqrt{1 - \frac{b^2}{h^2}\sin^2\alpha}\, \cos \ell\alpha d\alpha \quad ,$$

$$(\ell = 2,3,4, \ldots)$$

(2.38b)

$$\varphi_o = \varphi_\ell = 0 \quad , \qquad (\ell = 1,2,3, \ldots) \quad . \tag{2.39b}$$

The function $\mathbb{E}\left(\frac{b}{h}\right)$ in (2.38b) is the complete elliptic integral of the second kind and is given by

$$\mathbb{E}(x) = \frac{\pi}{2}\left(1 - \frac{1}{2^2}x^2 - \frac{1^2 \cdot 3}{2^2 \cdot 4^2}x^4 - \ldots\right) \quad , \quad (x^2 < 1) \quad . \tag{2.40}$$

By comparing the solution given by (2.17) - (2.19) at $r = r(\alpha)$ and $\xi = \xi(\alpha)$ with the boundary conditions (2.37) - (2.39) together with

the matching conditions (2.30), (2.32) - (2.36), we can, at least in principle, determine all the coefficients $c_3, c_4, c_5, c_6, A_n, G_n, H_n, B_n$, D_n and $E_n (n=1,2, \ldots)$. Consequently, the pressure and velocity distributions are completely determined.

A final remark about the matching condition is that it can only be done at some r in $h-b < r < h+b$, and $r = h$ is a convenient one. Suppose we want to match two solutions at $r = h + \epsilon$, $|\epsilon| > b$ then in $(D - D_o) \cap (r = h + \epsilon)$, ξ varies over the whole interval $[-\pi, \pi]$ and the set $\{1, \sin n\xi, \cos n\xi\}$ $(n=1,2,3, \ldots)$ becomes complete. To make a Fourier series vanish, say $\sum_{n=1}^{\infty} a_n \sin n\xi = 0$, each coefficient must be zero, i.e. $a_n = 0$ $(n=1,2,3, \ldots)$. Due to the fact that the Wronskian of $K_n(z)$ and $I_n(z)$ does not vanish,

$$W\{K_n(z), I_n(z)\} = \begin{vmatrix} K_n(z) & K_n'(z) \\ I_n(z) & I_n'(z) \end{vmatrix} = \frac{1}{z} \quad , \qquad (2.41)$$

conditions (2.30), (2.32) - (2.36) cannot be satisfied simultaneously unless $P(r,\xi) = u(r,\xi) = v(r,\xi) = 0$, $w(r,\xi) = c_5 = c_6$, which is a trivial solution.

2.3 Torque exerted on the flagellum

As an infinitely long flagellum propels itself through a viscous fluid by propagating a helical wave along it, there will be a constant torque (or a moment of force) exerted on the flagellum by the surrounding fluid about an axis lying in the direction of its forward motion. This torque is induced as a result of the helical movement of flagellum and

it tends to rotate the flagellum in the opposite direction to that of its forward motion. Thus, in order to make the helical movement of flagellum possible, a constant torque of the same magnitude but in opposite direction of the induced torque must be applied on the flagellum. For self-propelling microscopic organisms, this counter-torque is provided by having an inertial head. Without such counter-torque, helical waves will cease to exist and the flagellum becomes motionless.

The torque exerted on a flagellum in a wavelength by the surrounding fluid due to the helical wave motion can be calculated by the following formula,

$$M = b \int_{x=0}^{\lambda} \int_{\alpha=-\pi}^{\pi} \left[r(\tau_{\theta r} n_r + \tau_{\theta\theta} n_\theta + \tau_{\theta x} n_x) \sqrt{1+k^2 h^2} \left(1 + \frac{b \cos\alpha}{\sqrt{h^2 - b^2 \sin^2\alpha}} \right) \right]_{\substack{r=r(\alpha) \\ \xi=\xi(\alpha)}} d\alpha dx \quad , \quad (2.42)$$

where $\tau_{\theta r}, \tau_{\theta\theta}$ and $\tau_{\theta x}$ are the stress tensor components, given by

$$\tau_{\theta r} = \mu \left(\frac{\partial v}{\partial r} - \frac{v}{r} + \frac{1}{r} \frac{\partial u}{\partial \xi} \right) \quad , \quad (2.43a)$$

$$\tau_{\theta\theta} = - P + 2\mu \left(\frac{1}{r} \frac{\partial v}{\partial \xi} + \frac{u}{r} \right) \quad , \quad (2.43b)$$

$$\tau_{\theta x} = \mu \left(\frac{1}{r} \frac{\partial w}{\partial \xi} - k \frac{\partial v}{\partial \xi} \right) \quad . \quad (2.43c)$$

n_r, n_θ and n_x are the components of the unit outward normal to the flagellum surface in the r, θ, and x directions respectively. They may be found without much difficulty as

$$n_r = \frac{\cos\alpha}{\sqrt{1+k^2 h^2 \sin^2(\alpha+\xi)}} \quad , \quad (2.44a)$$

$$n_\theta = \frac{\sin\alpha}{\sqrt{1+k^2h^2\sin^2(\alpha+\xi)}} \quad , \tag{2.44b}$$

and

$$n_x = -\frac{kh\sin(\alpha+\xi)}{\sqrt{1+k^2h^2\sin^2(\alpha+\xi)}} \quad , \tag{2.44c}$$

ξ and α being related by (2.5b).

Once the pressure and velocity components are found, we can obtain the stress components $\tau_{\theta r}$, $\tau_{\theta\theta}$ and $\tau_{\theta x}$ by substituting (2.16) - (2.19) into (2.43). Finally, substituting (2.43) and (2.44) into (2.42), the torque acting on a flagellum in a wavelength could be determined.

2.4 Energy required to maintain the flagellum in motion

The energy E required in a wavelength of the flagellum for maintaining the helical motion may be found by integration, over the flagellum surface, of the time-rate of work done by the surface stresses. This calculation yields

$$E = b\int_{x=0}^{\lambda}\int_{\alpha=-\pi}^{\pi}\left[\sum_{i=r,\theta,x}(\omega h\tau_{ri}\sin\xi+\omega h\tau_{\theta i}\cos\xi+U\tau_{xi})\, n_i\sqrt{1+k^2h^2}\left(1+\frac{b\cos\alpha}{\sqrt{h^2-b^2\sin^2\alpha}}\right)\right]_{\substack{r=r(\alpha)\\ \xi=\xi(\alpha)}} d\alpha dx \tag{2.45}$$

where $\tau_{\theta i}(i=r,\theta,x)$ and n_i are given by (2.43) and (2.44) respectively, τ_{ri} and τ_{xi} are as follows,

$$\tau_{rr} = -P + 2\mu\frac{\partial u}{\partial r} \quad , \tag{2.46a}$$

$$\tau_{xx} = - P - 2\mu k \frac{\partial w}{\partial \xi} \quad , \tag{2.46b}$$

$$\tau_{r\theta} = \tau_{\theta r} = \mu\left(\frac{1}{r}\frac{\partial u}{\partial \xi} + \frac{\partial v}{\partial r} - \frac{v}{r}\right) \quad , \tag{2.46c}$$

$$\tau_{rx} = \tau_{xr} = \mu\left(-k\frac{\partial u}{\partial \xi} + \frac{\partial w}{\partial r}\right) \quad , \tag{2.46d}$$

$$\tau_{x\theta} = \tau_{\theta x} = \mu\left(\frac{1}{r}\frac{\partial w}{\partial \xi} - k\frac{\partial v}{\partial \xi}\right) \quad . \tag{2.46e}$$

2.5 Approximate propulsion velocity when $b \ll h$

For most flagellum-propelling microorganisms, the radius of the circular cross-section of flagellum is small in comparison with the amplitude of helical waves. In the limiting case when $b/h \ll 1$, boundary conditions (2.37) - (2.39) reduce to

$$u(r(\alpha), \xi(\alpha)) = \omega b \sin\alpha \quad , \tag{2.47}$$

$$v(r(\alpha), \xi(\alpha)) = \omega h + O\left(\frac{b}{h}\right)^2 \quad , \tag{2.48}$$

$$w(r(\alpha), \xi(\alpha)) = 0 \quad . \tag{2.49}$$

By (2.5b), we see that $\sin\alpha = \frac{h}{b}\sin\xi$. As is clearly suggested by (2.47) - (2.49), we assume, as a first approximation, that for $r > h$,

$$P(r,\xi) \simeq k\mu A_1 \frac{K_1(kr)}{K_1(kh)} \sin\xi \quad , \tag{2.50}$$

$$u(r,\xi) \simeq \frac{1}{2}\left[G_1 \frac{K_o(kr)}{K_o(kh)} + A_1 kr \frac{K_1(kr)}{K_1(kh)} + H_1 \frac{K_2(kr)}{K_2(kh)}\right]\sin\xi \quad , \tag{2.51}$$

$$v(r,\xi) \simeq \frac{c_3}{2}\frac{h}{r} + \frac{1}{2}\left[G_1 \frac{K_o(kr)}{K_o(kh)} - H_1 \frac{K_2(kr)}{K_2(kh)}\right]\cos\xi \quad , \tag{2.52}$$

$$w(r,\xi) \simeq \frac{c_5}{2} + \frac{1}{2}\left[G_1 \frac{K_1(kr)}{K_o(kh)} + H_1 \frac{K_1(kr)}{K_2(kh)} + A_1 kr \frac{K_o(kr)}{K_1(kh)} - A_1 \frac{K_1(kr)}{K_1(kh)}\right]\cos\xi . \tag{2.53}$$

The boundary surface, in the limit of $b/h \ll 1$, reduces to

$$r(\alpha) = h\left[1 + \frac{b}{h}\cos\alpha + O\left(\frac{b}{h}\right)^2\right] \quad ,$$

and

$$\xi(\alpha) = \frac{b}{h}\sin\alpha + O\left(\frac{b}{h}\right)^3 \quad . \tag{2.54}$$

Neglecting terms of order $O\left(\frac{b}{h}\right)^2$ and higher orders in applying the boundary conditions, and noting that for arbitrary analytic function $f(r(\alpha))$,

$$f(r(\alpha)) = f(h) + b\cos\alpha\, f'(h) + O\left(\frac{b}{h}\right)^2 \quad ,$$

we obtain the following simultaneous equations,

$$G_1 + A_1 kh + H_1 = 2\omega h \quad , \tag{2.55a}$$

$$c_3 + G_1 - H_1 = 2\omega h \quad , \tag{2.55c}$$

$$-c_3 + khG_1 \frac{K_0'(kh)}{K_0(kh)} - kh\,H_1 \frac{K_2'(kh)}{K_2(kh)} = 0 \quad , \tag{2.55d}$$

$$c_5 + G_1 \frac{K_1(kh)}{K_0(kh)} + H_1 \frac{K_1(kh)}{K_2(kh)} + kh\,A_1 \frac{K_0(kh)}{K_1(kh)} - A_1 = 0 \quad , \tag{2.55e}$$

$$G_1 \frac{K_1'(kh)}{K_0(kh)} + H_1 \frac{K_1'(kh)}{K_2(kh)} + A_1 \frac{K_0(kh)}{K_1(kh)} + khA_1 \frac{K_0'(kh)}{K_1(kh)} - A_1 \frac{K_1'(kh)}{K_1(kh)} = 0 \quad , \tag{2.55f}$$

where $K_n'(z)\ (n=0,1,2)$ denotes $dK_n(z)/dz$. The solution of the above simultaneous equations is

$$G_1 = \frac{2\omega h}{\Delta}\left[-\frac{1}{2}k^3h^3 + \left(kh + \frac{1}{2}k^3h^3\right)\frac{K_0(kh)}{K_2(kh)}\right] , \tag{2.56a}$$

$$A_1 = \frac{2\omega h}{\Delta}\left[\frac{1}{2}k^2h^2 + kh\frac{K_1(kh)}{K_0(kh)} - \frac{1}{2}k^2h^2\frac{K_0(kh)}{K_2(kh)}\right] , \tag{2.56b}$$

$$H_1 = \frac{2\omega h}{\Delta}\left[3kh + (2-k^2h^2)\,\frac{K_1(kh)}{K_0(kh)}\right] \quad , \tag{2.56c}$$

$$c_3 = \frac{2\omega h}{\Delta}\left[6kh + \frac{1}{2}k^3h^3 + (4-k^2h^2)\,\frac{K_1(kh)}{K_0(kh)} - \frac{1}{2}k^3h^3\,\frac{K_0(kh)}{K_2(kh)}\right], \tag{2.56d}$$

$$c_5 = \frac{2\omega h}{\Delta}\left[-2k^2h^2 - \frac{1}{2}k^4h^4 + k^3h^3\,\frac{K_1(kh)}{K_0(kh)} + \frac{1}{2}k^4h^4\,\frac{K_0(kh)}{K_2(kh)}\right], \tag{2.56e}$$

where

$$\Delta = 3kh + 2\,\frac{K_1(kh)}{K_0(kh)} + kh\,\frac{K_0(kh)}{K_2(kh)} \quad . \tag{2.56f}$$

Since the modified Bessel function of the second kind $K_m(nkr)$ $(m = 0,\pm1,\pm2, \ldots; n = 1,2,3, \ldots)$ decreases exponentially as r approaches to infinity, the boundary conditions at infinity, (2.14) and (2.15), are satisfied automatically with the propulsion velocity U given by $U = -\frac{c_5}{2}$ or

$$\frac{U}{c} = k^3h^3\,\frac{2 + \frac{1}{2}k^2h^2 - kh\,\frac{K_1(kh)}{K_0(kh)} - \frac{1}{2}k^2h^2\,\frac{K_0(kh)}{K_2(kh)}}{3kh + 2\,\frac{K_1(kh)}{K_0(kh)} + kh\,\frac{K_0(kh)}{K_2(kh)}} \quad . \tag{2.57}$$

The value of U/c given by (2.57) is plotted versus the kh value in Fig. 3. The limiting value of U/c as kh approaches to zero is

$$\lim_{kh \to o}\frac{U}{c} = k^3h^3\,\frac{2K_0(kh) - khK_1(kh)}{2K_1(kh)} \quad . \tag{2.58}$$

To determine the accuracy of the present single-harmonic approximation for the outer solution $(r > h)$, (2.50) - (2.53), and to show that it may differ from the exact solutions, (2.16) - (2.19), only by

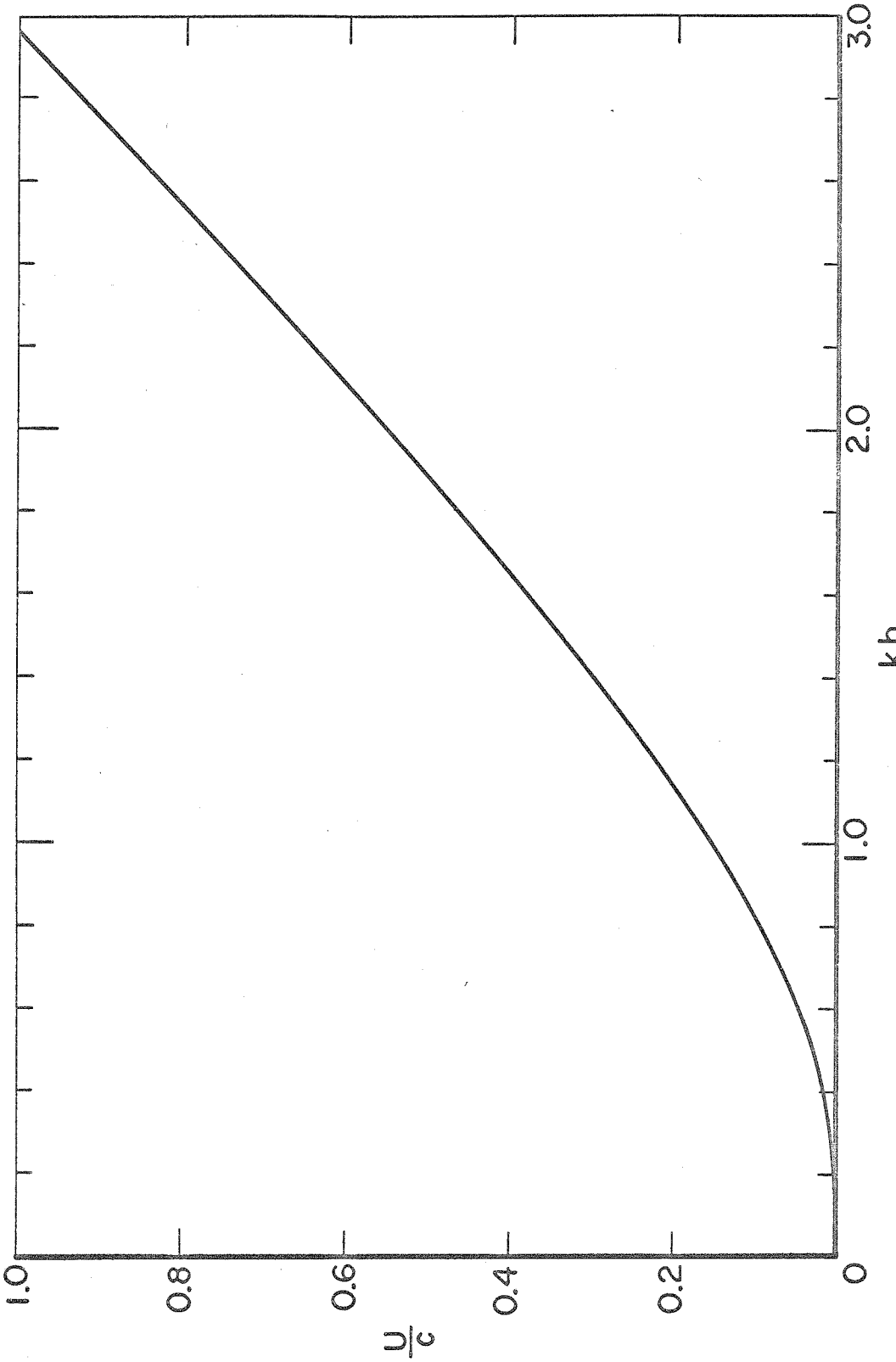

Fig. 3 Propulsion velocity of an infinitely long flagellum when $b < h$.

terms of order $O(b/h)^2$, we proceed as follows. By (2.54), we have

$$\sin n\xi(\alpha) = \sin\left(n\,\frac{b}{h}\,\sin\alpha\right) + O\left(\frac{b}{h}\right)^3 \quad (n=1,2,3,\ .\ .\ .) \ ,$$

and

$$\cos n\xi(\alpha) = \cos\left(n\,\frac{b}{h}\,\sin\alpha\right) + O\left(\frac{b}{h}\right)^3 \quad (n=1,2,3,\ .\ .\ .) \ .$$

From the integral representation of the Bessel function of the first kind, $J_\ell(x)$, we have for $\ell = 0, \pm1, \pm2, \ .\ .\ .$

$$\frac{2}{\pi}\int_0^\pi \sin\left(n\,\frac{b}{h}\,\sin\alpha\right)\sin\ell\alpha\,d\alpha = [\,1-(-1)^\ell\,]\,J_\ell\left(n\,\frac{b}{h}\right) \ ,$$

$$\frac{2}{\pi}\int_0^\pi \cos\left(n\,\frac{b}{h}\,\sin\alpha\right)\cos\ell\alpha\,d\alpha = [\,1+(-1)^\ell\,]\,J_\ell\left(n\,\frac{b}{h}\right) \ .$$

Thus, for the exact solution (2.16) - (2.19), the boundary conditions (2.47) - (2.49) yield that, for $\ell = 0,2,4,6, \ .\ .\ .\ ,$

$$\sum_{n=1}^{\infty} u_n(h)\ J_{\ell+1}\left(n\,\frac{b}{h}\right) = \frac{\omega b}{2}\,\delta_{\ell 0} + O\left(\frac{b}{h}\right)^2 \ , \tag{2.59a}$$

$$\sum_{n=1}^{\infty} b u_n'(h)\left[J_{\ell+1}\left(n\,\frac{b}{h}\right) + J_{\ell+3}\left(n\,\frac{b}{h}\right)\right] = O\left(\frac{b}{h}\right)^2 \ , \tag{2.59b}$$

$$\frac{1}{2}\,c_3\,\delta_{\ell 0} + \sum_{n=1}^{\infty} v_n(h) J_\ell\left(n\,\frac{b}{h}\right) = \omega h\,\delta_{\ell 0} + O\left(\frac{b}{h}\right)^2 \ , \tag{2.59c}$$

$$-\frac{b}{2h}\,c_3\,\delta_{\ell 0} + \sum_{n=1}^{\infty} b\,v_n'(h)\left[J_\ell\left(n\,\frac{b}{h}\right) + J_{\ell+2}\left(n\,\frac{b}{h}\right)\right] = O\left(\frac{b}{h}\right)^2 \ , \tag{2.59d}$$

$$\frac{1}{2}\,c_5\,\delta_{\ell 0} + \sum_{n=1}^{\infty} w_n(h)\ J_\ell\left(n\,\frac{b}{h}\right) = O\left(\frac{b}{h}\right)^2 \ , \tag{2.59e}$$

$$\sum_{n=1}^{\infty} b\, w_n'(h)\left[J_\ell\left(n\,\frac{b}{h}\right) + J_{\ell+2}\left(n\,\frac{b}{h}\right)\right] = 0\left(\frac{b}{h}\right)^2 \quad , \tag{2.59f}$$

where $u_n(r)$, $v_n(r)$ and $w_n(r)$ are given by (2.26) - (2.28), $u_n'(r)$ denotes $du_n(r)/dr$ and $\delta_{\ell o}$ is the Kronecker delta.

Since the ascending series for the Bessel function of the first kind is

$$J_\ell(x) = \left(\frac{1}{2}\,x\right)^\ell \sum_{m=o}^{\infty} \frac{\left(-\frac{1}{4}\,x^2\right)^m}{m!\Gamma(\ell+m+1)} \quad ,$$

we see immediately that the single-harmonic approximation (2.50) - (2.53) with the coefficients determined by (2.55) and $A_n=G_n=H_n=0$ $(n=2,3,4,\ .\ .\ .)$ satisfies the simultaneous equations (2.59) $(\ell = 0,2,4,6,\ .\ .\ .)$ up to the order $O(b/h)^2$.

In order to make the solutions smooth at $r = h$, and that the matching conditions (2.30), (2.32) - (2.36) be satisfied, we have to take infinitely many terms for the solutions in the region $(D - D_o)\cap(r < h)$. Thus, for $r < h$,

$$P(r,\xi) = k\mu \sum_{n=1}^{\infty} B_n \frac{I_n(nkr)}{I_n(nkh)} \sin n\xi \quad , \tag{2.60}$$

$$u(r,\xi) = \frac{1}{2}\sum_{n=1}^{\infty}\left[D_n \frac{I_{n-1}(nkr)}{I_{n-1}(nkh)} + kr\, B_n \frac{I_n(nkr)}{I_n(nkh)} + E_n \frac{I_{n+1}(nkr)}{I_{n+1}(nkh)}\right]\sin n\xi \quad , \tag{2.61a}$$

$$v(r,\xi) = \frac{c_4\, r}{2h} + \frac{1}{2}\sum_{n=1}^{\infty}\left[D_n \frac{I_{n-1}(nkr)}{I_{n-1}(nkh)} - E_n \frac{I_{n+1}(nkr)}{I_{n+1}(nkh)}\right]\cos n\xi \quad , \tag{2.61b}$$

$$w(r,\xi) = \frac{c_6}{2} + \frac{1}{2}\sum_{n=1}^{\infty}\left[-D_n \frac{I_n(nkr)}{I_{n-1}(nkh)} - E_n \frac{I_n(nkr)}{I_{n+1}(nkh)} - kr\, B_n \frac{I_{n-1}(nkr)}{I_n(nkh)} + \left(1 - \frac{2}{n}\right) B_n \frac{I_n(nkr)}{I_n(nkh)}\right]\cos n\xi \quad . \tag{2.61c}$$

The coefficients c_4, c_6, D_n, B_n and $E_n (n=1,2,3,\ .\ .\ .)$ are to be

determined by (2.11) - (2.13), (2.30), (2.32) - (2.36). Theoretically this is possible, but practically it is a very tedious task because we have to keep an infinite number of terms in the calculations. Any finite-term approximations will make the solutions un-smooth at $r = h$.

2.6 Comparison with G.I. Taylor's and G. J. Hancock's solutions

To study the flagellated propulsion of microscopic organisms, Taylor (1952) applied the Stokes equations in a cylindrical polar co-ordinate system and analyzed the motion of an infinitely long cylindrical tail which makes progressive helical waves of small amplitude, i.e. $h \ll b$ (in the present notation). He was able to find that the propulsion velocity U of this cylindrical tail is in the opposite direction to the phase velocity c of the helical waves and the magnitude of U for arbitrary values of kb is

$$\frac{U}{c} = k^2 h^2 \frac{K_o(kb) - \frac{1}{2} kb K_1(kb) + \frac{1}{2} kb \frac{K_o^2(kb)}{K_1(kb)}}{kbK_1(kb)\left\{\frac{1}{2} + \frac{1}{2}\frac{K_o(kb)}{K_2(kb)} - \left[\frac{K_o(kb)}{K_1(kb)}\right]^2\right\} + K_o(kb)} \quad . \tag{2.63}$$

In the limiting case when kb approaches to zero, (2.63) reduces to

$$\lim_{kb \to 0} \frac{U}{c} = k^2 h^2 \frac{K_o(kb) - \frac{1}{2}}{K_o(kb) + \frac{1}{2}} \quad . \tag{2.64}$$

Furthermore, Taylor found that a constant couple (or torque) must be applied to the tail about its length in order that it may not rotate. In the limiting case when kb approaches to zero, the torque M exerted by the surrounding fluid on the cylinder per wavelength is (Drummond,

1966)

$$\lim_{kb \to 0} M = -4\pi\mu kh^2 c\lambda \Big/ \left[K_o(kb) + \frac{1}{2} \right] . \qquad (2.65)$$

The negative sign in front of the expression (2.65) means that the torque acting on the tail is in the direction opposite to that of the forward propulsion.

The assumption made in Taylor's work that the amplitude of the helical wave, h, is small in comparison with the radius of the circular cylindrical tail, b, is not generally met in nature, since even though kh may be small, h is usually observed to be greater than b. For a great variety of motions employed by microscopic organisms, the kh value is about 1 as a typical estimate. It is necessary then to develop a theory capable of solving problems involving helical waves of arbitrary amplitude. However, the extension of the method used by Taylor in an attempt to determine further terms in the series for the velocity is very difficult, as has been noted by Hancock(1953). An alternative approach was suggested by Hancock(1953). He analyzed the movement of a long thin cylindrical filament along which helical waves of lateral displacement are propagated. The flow around the filament is determined by distributing a system of 'doublets' and 'Stokeslets' inside the surface of the filament whose strengths are determined from the no-slip boundary conditions on the filament surface together with the condition that the total energy of the induced velocity field remains finite. In Hancock's theory, the amplitude of propagating helical waves, h, need not be small as compared with the wavelength λ, yet the radius of the

filament, b, shrinks to zero. Under these conditions, he was able to find that the propulsion velocity U is

$$\frac{U}{c} = \frac{k^2 h^2}{1+2k^2 h^2} \quad . \tag{2.67}$$

However, he did not obtain an expression for the torque exerted on the filament by the surrounding fluid, the reason for this difficulty is because of his initial assumption that kb must be very small. Even when no "zero radius" assumption is made, he still could not find the torque by means of his theory because it is only $\left(\ell n \frac{b}{\lambda}\right)^{-1}$ which is of an order of magnitude not neglected in his calculations, but $\frac{b}{\lambda}$ itself.

In order to have a better understanding of the nature of helical waves, we suggest here a third approach as presented in the previous sections of this chapter. In this new approach, a helical coordinate system (r,ξ,x) is employed. All the operators are expressed in terms of this helical coordinate while the velocity components u, v and w are still kept in the r,θ and x directions with r,ξ as the independent variables. In so doing, the solutions for helical waves of arbitrary amplitude h produced by an infinitely long flagellum of radius b, with $b < h$, can be found for the two regions $(r > h)$ and $(r < h)$ separately. Based on the theorem proved in the foregoing, the outer solution (corresponding to $r > h$) and the inner solution (corresponding to $0 \leqslant r < h$) can be matched infinitely smoothly at $r = h$. Expressions for calculating the induced torque M and the energy required to maintain such helical motion E are presented. In the extreme case when $b \ll h$, by a single-harmonic approximation for

the outer solution and neglecting second-order terms $O\left(\frac{b}{h}\right)^2$ in applying the boundary conditions, the propulsion velocity is found to be

$$\frac{U}{c} = k^3 h^3 \frac{2 + \frac{1}{2} k^2 h^2 - kh \frac{K_1(kh)}{K_0(kh)} - \frac{1}{2} k^2 h^2 \frac{K_0(kh)}{K_2(kh)}}{3kh + 2 \frac{K_1(kh)}{K_0(kh)} + kh \frac{K_0(kh)}{K_2(kh)}} \quad . \qquad (2.57)$$

When kh is small, (2.57) reduces to

$$\lim_{kh \to 0} \frac{U}{c} = k^3 h^3 \frac{2K_0(kh) - kh K_1(kh)}{2K_1(kh)} \quad . \qquad (2.58)$$

However, the author has not been able to provide explicit solutions for the induced torque M and the energy required E, because it requires the knowledge of all coefficients, infinitely many of them, in the inner solution.

For small values of kb and kh, Taylor's (2.64), Hancock's (2.67) and present (2.58) solutions are plotted in Fig. 4 for comparison. From Taylor's or Hancock's solution, (2.64) and (2.67), we observe that the propulsion velocity U is proportional to the square of kh. According to the present approximate solution (2.58), however, U/c is proportional to the product of $(kh)^4$ and log kh (i.e. $U \propto - k^4 h^4 \log kh$), the order of which is between the third and fourth powers of kh. In other words, the propulsion velocity U given by the present approximation is smaller than that predicted by Taylor or Hancock for the same phase velocity c. It was reported by many biologists (e.g. Rikmenspoel, 1962) that the velocities predicted by Taylor (1952) or Hancock (1953) are too high, by a factor of 10 for the model of Taylor or a factor of 5 for that of Hancock. Hence the

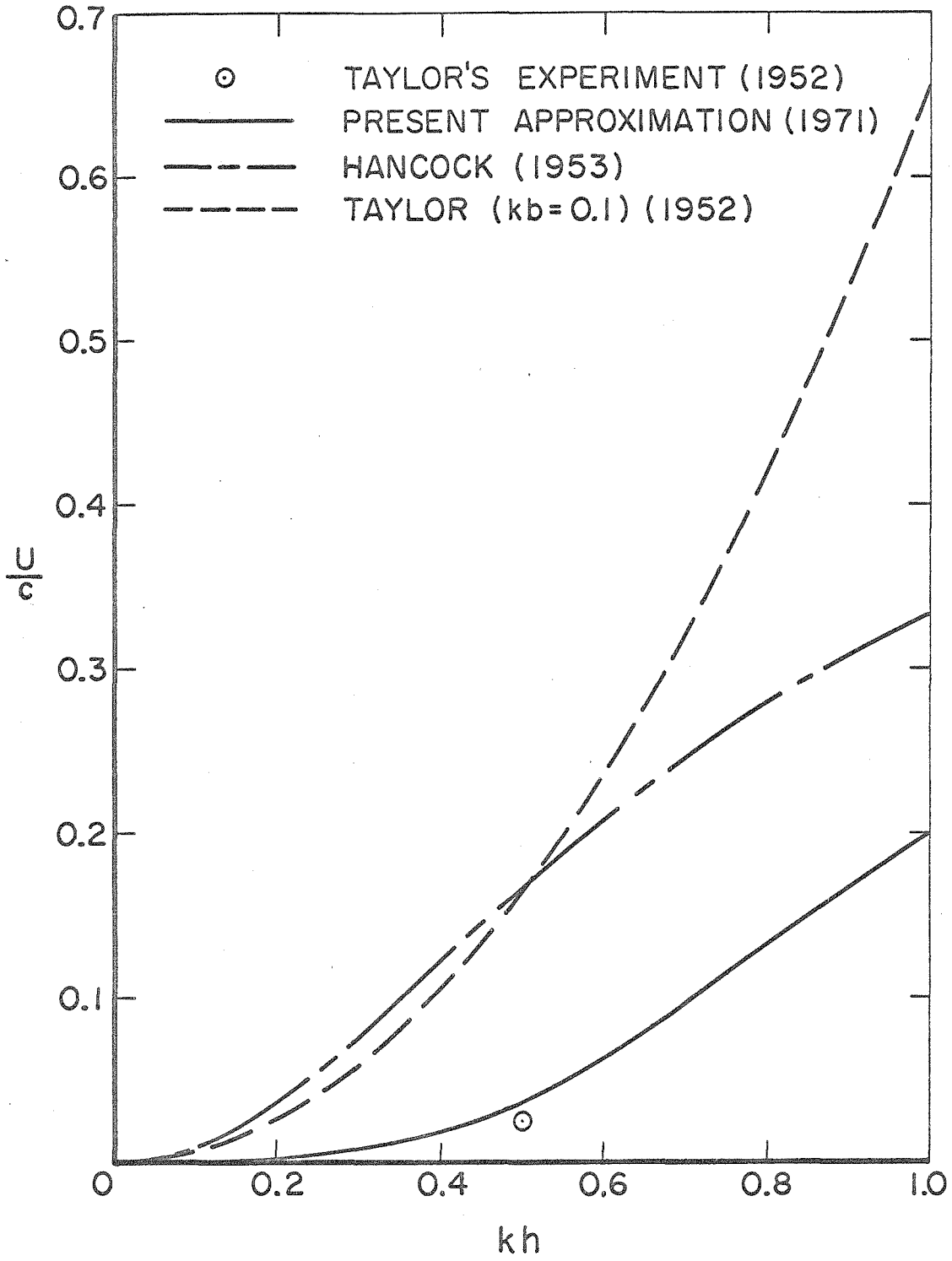

Fig. 4 Propulsion velocity of flagellum at small values of kb and kh.

present approximation is in a better agreement with the experimental data measured by biologists.

Another interesting fact worth mentioning is that Taylor (1952) made a working model of swimming spermatozoan which, when released after being wound up, can make a helical wave to travel down its rubber tail without rotating relative to the body. The only experimental result on this model reported in his paper is the one in which (in the present notation) $kb = 0.1$, $kh = 0.5$ and the observed value of U/c is

$$(U/c)_{observed} = 0.025$$

which is also plotted in Fig. 4. Comparing this experimental result with three theoretical curves, it further adds to one's confidence in the present solution.

III. THE SELF-PROPULSION OF A MICROORGANISM BY SENDING HELICAL WAVES DOWN ITS FLAGELLATED TAIL

3.1 First principles of mechanics

In order to facilitate applications to the self-propulsion of flagellated microscopic organisms, Gray and Hancock (1955) derived two very useful approximate formulae based on the first principles of mechanics and the concept of 'Stokeslets' for calculating the tangential and normal coefficients of viscous resistance acting on the surface of a long thin cylindrical element which is in motion through a viscous fluid. If the tangential and normal velocities of this cylindrical element of length ds are $\vec{V}_s$ and $\vec{V}_n$ respectively with respect to the surrounding fluid, the tangential viscous force acting on this element ds will be $d\vec{F}_s = - C_s \vec{V}_s ds$, and the normal viscous force, $d\vec{F}_n = -C_n \vec{V}_n ds$, where C_s and C_n are the corresponding coefficients of resistance, which are given by Gray and Hancock (1955) as

$$C_n = 2 C_s \quad , \tag{3.1}$$

and

$$C_s = \frac{2\pi\mu}{\log\left(\frac{2\lambda}{b}\right) - \frac{1}{2}} \quad , \tag{3.2}$$

where b is the radius of the slender filament, μ the viscosity coefficient.

Equations (3.1) and (3.2) given by Gray and Hancock (1955) have been adopted by many authors to make theoretical analyses of planar waves generated by minute creatures, including the propulsion of

sea-urchin spermatozoa, Psammechinus miliaris (Gray and Hancock, 1955) and the movement of spermatozoa of a bull (Gray, 1958). The results are remarkably good for planar waves. Based also on the above formulae, Carlson (1959) derived an expression for the motile power required to make such plane waves. However, when Gray and Hancock's method is adopted to study the helical movement of flagellated microorganisms, both the linear and angular momentum must be simultaneously taken into account. For a body propelling itself at a constant mean velocity in a viscous fluid, both the resultant force and the resultant torque acted on the body by the fluid must vanish. The purpose of this chapter is to demonstrate that conditions of conservation of both linear and angular momentum yield two equations relating four flow quantities, the forward speed of propulsion, U, the induced angular velocity Ω of body about the axis of propulsion, the resultant thrust F_x and resultant torque M_x experienced by the organism. The forward speed U and angular velocity Ω of a flagellated organism in helical waving motion posterior to its head are thereby determined by the conditions that both F_x and M_x vanish.

Consider a model creature, which has a head and a flagellum, swimming in a viscous fluid by making helical waves which propagate distally. The motion will be considered here in two steps. For the first, the flagellum bends itself simultaneously in two internal planes normal to each other, and the cross sections of body do not rotate about the body-axis (Fig. 5a, b). In terms of a cylindrical polar coordinate system (r, θ, x) fixed with respect to the fluid at infinity, this type of helical wave form can be described by

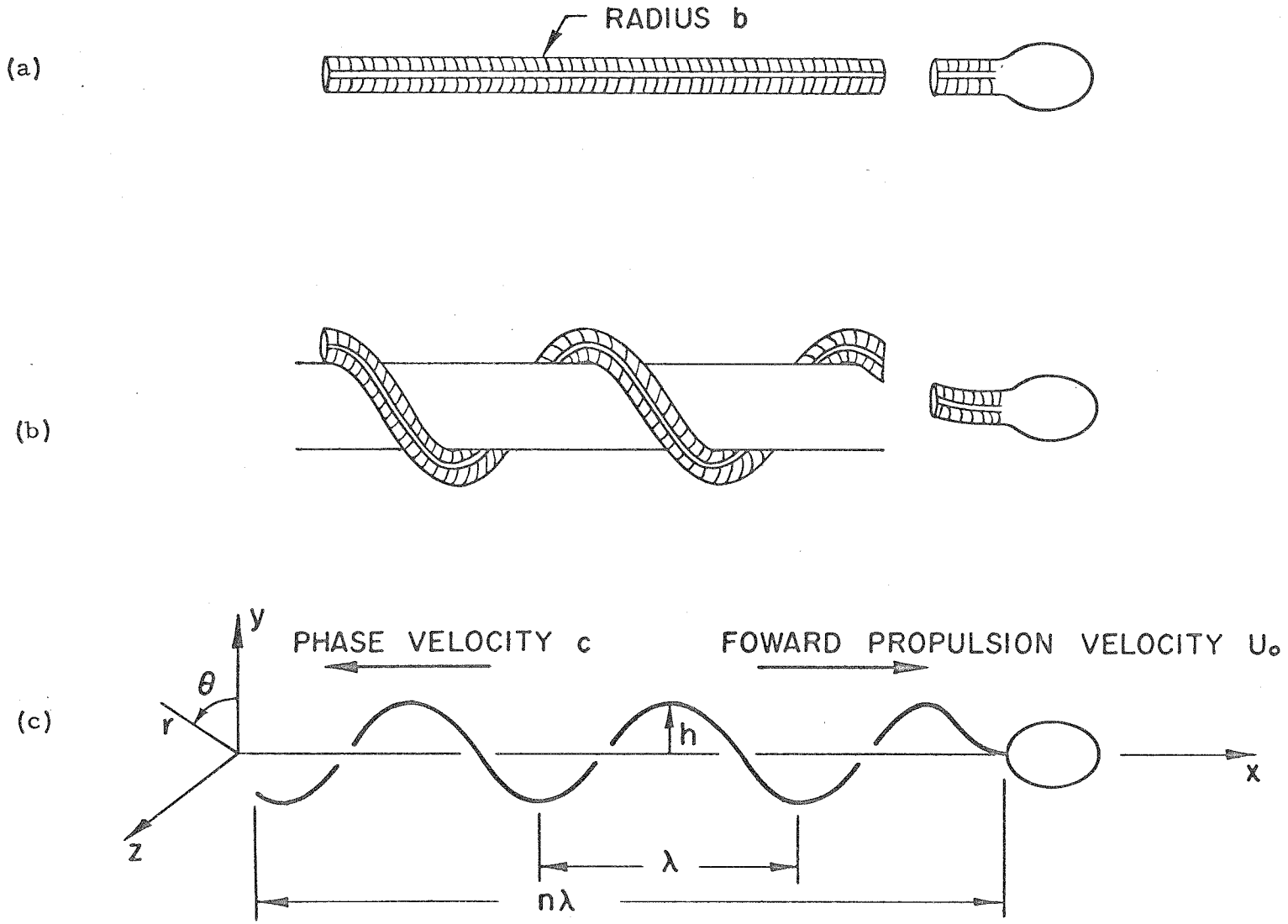

Fig. 5 Schematic diagrams of a model microorganism employing helical waves along its flagellum.

(d)

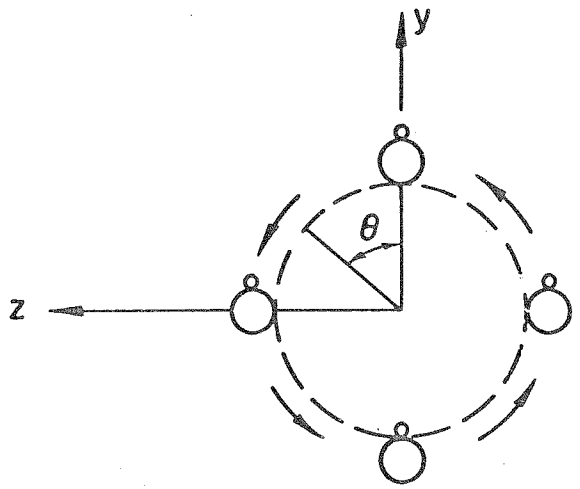

$\omega = kc$

(e)

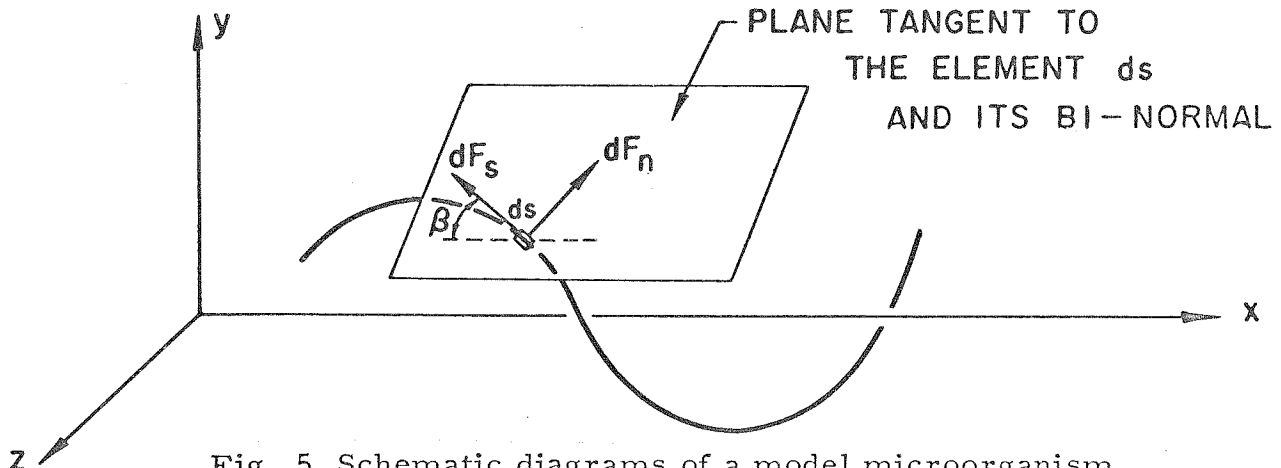

Fig. 5 Schematic diagrams of a model microorganism employing helical waves along its flagellum.

$$r = h \quad ,$$

$$\theta = k(x+ct) = kx + \omega t \quad , \qquad (3.3)$$

where $k = 2\pi/\lambda$ is the wave number and $c = \omega/k$ is the phase velocity. Every element of the flagellum rotates about the x-axis with a frequency $f = \omega/2\pi$ cycles/sec in the θ-direction, but does not "gyrate" around any point within the body, and moves parallel to the x-axis with velocity U_o (Fig. 5c, d). The head and its attached tail, as a whole, do not rotate about the x-axis, while they move along the x-axis with velocity U_o.

Now, from the free-body diagram of the forces acting on an element ds of the tail, the propulsive force in the x-direction is seen to be

$$dF_x = (dF_n \sin\beta - dF_s \cos\beta) \quad , \qquad (3.4)$$

and the force in the θ-direction is $dF_\theta = -(dF_n \cos\beta + dF_s \sin\beta)$, which gives a torque, or a moment of force about the x-axis,

$$dM_x = h dF_\theta = -h(dF_n \cos\beta + dF_s \sin\beta) \quad , \qquad (3.5)$$

where β is the constant pitch-angle between the tail and the x-axis,

$$\tan\beta = \frac{2\pi}{\lambda} h = kh \quad , \qquad (3.6)$$

and dF_n/ds, dF_s/ds are the bi-normal and tangential components, respectively, of the resultant force acting on the filament of unit length. The negative sign in Eq. (3.5) means that the torque tends to rotate the body in the $(-\theta)$-direction, i.e. clockwise in the yz plane. The total

force in the x-direction can be balanced, $\int_{x=o}^{n\lambda} dF_x - F_{head} = 0$ (where $n\lambda$ is the extension of flagellum in the x-direction, F_{head} is the viscous drag on the head, but the net torque, $\int_{x=o}^{n\lambda} dM_x$, cannot vanish as will be shown explicitly later. Hence the creature, head and tail as a whole, starts to rotate about the x-axis in the $(-\theta)$-direction. While the microorganism rotates clockwise, the viscous fluid will exert on it an additional counter torque. This effect of body rotation reduces the speed at which the waves travel relative to the environment, and in turn reduces both the propulsive thrust and the torque acting on the tail. Only until the creature reaches an induced angular velocity $\Omega (= 2\pi f_{ind}, f_{ind}$ being the induced angular frequency of the head and tail as a whole) at which the net torque and net force acting on the entire body both vanish identically does the motion become steady.

The resulting body motion in the Lab-system (i.e. in this same coordinate system (x, y, z) fixed with respect to the fluid at large distances) is clearly the one in which every cross-section of the tail rotates about the x-axis with an apparent angular velocity $\omega_{app} = \omega - \Omega$, in the θ-direction (counter-clockwise), whereas the head rotates (clockwise) about the x-axis with the induced angular velocity Ω, while the body as a whole moves along the x-axis with a velocity U, which in general may be different from U_o. Moreover, every cross-section of the tail, like the head, also rotates about its own center with angular velocity Ω (about a line parallel to the x-axis) in the

clockwise direction (see Fig. 6). Thus the motion of the central curve of the tail can be described as

$$\begin{aligned} &r = h \quad , \\ &\theta = kx + (\omega - \Omega)t \quad , \\ &\text{propulsion velocity:} \quad \frac{dx}{dt} = U \quad . \end{aligned} \tag{3.7}$$

The viscous torque resulted from the fluid reaction on an element of the cylindrical tail of radius b and arc length ds, which rotates about the tangent of its central curve (given by (3.7)) with angular velocity (clockwise) $\Omega_s = \Omega \cos\beta$, is given by (see, e.g. Lamb (1932), p. 588) $d\vec{M}_s = 4\pi\mu b^2 \Omega_s d\vec{s}$. The x-component of this torque is

$$dL_{tail} = \vec{e}_x \cdot d\vec{M}_s = dM_s \cos\beta = 4\pi\mu b^2 \Omega \cos\beta \, dx \quad , \tag{3.8}$$

whereas its circumferential component (in the θ-direction) yields zero resultant over a whole wavelength. The equilibrium conditions concerning the net force and torque now become

$$\int_{x=o}^{n\lambda} dF_x - F_{head} = \int_{x=o}^{n\lambda} (dF_n \sin\beta - dF_s \cos\beta) - F_{head} = F_x^{(e)} \quad , \tag{3.9}$$

$$\int_{x=o}^{n\lambda} (dM_x + dL_{tail}) + M_{head} = -h \int_{x=o}^{n\lambda} (dF_n \cos\beta + dF_s \sin\beta) + L_{tail} + M_{head} = M_x^{(e)} \quad , \tag{3.10}$$

where

$$dF_n = C_n (V_\theta \cos\beta - U \sin\beta) \sec\beta \, dx \quad , \tag{3.11}$$

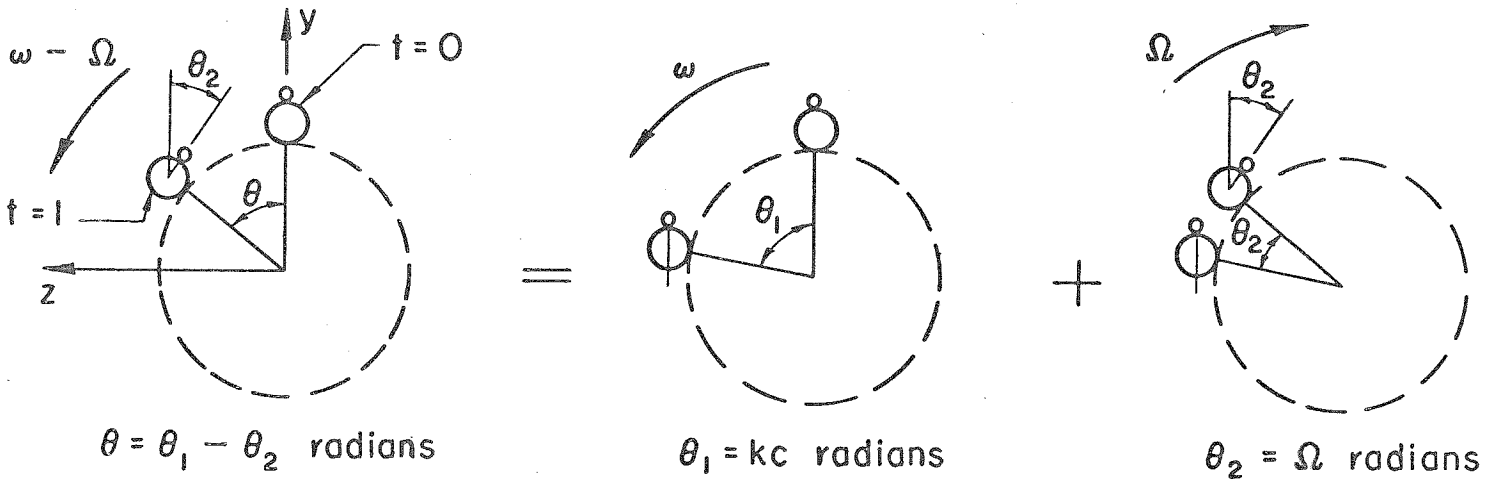

(a) Relative positions of a section of tail in unit time apart.

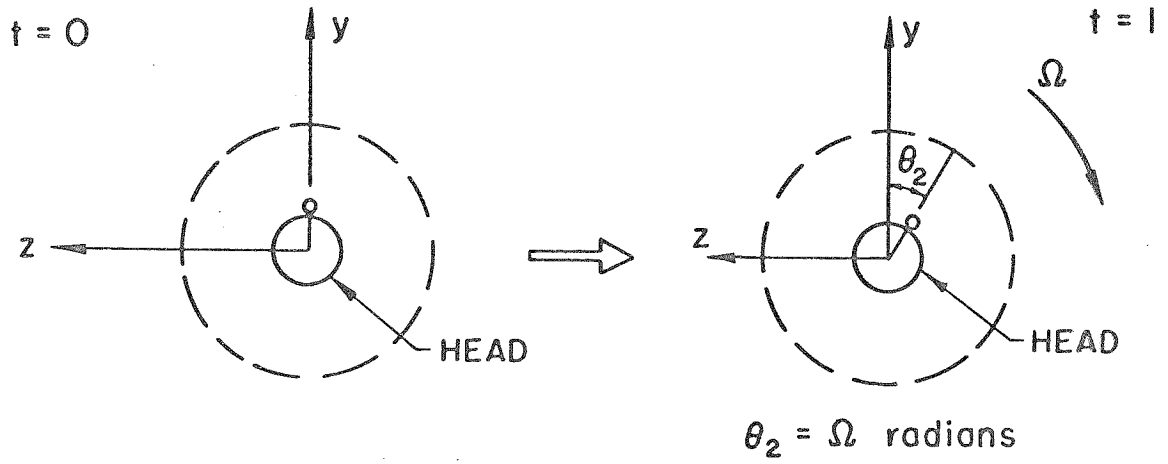

Fig. 6

(b) Relative positions of the head in unit time apart.

$$dF_s = C_s(V_\theta \sin\beta + U\cos\beta)\sec\beta\, dx \quad , \qquad (3.12)$$

$$V_\theta = h\frac{\partial\theta}{\partial t} = h\omega_{app} = h(\omega-\Omega) \quad , \qquad (3.13)$$

and $F_x^{(e)}$ denotes the extraneous thrust, and $M_x^{(e)}$ the extraneous torque, both being applied on the body by external agencies such as gravity or mechanical pull other than the fluid (whose contributions are already given by the left hands of (3.9), (3.10)). For self-propelling bodies at constant forward speed in the absence of external agencies, $F_x^{(e)} = 0$ and $M_x^{(e)} = 0$, Eqs. (3.9) and (3.10) then provide two basic equations to be solved for two unknowns, namely the propulsion velocity U and the induced angular velocity Ω. The force exerted on the head F_{head} by the viscous fluid is a function of U, $F_{head}=F_{head}(U)$ and the torque acting on the head is a function of Ω, $M_{head}=M_{head}(\Omega)$, explicit relations of which will be given later in Section 3.2. We note here that expressions (3.11), (3.12) for the forces exerted by the fluid are written according to the theory of Gray and Hancock (1955).

It may be noted that although every cross-section of the flagellum (or the tail) rotates about the x-axis with an apparent angular velocity $\omega_{app} = \omega - \Omega$ counter-clockwise, which is in general different from that of the head (Ω, clockwise), yet the tail (i.e. with its material substances) does <u>not</u> rotate as a whole relative to the head. This state of operation can be realized by sending a helical wave with only its wave <u>form</u> progressing distally with angular velocity ω relative to the head, without twisting the flagellum into a rope-like strand (as the latter situation would be a torture no creature could stand), as can also be seen from Fig. 6. To an observer in a moving frame of reference

which rotates about the x-axis with angular velocity Ω clockwise, the microorganism will appear to make helical waves exactly the same as in Fig. 5 and as described by Eq. (3.3), except that the propulsive mechanism is quite different since it is now affected by Ω. In the extreme case when $\omega = \Omega$, i.e. $\omega_{app} = 0$ (which will be shown later to correspond to the case of a very small head), the tail will cease to exhibit any bending waves (only in a stationary helical shape, although it rotates about its longitudinal axis with a frequency Ω clockwise), whilst its forward propulsion speed reduces to zero. The above argument roughly answers the question raised by Lord Rothschild (1961) "Can a spermatozoon roll about its longitudinal axis when its tail exhibits no bending waves?" It may further be noted that the effort made by a spermatozoon to roll without exhibiting bending waves is not in the form of a torsion, but a bending simultaneously in two perpendicular internal planes. This may sound paradoxical, but it is not.

From the preceeding consideration of the first principles we have seen that propagation of helical waves along a flagellum must be accompanied by a rotation of the head in a direction opposite to that of the angular phase velocity of the helical waves. The solution of Stokes' equations involving rotation of a body may be comprised of the 'doublets', 'Stokeslets', and 'rotlets' (Childress, 1964). Before leaving for the determination of the 'rotlet' and the torque exerted by a viscous fluid on the head, it may be pointed out that it may be desirable to improve the accuracy of (3.1) and (3.2) if higher accuracies are needed. For instance, the normal coefficient of quasi-steady resistance based on the Oseen equation, given by (see, e.g. Lamb (1932))

$$C_n = \frac{4\pi\mu}{\frac{1}{2} - \gamma + \log\left(\frac{4\mu}{\rho b V_n}\right)} \quad , \tag{3.1a}$$

can be tried out, where γ is the Euler's constant, $\gamma = 0.577 \ldots$, b is the radius of cylindrical tail, μ the coefficient of viscosity, and ρ the density of fluid. The tangential coefficient of resistance, again based on the quasi-steady assumption, was employed by Wu (1966) as

$$C_s = 4\pi\mu\left(\frac{1}{\beta_o} + \frac{2\gamma-1}{\beta_o^2}\right) \quad , \quad \beta_o \equiv \log\left(\frac{4\mu \cdot 1}{\rho b^2 V_s}\right) . \tag{3.2a}$$

3.2 The Rotlet and Torque

We summarize below the fundamental singular solutions of the Stokes' equations (Hancock (1953) and Childress (1964)). For an incompressible viscous fluid, the Stokes' equations are

$$\nabla \cdot \vec{u} = 0 \quad , \tag{3.14}$$

$$0 = -\nabla P + \mu \nabla^2 \vec{u} \quad , \tag{3.15}$$

where P is the pressure and $\vec{u} = u\vec{e}_x + v\vec{e}_y + w\vec{e}_z$ the velocity vector, $\vec{e}_x$, $\vec{e}_y$, $\vec{e}_z$ being unit vectors in x, y, and z directions, respectively. Taking the divergence of (3.15) and making use of (3.14) we have

$$\nabla^2 P = 0 \quad , \tag{3.16}$$

hence P is harmonic. For a 'Stokeslet' situated at the origin and oriented in the direction of an arbitrary vector $\vec{\alpha}$ with strength $\alpha = |\vec{\alpha}|$, the pressure assumes the value

$$P_s = 2\mu \frac{\vec{\alpha}\cdot\vec{R}}{R^3} \quad , \tag{3.17}$$

where $\vec{R} = x\vec{e}_x + y\vec{e}_y + z\vec{e}_z$, $R^2 = x^2 + y^2 + z^2$. Substituting (3.17) into (3.15), and integrating (3.15) together with (3.14), we obtain

$$\vec{u}_s = \frac{\vec{\alpha}}{R} + \frac{\vec{R}(\vec{\alpha}\cdot\vec{R})}{R^3} \quad . \tag{3.18}$$

The force given by the Stokeslet of strength $\vec{\alpha}$ is

$$\vec{F}_s = \int_s \sigma\cdot d\vec{S} = -8\pi\mu\,\vec{\alpha} \quad , \tag{3.19}$$

where $d\vec{S}$ is a surface element, σ is the stress tensor, given by $\sigma_{ij} = -P\delta_{ij} + \mu(\partial u_i/\partial x_j + \partial u_j/\partial x_i)$, δ_{ij} being the Kronecker delta. The above result can be shown by integration over the entire surface of the body represented by the above singular solution.

The pressure field of Stokes' flow is unchanged by superposition on the velocity of an irrotational component $\vec{u}_d$ which has a scalar potential ϕ,

$$\vec{u}_d = \nabla\phi \quad . \tag{3.20}$$

Taking the divergence of (3.20) gives

$$\nabla^2\phi = 0 \quad . \tag{3.21}$$

For a 'doublet' in the direction of arbitrary vector $\vec{\beta}$ with strength $\beta = |\vec{\beta}|$,

$$\phi = \frac{\vec{\beta}\cdot\vec{R}}{R^3} \quad . \tag{3.22}$$

By substituting (3.22) into (3.20), the velocity vector of the doublet is

$$\vec{u}_d = \frac{\vec{\beta}}{R^3} - \frac{3\vec{R}(\vec{\beta}\cdot\vec{R})}{R^5} \quad . \tag{3.23}$$

Doublets do not give any force.

To derive the third type singular solution, or the 'rotlet', we first note that the vorticity vector $\vec{\zeta} = \nabla \times \vec{u}$ satisfies automatically the equation

$$\nabla\cdot\vec{\zeta} = 0 \quad . \tag{3.24}$$

If P = constant, $\vec{\zeta}$ can be derived from a scalar potential, χ, $\vec{\zeta} = \nabla\chi$, since by (3.14) and (3.15)

$$\nabla \times \vec{\zeta} = \nabla \times (\nabla \times \vec{u}) = -\nabla^2\vec{u} = -\frac{1}{\mu}\nabla P = 0 \quad .$$

From (3.24) and $\vec{\zeta} = \nabla\chi$ it follows that $\nabla^2\chi = 0$. For a 'rotlet' in the direction of an arbitrary vector $\vec{\Omega}$ with strength $\Omega = |\vec{\Omega}|$,

$$\chi = 2\frac{\vec{\Omega}\cdot\vec{R}}{R^3} \quad , \tag{3.25}$$

hence

$$\vec{u}_r = \frac{1}{2}\vec{\zeta}\times\vec{R} = \left[\nabla\left(\frac{\vec{\Omega}\cdot\vec{R}}{R^3}\right)\right]\times\vec{R} = \frac{\vec{\Omega}\times\vec{R}}{R^3} \quad . \tag{3.26}$$

The torque applied on the body by a rotlet $\vec{\Omega}$ is found to be

$$\vec{M} = -\int_S \vec{R}\times(\sigma\cdot d\vec{S}) = -8\pi\mu\vec{\Omega} \quad . \tag{3.27}$$

In summary, Stokeslets give singular forces but no torque, rotlets give singular torques but no net force, whereas doublets generate neither. We now proceed to construct the solution to approximate the flow around the head by employing these three types of singular

solutions.

Suppose the head of the microorganism depicted in Fig. 5 is a sphere of radius a. It moves along the x-axis with a velocity of $U\vec{e}_x$ and rotates about the x-axis with an angular velocity $-\Omega\vec{e}_x$. At the instant when the center of sphere coincides with the origin $x = 0$, the instantaneous velocity field can be shown as

$$\vec{u} = \frac{(-a^3\Omega\vec{e}_x)\times\vec{R}}{R^3} + \frac{3aU}{4}\left[\frac{\vec{e}_x}{R} + \frac{\vec{R}(\vec{e}_x\cdot\vec{R})}{R^3}\right] + \frac{a^3U}{4}\left[\frac{\vec{e}_x}{R^3} - \frac{3\vec{R}(\vec{e}_x\cdot\vec{R})}{R^5}\right], \tag{3.28}$$

in which the strength of the rotlet, Stokeslet and doublet are determined to satisfy the no-slip condition at the spherical surface. Hence, by (3.27) and (3.28), the torque acting on the head is

$$\vec{M}_{head} = -8\pi\mu(-a^3\Omega\vec{e}_x) = 8\pi\mu a^3\Omega\vec{e}_x \quad . \tag{3.29}$$

The above result was given earlier by Lamb (1932). The force acting on the head is obtained from Eqs. (3.19) and (3.28)

$$\vec{F}_{head} = -8\pi\mu\left(\frac{3aU}{4}\vec{e}_x\right) = -6\pi\mu aU\vec{e}_x \tag{3.30}$$

which is the well-known Stokes' drag formula.

3.3 Propulsion Velocity U and Induced Angular Velocity Ω

We are now in position to give a complete account of the motion of a microorganism having a spherical head of radius a, propelling itself through a viscous fluid, with velocity U in the positive x direction, by propagating along its flagellum a helical wave of radial

amplitude h, wavelength λ, and phase velocity c. As a result of this movement, the head will rotate at an induced angular velocity Ω in the negative θ direction, and the movement of the flagellum is given by (3.7). The total number of helical waves along the tail is n (which need not be an integer) and the radius of the tail cross-section is b (see Fig. 7). Substituting (3.1), (3.6) and (3.13) into (3.11), we have

$$dF_n = 2C_s[(kc-\Omega)h - Ukh]dx \quad . \tag{3.31}$$

Similarly, from (3.6), (3.13) and (3.12),

$$dF_s = C_s[(kc-\Omega)kh^2 + U]dx \quad . \tag{3.32}$$

Upon substituting (3.29) - (3.32) in (3.9), (3.10), the force and torque balance conditions $F_x^{(e)} = 0$, $M_x^{(e)} = 0$, yield two simultaneous equations for two unknowns U and Ω,

$$(1 + 2\kappa^2 + A)U + \kappa\Omega h = \kappa^2 c \quad , \tag{3.33a}$$

$$\kappa U + (2 + \kappa^2 + B)\Omega h = \kappa(2 + \kappa^2)c \quad , \tag{3.33b}$$

where

$$\kappa = kh \quad , \quad A = \frac{3\mu\kappa}{nC_s}\left(\frac{a}{h}\right)(1+\kappa^2)^{\frac{1}{2}} \quad , \quad B = \frac{4\mu}{nC_s}\left[\pi n\left(\frac{b}{h}\right)^2 + \left(\frac{a}{h}\right)^3 \kappa(1+\kappa^2)^{\frac{1}{2}}\right] \quad , \tag{3.34}$$

C_s being the tangential force coefficient as given by (3.2), and n the number of wavelength along the tail. From (3.33) it readily follows that

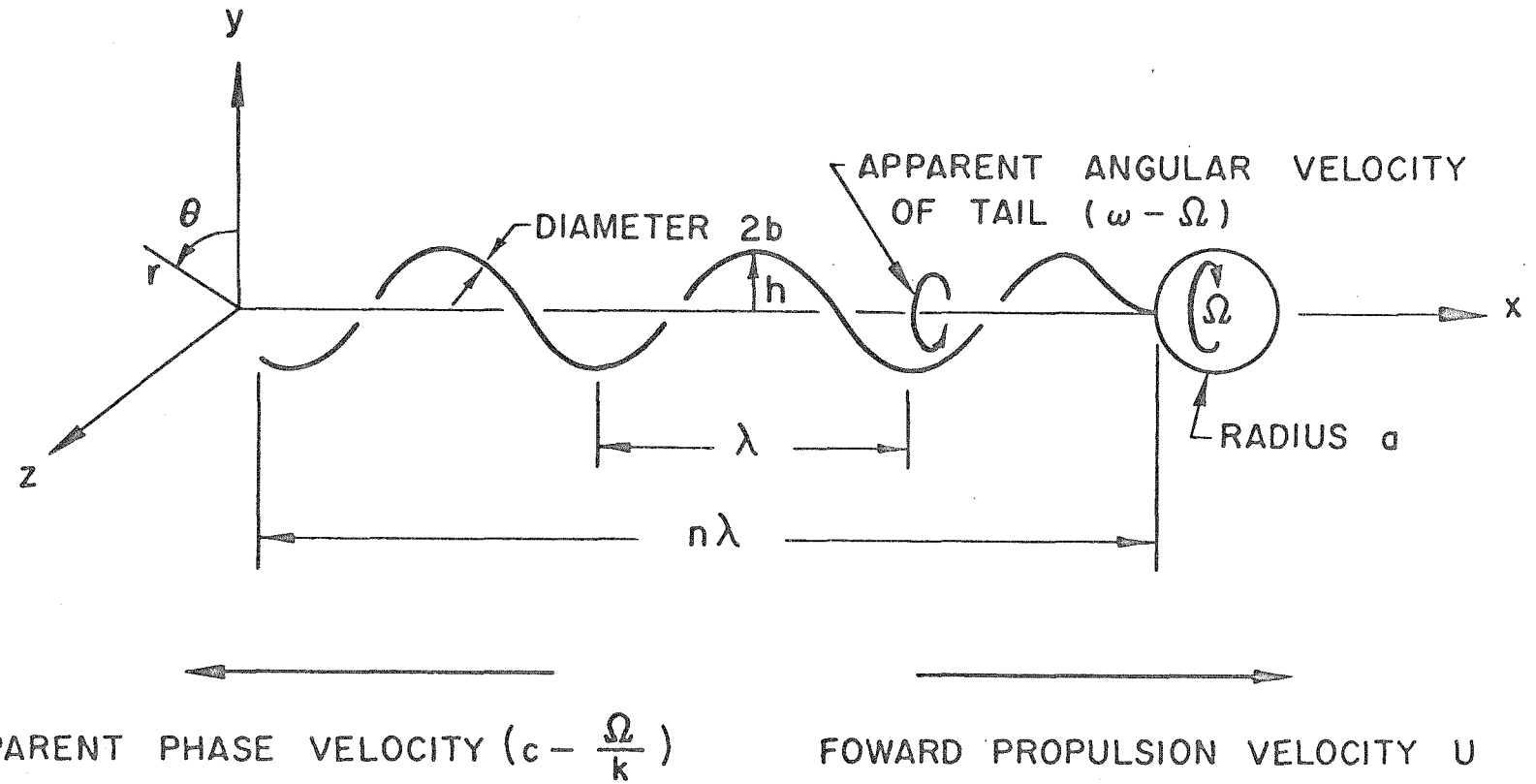

Fig. 7 Schematic diagram of the helical wave motion of a flagellated microorganism with a spherical head.

$$\frac{c}{U} = \frac{1+2\kappa^2+A}{\kappa^2}\left\{1 + \frac{2(1+\kappa^2)^2 + (2+\kappa^2)A}{(1+2\kappa^2+A)B}\right\} , \qquad (3.35)$$

$$\frac{\omega}{\Omega} = 1 + \frac{(1+2\kappa^2+A)B}{2(1+\kappa^2)^2 + (2+\kappa^2)A} \quad . \qquad (3.36)$$

From Eqs. (3.35) and (3.36) it is of interest to note the following result. When the radius of the head of a microorganism becomes negligible $(a \to 0)$, while the wave motion of tail is of such a significant amplitude that $\kappa = kh = O(1)$ and $b \ll h$, as is rather typical in natural environment, (3.34) indicates clearly that $B = O(b/h)^2$ whereas $A \simeq 0$. Consequently, by (3.35) and (3.36), the forward propulsion velocity, $U/c = O(b/h)^2$, will also be small, and the induced angular velocity Ω becomes nearly equal to the circular frequency, $\omega = kc$, of the helical wave. In this limit

$$\lim_{a/h,\, b/h \to 0} U = O(b/h)^2 \quad , \quad \lim_{a/h,\, b/h \to 0} \Omega = \omega \quad , \quad (\kappa = kh = O(1)) \ .$$

Thus, the apparent angular velocity $\omega_{app} = \omega - \Omega$ is practically zero. That is to say, to an observer in the fixed x, y, z space, the tail appears "motionless", thus indicating that all motions of this class tend to cease, and the organism becomes unable to propel itself by means of helical waves.

The above conclusion is at variance with that of Holwill and Burge (1963), and Holwill (1966). They claimed that when the radius, a, of the head, approaches zero, the forward propulsion velocity will approach to the value (in the present notation)

$$\frac{U}{c} = \frac{k^2 h^2}{1+2k^2 h^2} \quad ,$$

which is not correct. The error in Holwill's work is due to neglecting a correct consideration of the balance between the torque and the angular momentum. As indicated earlier in the present chapter, application of the Gray and Hancock (1955) method to helical wave motions must be accompanied by inclusion of 'rotlets' as a characteristic element of rotational movements. Note that the above equation for U/c is obtained from (3.33a) by substitution of $\Omega = 0$, but this result is not compatible with (3.33b) for real kh.

As was pointed out by Gray in his famous work (1953), the difference between planar and helical motions "lies in the fact that whereas the lateral components of all normal and tangential forces of a two-dimensional wave summate to zero; those of a helical wave yield couples tending to rotate the body in the opposite direction to that in which the elements are moving round the median axis of motion." "In freely swimming systems, however, some amount of spin is inevitable. Its effect is to reduce the effective speed at which the waves travel relative to the environment, and since the latter factor determines the magnitude of the propulsive thrust, the speed of progression must inevitably be less than when all spin is eliminated. If the frequency of spin were equal to the frequency of propagation of the waves down the body, the waves would remain stationary relative to the medium and no forward thrust would develop." Unfortunately, no successful mathematical analysis has appeared since then. This author hopes that the

present chapter will do its part in providing a theoretical basis for supporting Gray's statement.

3.4 The Optimum Head-Tail Ratio for Maximum Propulsion Velocity

We have just seen that the propulsion velocity U tends to $O(b/h)^2$ as the radius, a, of the head diminishes. The physical interpretation of this result is now clear because a microorganism which has no head to resist the rotation given rise by the viscous torque due to its tail wave motion simply cannot manifest helical waves. It therefore cannot propel itself by means of helical waves, although it may be possible for the organism to derive propulsion by plane waves along its tail. To the other extremity, as the radius a of the head becomes exceedingly large compared with both h and b, we note from (3.34) that $A = O(a/h)$, $B = O(a/h)^3$, assuming κ and n to be of $O(1)$. Consequently, by (3.35), (3.36)

$$\lim_{a/h,\, a/b \to \infty} U = 0 \quad , \qquad \text{and} \qquad \lim_{a/h,\, a/b \to \infty} \Omega = 0 \quad .$$

Physically this means that the head of the microorganism is, in this limit, too big to be propelled by its tail.

Between these two extremities, the numerical results reveal that the propulsion velocity U actually reaches a maximum at a certain value of a/b for each fixed set of values of κ, kb, and $\ell \equiv n\lambda/b$ (ℓ being the ratio of the total extension of the flagellum in the direction of propulsion to its radius). Generally ℓ is of order $O(100)$. The optimum head-tail ratio a/b can be determined numerically from the curve U/c versus a/b for given values of κ, kb, and

ℓ, as is demonstrated in Figs. 8 - 9 where ℓ is taken to be 156 as a typical value derived from experimental observations. For example, at $kb = 0.1$, $\kappa = kh = 1$, the optimum value of a/b is 21.4, and for $kb = 0.05$, $\kappa = 0.5$, it is 18.4. From these results the optimum a/b is further cross-plotted in Fig. 10 versus κ for several values of kb, alternately, h/b. It is noted that the optimum a/b increases gradually with the pitch $\kappa = kh$ of the helical wave at fixed h/b and increases more rapidly as the wave amplitude h increases for fixed pitch κ. As mentioned earlier, for a great variety of motions employed by microorganisms the pitch $\kappa = kh$ is generally of order O(1). In this neighborhood the present analysis indicates, as shown by Fig. 10, that the optimum head-tail ratio a/b lies in the range somewhere between 15 and 40 for $5 < h/b < 40$, the latter about covering the range actually observed. Although it would take further quantitative evaluations (such as of the speed of propulsion U, induced angular velocity Ω, and the hydromechanical efficiency, as well as their comparison with experimental observations) in order to ascertain whether most microorganisms may utilize this feature of the optimum head-tail ratio in achieving the speed U to their advantage, it is nevertheless more than a passing interest to note here that the above predicted values of optimum a/b are fairly well supported by observed data. For instance, the organism studied by Lowy and Spencer (1968, plate 6) has a head-tail ratio of about 25:1. Leifson (1960) gave excellent photographs of a number of different bacteria, showing that the head-tail ratios of these bacteria are generally of order O(10).

The ratio of the propulsion velocity to the wave phase velocity,

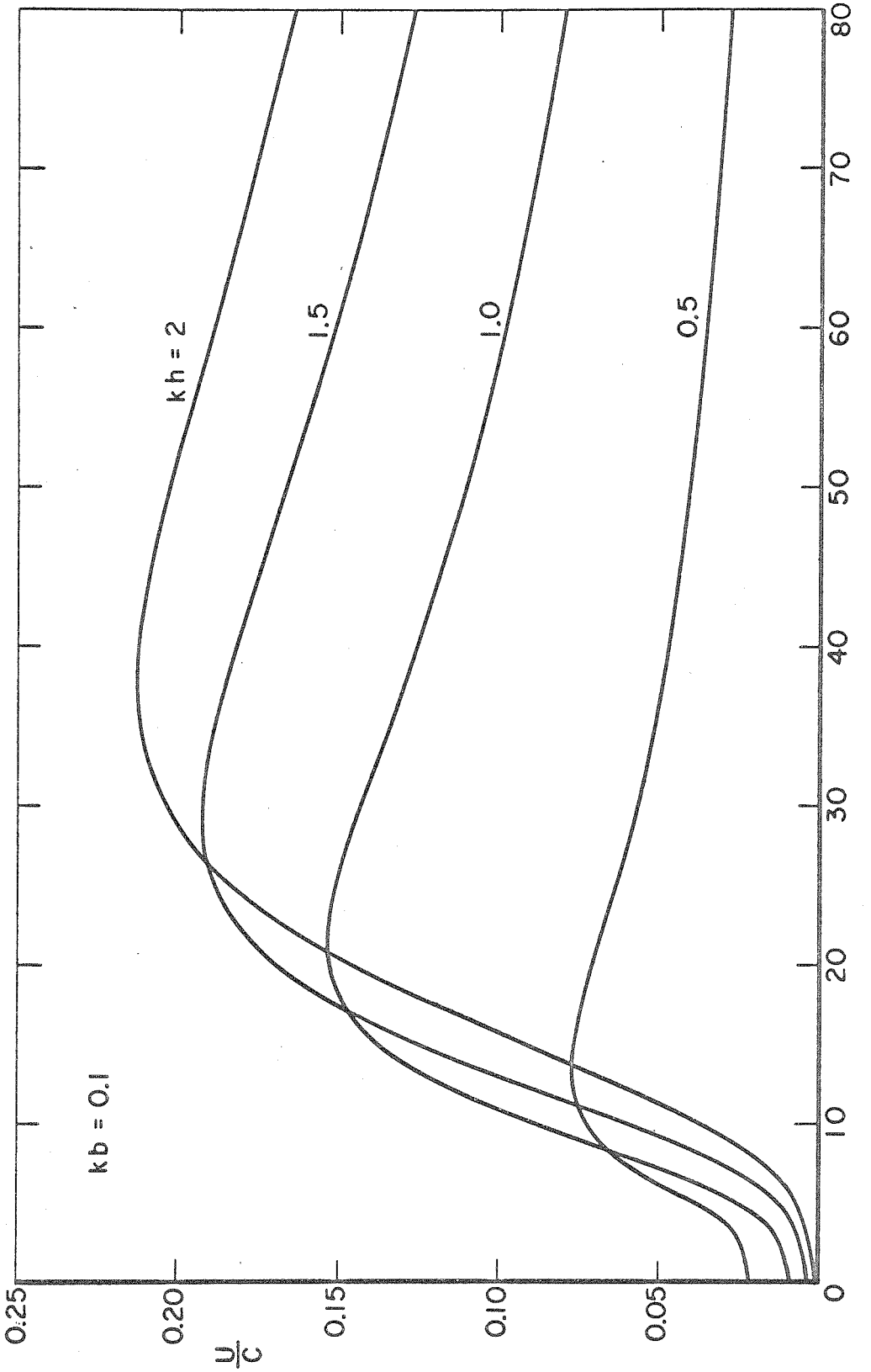

Fig. 8 Variation of propulsion velocity U with the head-tail ratio a/b at kb = 0.1.

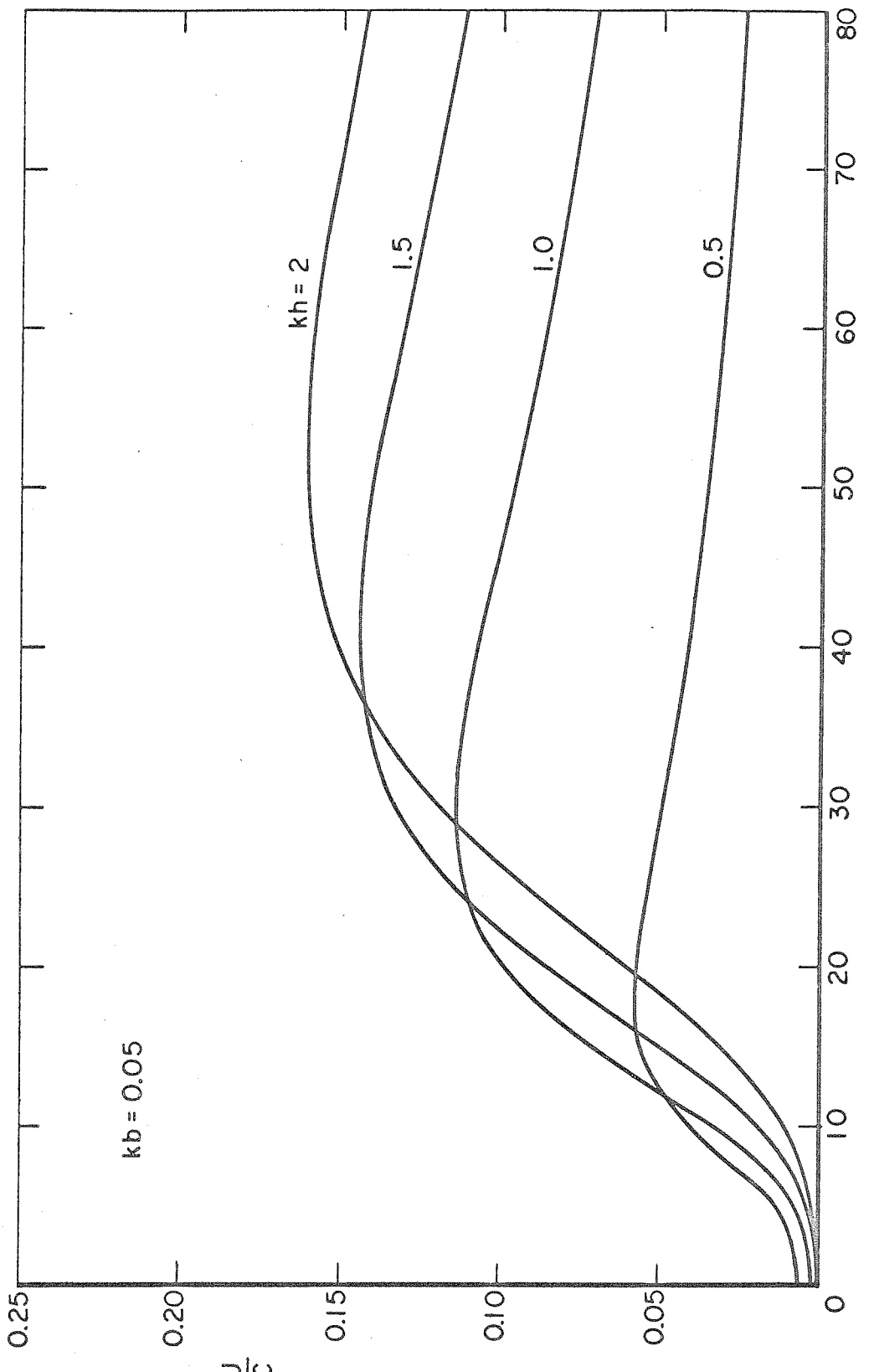

Fig. 9 Variation of propulsion velocity U with the head-tail ratio a/b at kb = 0.05.

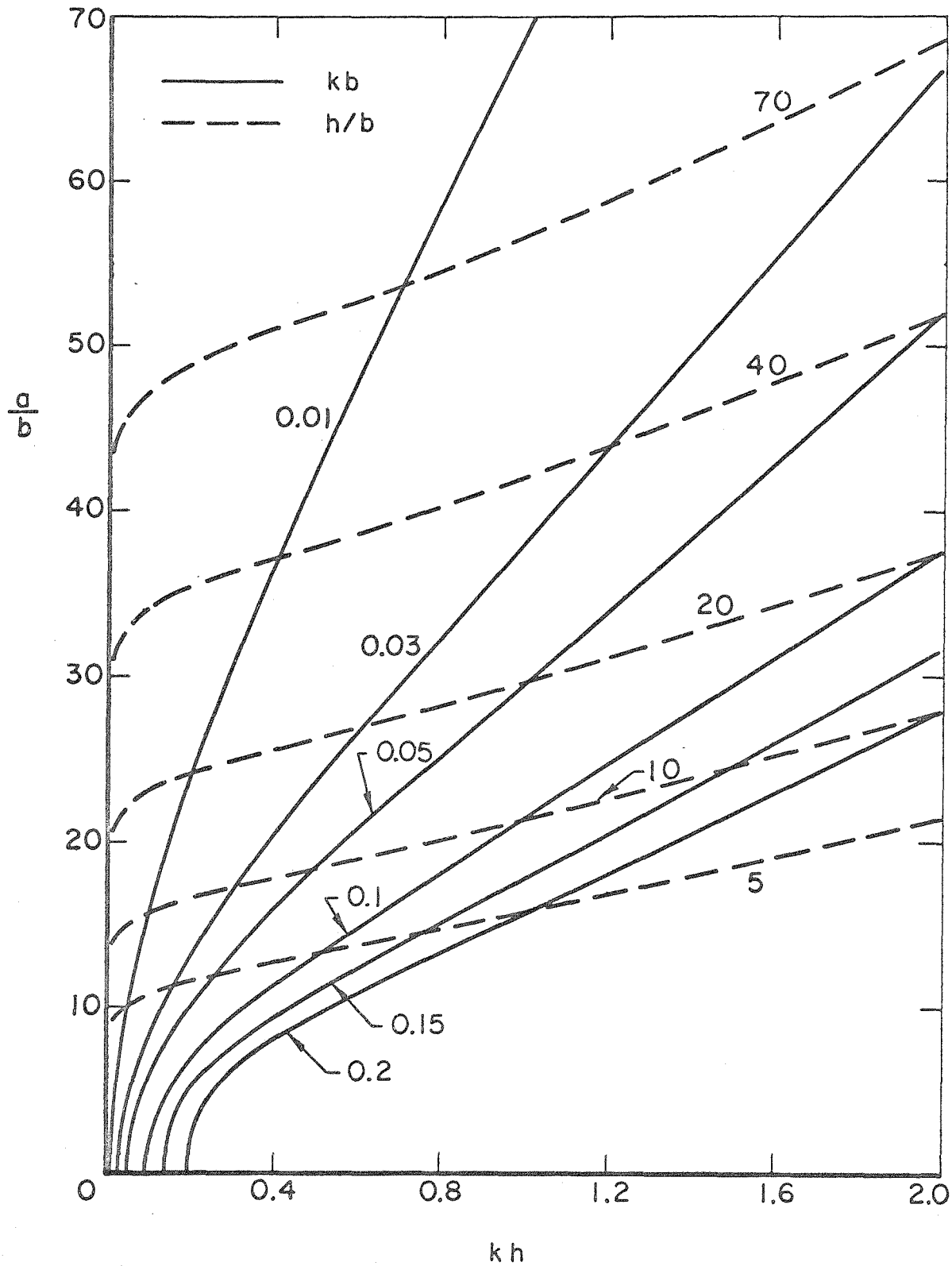

Fig. 10 Dependence of the optimum head-tail ratio on the wave pitch-ratio kh and kb.

U/c, of microorganisms having the optimum head-tail ratio is plotted versus the wave pitch $\kappa = kh$ in Fig. 11 for several fixed values of kb (again with $\ell = 156$). This optimum U/c increases with the pitch κ and with increasing kb. In the vicinity of $\kappa = 1$, U/c is seen to have a value between 0.09 at $kb = 0.03$ and 0.19 at $kb = 0.2$.

The ratio of the induced angular velocity Ω of the head to the wave circular frequency ω, again for microorganisms with the optimum head-tail ratio, is plotted versus κ in Fig. 12 for various kb. The result shows that Ω/ω increases with decreasing kb. For each fixed kb, however, it is of interest to note that Ω/ω reaches a maximum, at about $\kappa = 0.8$ for $kb < 0.1$. The significance of this maximum of Ω/ω is further enlightened by the following consideration of the hydromechanical efficiency.

3.5 Energy Consideration and Hydromechanical Efficiency

The power required to move the spherical head through the fluid with a forward velocity U and an angular velocity Ω is

$$P_{head} = F_{head}\, U + M_{head}\, \Omega = 6\pi\mu a U^2 + 8\pi\mu a^3 \Omega^2 \quad . \quad (3.37)$$

The power expended by the tail in propagating the helical wave distally is given by the time-rate of work done by the force exerted by the tail element, with the x-component $-dF_x$ and θ-component $-dF_\theta$ (the negative signs signifying the reaction to the force acted by the fluid on the tail), plus the time-rate of work done by the torque associated with the tail rotation about its centroid, or

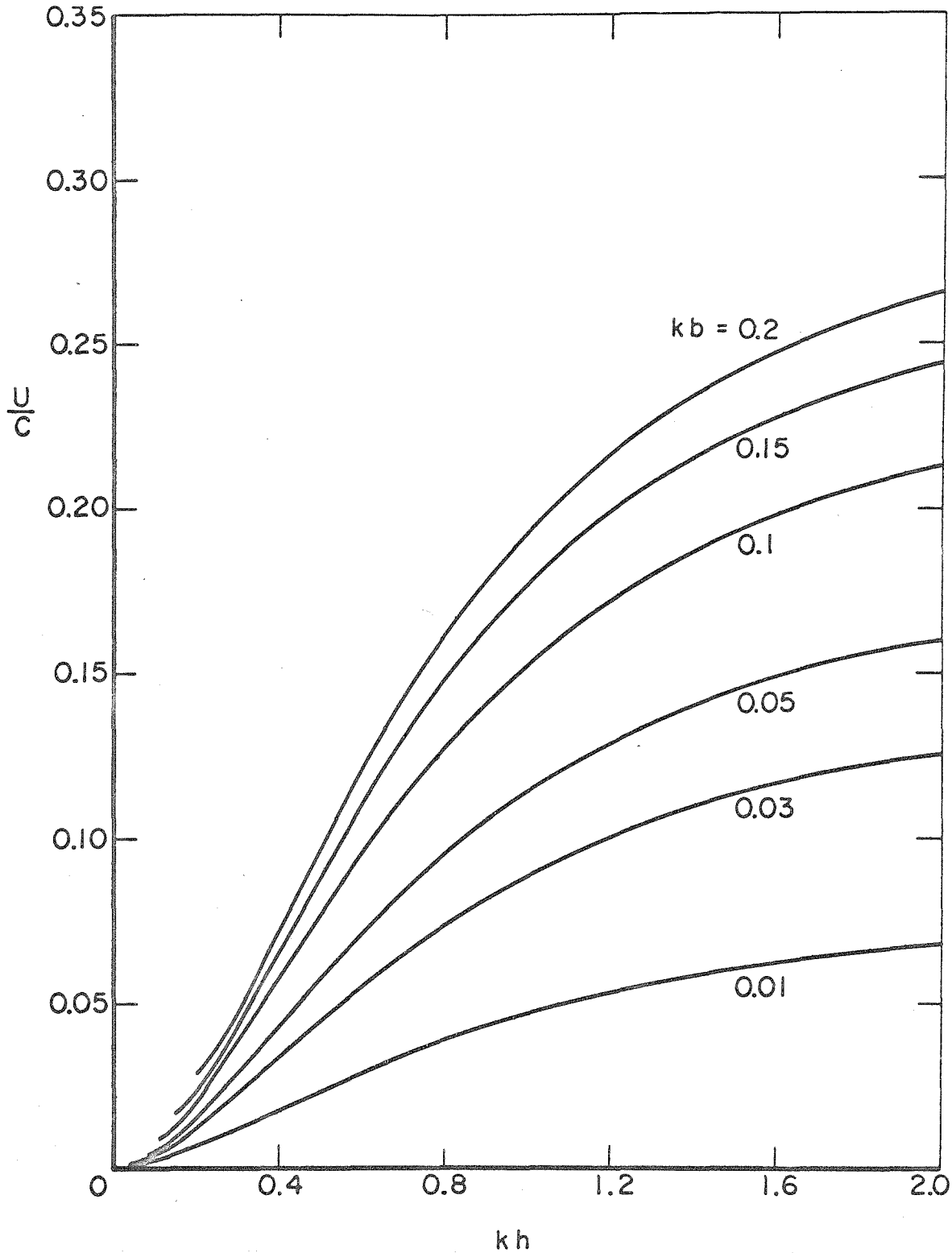

Fig. 11 The propulsion velocity of a microorganism with the optimum head-tail ratio.

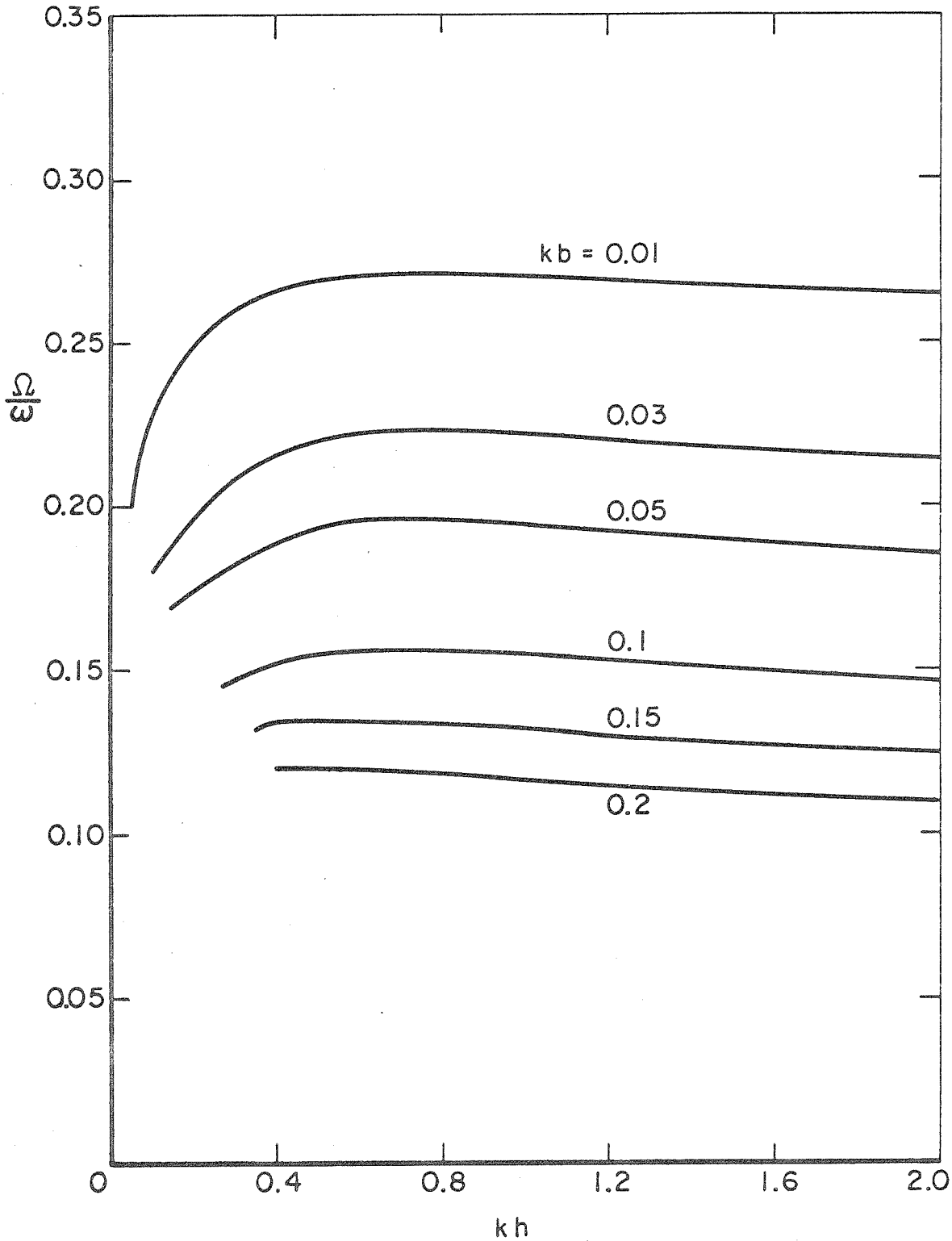

Fig. 12 The induced angular velocity Ω of the body of a microorganism with the optimum head-tail ratio.

$$P_{tail} = \int_{x=o}^{n\lambda} [\, -U dF_x - V_\theta dF_\theta + \Omega_s dM_s]$$

$$= \int_{x=o}^{n\lambda} [\, -U dF_x - (\omega-\Omega) dM_x + \Omega\, dL_{tail}]$$

$$= - U F_{head} + (\omega-\Omega)[\, M_{head} + L_{tail}] + \Omega\, L_{tail} \quad . \qquad (3.38)$$

In the second step above, use has been made of (3.5), (3.8), (3.13), and in the last step the force and torque balance conditions (3.9) and (3.10)(again with $F_x^{(e)}$, $M_x^{(e)} = 0$) have been applied*. The total power expended in propelling the microorganism by means of helical waves is therefore the sum of P_{head} and P_{tail}, giving

$$P = \omega[\, M_{head} + L_{tail}] = 4\pi\mu\omega\Omega[\, 2a^3 + b^2 n\lambda \cos\beta\,] \quad . \qquad (3.39)$$

We shall define the hydromechanical efficiency η as the ratio of the power required for propelling the head alone to the total power expended in manifesting the whole motion,

$$\eta = \frac{P_{head}}{P} = \left(\frac{\Omega}{\omega}\right)\left[\, 1 + \frac{3}{4}\left(\frac{U}{a\Omega}\right)^2 \right] \Big/ \left[\, 1 + \frac{\ell}{2}\left(\frac{b}{a}\right)^3 (1+\kappa^2)^{-\frac{1}{2}} \right] \quad . \qquad (3.40)$$

This expression is general, whether or not the head-tail ratio is optimum. For the microorganisms with the optimum a/b, however, the two factors in square bracket of (3.40) are nearly equal to unity

---

*Equation (3.38) may also be stated as

$$P_{tail} = \int (C_n V_n^2 + C_s V_s^2)\, ds + P_{\text{rotation of flagellum}}$$

The detailed manipulation, however, is simpler by following the steps of (3.38).

within the range of κ and ℓ of practical interest and $kb \ll 1$ so that

$$\eta_{op} \simeq \Omega/\omega \quad . \tag{3.41}$$

The accuracy of this approximation is well substantiated by the numerical result of η computed from (3.40) for the case of optimum a/b, as shown in Fig. 13. For fixed kb, the hydromechanical efficiency η attains a maximum at about $\kappa = 0.9$ throughout the range of kb covered, $0.01 < kb < 0.2$. In fact, η_{max} increases from 0.14 at $kb = 0.2$ to about 0.28 at $kb = 0.01$. It is now clear that locomotion of microorganisms by means of helical waves can be made most efficiently by keeping kh around 0.9, the resulting motion being characterized by the state that the head is induced to rotate at a maximum rate with respect to the wave frequency ω. In view of the significance of this result, it is perhaps not altogether coincidental that most microorganisms do have their kh values about 1, as found in experimental observations.

Finally, we remark here as to how the present result based on the consideration of optimum performance can be utilized to predict the specific helical motion. Suppose a microorganism is given with known a and b. This value of a/b and $kh = 0.9$ determine, by Fig. 10, the value of kb, and hence also h/b, h/a, and therefore the wave amplitude h. The wavelength follows from $\lambda = 2\pi/k \simeq 2\pi h$. The values of U/c, Ω/ω, and efficiency η can be read from Figs. 11 - 13. However, separate determination of U and Ω will require the knowledge of the wave frequency ω, or the wave velocity $c = \omega/k$, which may be either observed experimentally or evaluated when a

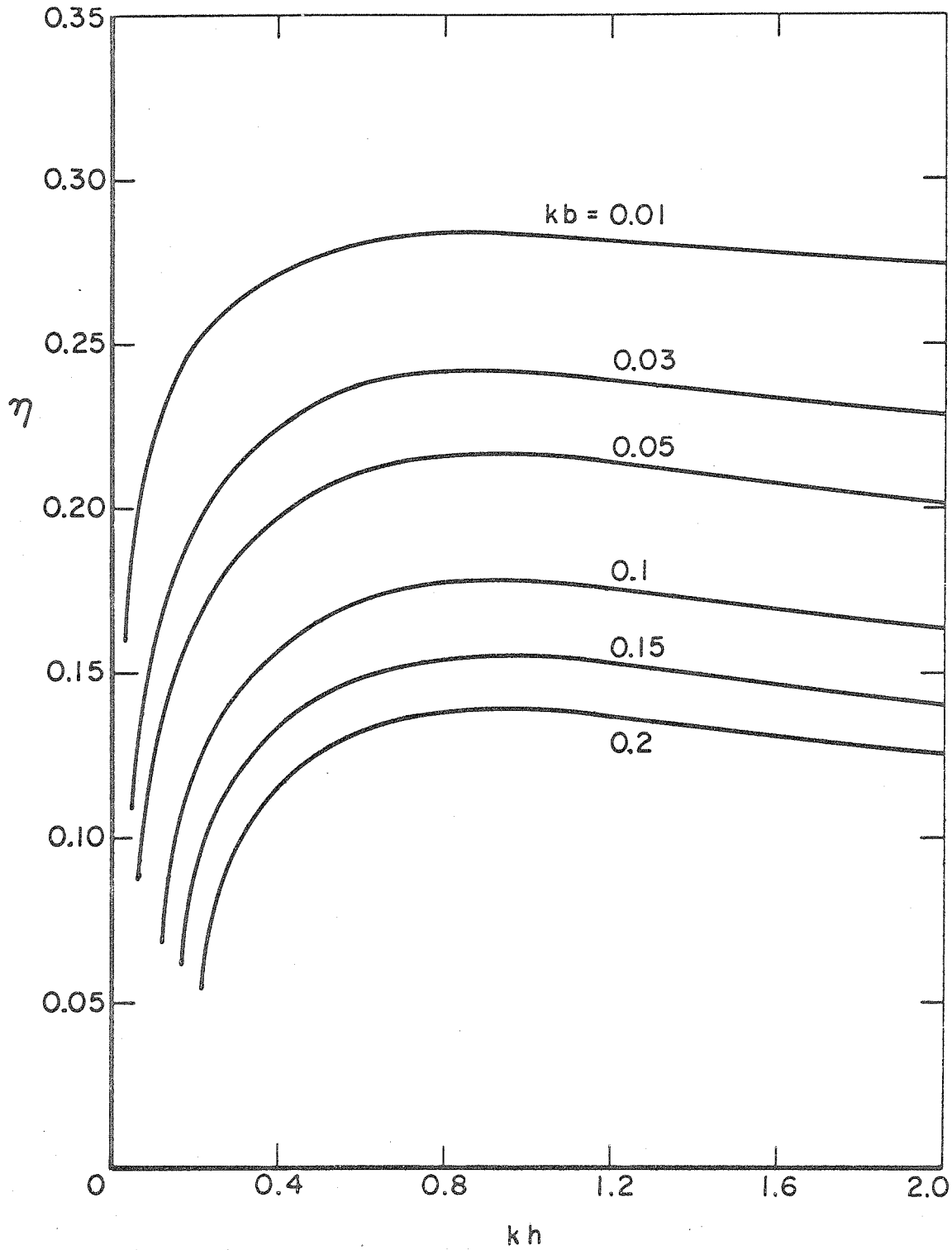

Fig. 13 The hydromechanical efficiency η for microorganisms with the optimum head-tail ratio.

bio-chemical estimate can be obtained of the energy available for delivering the tail power P_{tail}.

3.6 The Spirochete paradox

From the analysis given in the previous sections of this chapter, we have seen that for a microorganism to propel itself by manifesting helical waves, it must have some means to balance the viscous torque due to its tail wave motion. One possible way is for the microorganism to have an inertial head or body to resist the viscous torque, and by far it is the most general way. In particular, when the radius-amplitude ratio b/h approaches to zero, it is the only way as explained in Section 3.3. However, for arbitrary values of b/h, there is another possibility, namely with some amount of spin of the tail; a microorganism can still propel itself by propagating helical waves along it in this manner. One example of this type of microorganism is spirochete. In the past, scientists have been puzzled by the locomotion of spirochetes. How could a spirochete propel itself by helical waves without a head to balance the torque? Some biologists even suggested that it is not necessary for a spirochete to balance the torque provided that the torque is small (Jahn and Landman, 1965). However, this author believes that we should not, and we do not have to, give up the first principles in order to resolve this "Spirochete Paradox." In fact, the answer to this paradox is contained in Eqs. (3.34) - (3.36).

When the head vanishes (a = 0), (3.34) yields

$$A = 0 \qquad \text{and} \qquad B = \frac{4\pi\mu}{C_s}\left(\frac{b}{h}\right)^2 \quad . \tag{3.42}$$

Substituting (3.42) into (3.35) and (3.36), we have

$$\frac{U}{c} = \frac{B\kappa^2}{(1+2\kappa^2)B+2(1+\kappa^2)^2} \quad , \tag{3.43}$$

$$\frac{\Omega}{\omega} = \frac{2(1+\kappa^2)^2}{(1+2\kappa^2)B+2(1+\kappa^2)^2} \quad . \tag{3.44}$$

The value of U/c given by (3.43) is plotted in Fig. 14 versus $\kappa = kh$ for several values of the radius-amplitude ratio b/h, changing from 0 to 1. From Fig. 14, one further observes that the propulsion velocity increases with increasing b/h for fixed kh, and for fixed b/h it attains a maximum about $kh = 1$. Therefore a spirochete should keep its amplitude-wavelength ratio h/λ around 1:6($h/\lambda = kh/2\pi \approx 1/6$) in order to achieve a maximum propulsion velocity. By measuring the photographs given in Jahn and Landman (1965), we find that the amplitude-wavelength ratio h/λ for spirochetes is indeed 1:6. Thus, the value of $kh = 1$ is very significant, and it is a characteristic of all microorganisms employing helical waves whether the microorganism has an inertial head or not.

The ratio of the induced angular velocity Ω to the phase angular velocity ω is plotted in Fig. 15 versus the kh value for b/h between zero and one. This ratio Ω/ω increases as kh increases for fixed values of b/h. For fixed kh, Ω/ω increases as b/h decreases, and it becomes unity when b/h vanishes. At $kh = 1$, Ω/ω varies from 0.4 to 1 as b/h decreases from 1 to 0.

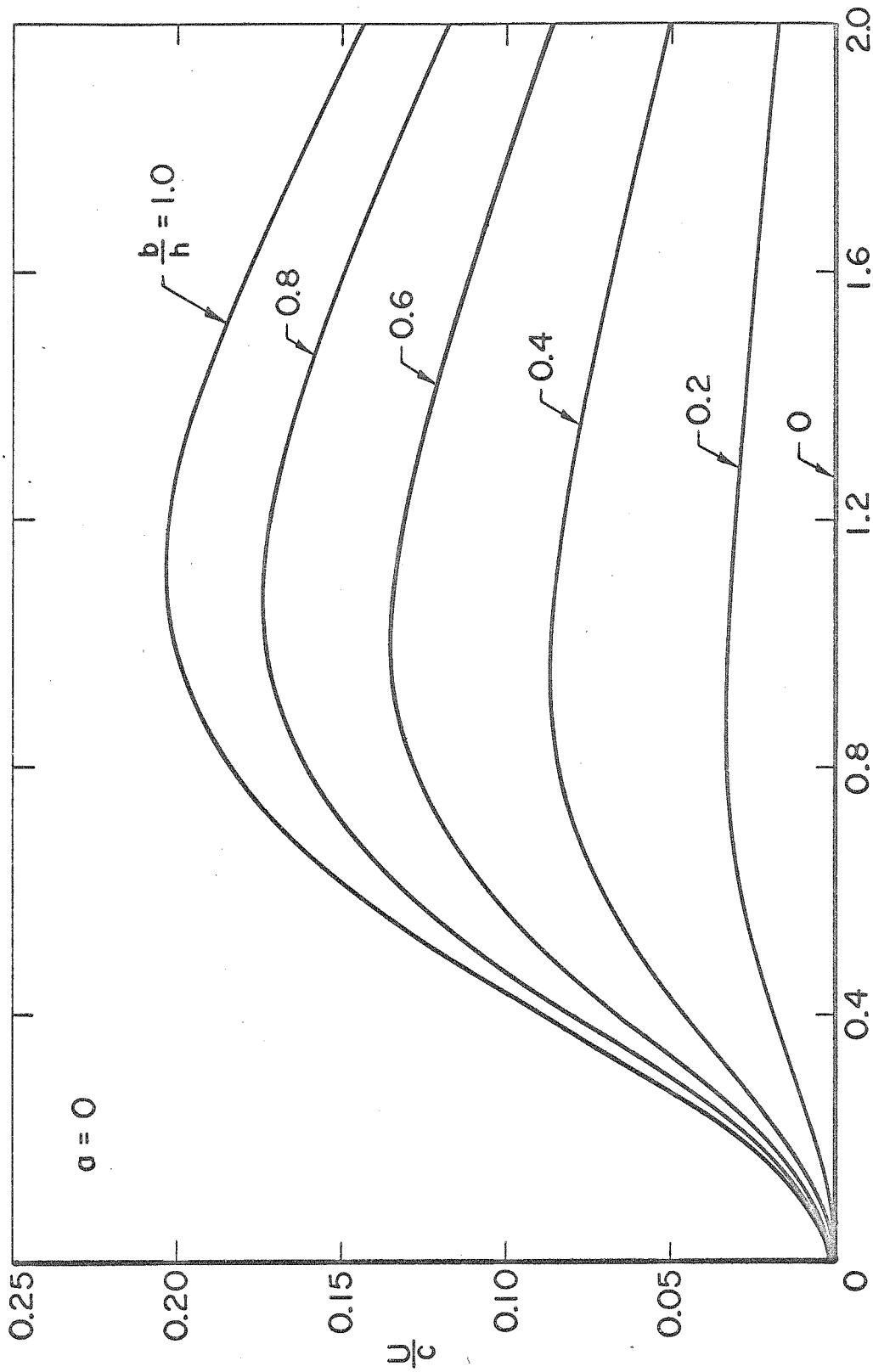

Fig. 14 Variation of propulsion velocity U with the wave pitch-ratio kh at a = 0.

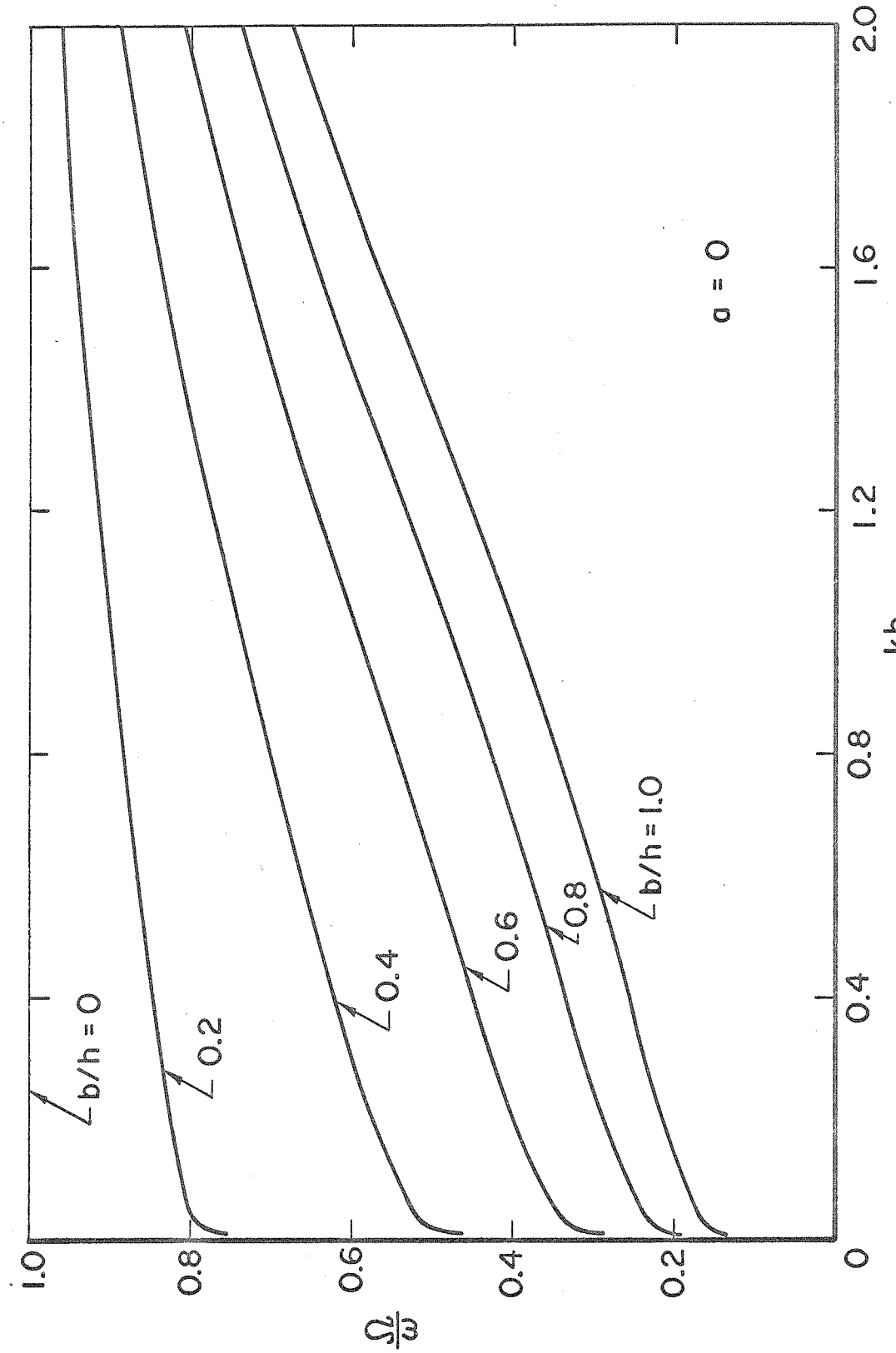

Fig. 15 Dependence of the induced angular velocity Ω on the wave pitch-ratio kh at a = 0.

IV. EXPERIMENTS ON THE NEIGHBORING EFFECT AND END EFFECT

4.1 The neighboring effect and end effect

It should be noted that the two approximate formulae (3.1) and (3.2) given by Gray and Hancock (1955) do not show dependence on the total number of waves n and the amplitude-wavelength ratio $kh = 2\pi h/\lambda$. Thus, two very important effects, namely the 'neighboring' effect and 'end' effect, have not been considered. By the 'neighboring' effect we mean the interaction between neighboring waves, which may be significant when kh is large. The force acted on an element of the body by the surrounding fluid is certainly influenced by the presence of elements in neighboring waves. The closer the neighboring waves (i.e. the larger the kh), the greater will be the neighboring effect. In the limit as kh tends to zero, the neighboring effect vanishes. The 'end' effect provides a measure of the difference between the flow near the flagellum produced by an infinitely long flagellum and that by a finite one. This effect of course decreases with increasing length of the flagellum. Furthermore, there is the 'wall' effect arising from the proximity of solid boundaries containing the fluid. Compared with the former two effects, the wall effect is usually less significant since microscopic organisms generally occupy a very small space in the surrounding fluid. That the end effect and neighboring effect may be significant is because of the known fact that an obstacle moving through a viscous fluid at a small Reynolds number drags along a large bulk of fluid with it.

A series of experiments have been carried out to determine the relative importance of these two effects and efforts have been made to estimate the accuracy of formulae (3.1) and (3.2) by taking these effects into account. The results are presented in the following sections.

4.2 Experimental procedures

In the experiments, enamel wires which are bent into uniform helices with various amplitudes and wavelengths are dropped down vertically into a cylindrical tank filled with glycerine. Four different sizes of enamel wires (No. 24, 26, 28 and 30) are used in these experiments, and the corresponding radii b are 0.25527 mm, 0.20244 mm, 0.16053 mm and 0.12738 mm respectively. The amplitudes h of the helices range from 0.242 cm to 0.734 cm and the wavelengths λ vary from 0.5 cm to 2 cm.

The cylindrical tank of 3/16 inch in wall thickness is 16 inches in outside diameter and 60 inches long (see Fig. 16). It has two rectangular observation windows, each of which is 6 inches wide and 30 inches long, opposite to each other on the side wall. The total weight of the tank with glycerine in it is supported by three legs welded to the lower end of the tank.

The density ρ of glycerine used in these experiments is 1.246 gm/cm^3, and its viscosity μ is listed in Table 1.

After the helical wire was released in glycerine, it moved steadily down the cylindrical tank and soon reached the terminal velocity under gravity, the only extraneous force. Two sets of data, namely

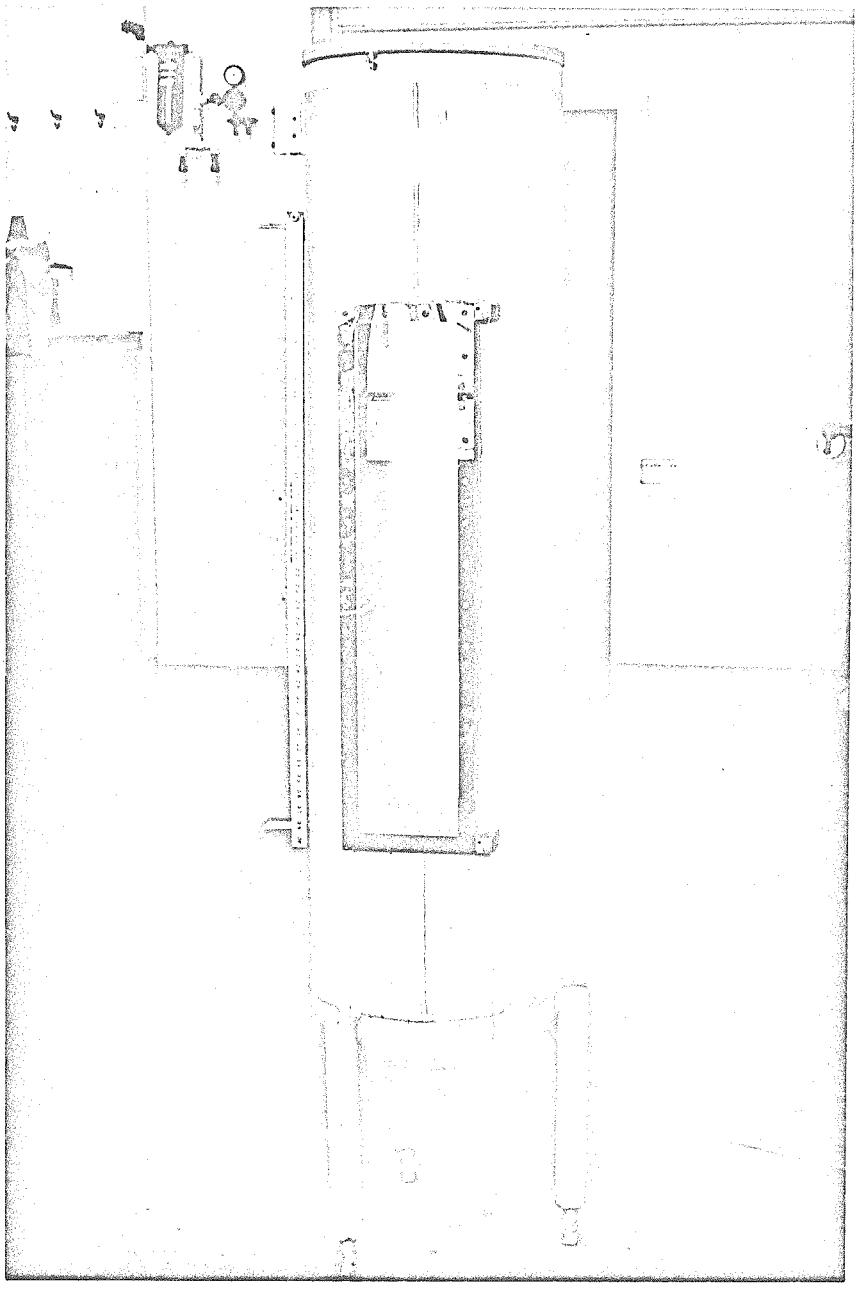

Fig. 16

TABLE I

Viscosity μ of glycerine with density $\rho = 1.246$ gm/cm^3

Temp., °C	Viscosity, poise	Temp., °C	Viscosity, poise
22.0	3.9810	23.5	3.5340
22.1	3.9512	23.6	3.5042
22.2	3.9214	23.7	3.4744
22.3	3.8916	23.8	3.4446
22.4	3.8618	23.9	3.4148
22.5	3.8320	24.0	3.3850
22.6	3.8022	24.1	3.3552
22.7	3.7724	24.2	3.3254
22.8	3.7426	24.3	3.2956
22.9	3.7128	24.4	3.2658
23.0	3.6830	24.5	3.2360
23.1	3.6532	24.6	3.2062
23.2	3.6234	24.7	3.1764
23.3	3.5936	24.8	3.1466
23.4	3.5638	24.9	3.1168

---

the propulsion velocity U and the angular velocity ω of the wire, were measured simultaneously. The measurements of the propulsion velocity U were accomplished by using a stop-watch to record the time spent for the helical wire to travel a given distance. The observation was made through the side observation window. In the mean time, the angular velocity ω was measured by observing from the top of

the cylindrical tank the rotational rate of the helical wire. The measured data were then compared with the theoretically predicted ones. To find the theoretical propulsion velocity U and angular velocity ω, we apply the basic equations (3.1), (3.2) and (3.8). By deleting the head and including the gravity as the sole external force, the equilibrium conditions (3.9) and (3.10) concerning the net force and torque on the rigid helical wire become

$$(1 + 2\kappa^2)U - \kappa\omega h = W(1 + \kappa^2)/C_s \quad , \tag{4.1}$$

$$\kappa U - \left[2 + \kappa^2 + \frac{4\pi\mu}{C_s}\left(\frac{b}{h}\right)^2\right]\omega h = 0 \quad , \tag{4.2}$$

where $\kappa = kh$, C_s is the tangential force coefficient as given by (3.2), and W is the net weight per unit length of the helical wire in glycerine, which is the same as the difference between the weight and the buoyant force per unit length of the wire. For No. 24, 26, 28 and 30 enamel wires in glycerine of density $\rho = 1.246$ gm/cm^3, W is 15.3368, 9.6461, 6.0659 and 3.8141 dynes/cm respectively. The presence of the last term on the left hand side of Eq. (4.2) is due to the fact that the wire is rigid. The motion of a rigid wire is equivalent to the motion of a living flagellum plus that due to a spin of the flagellum (see Fig. 17).

From (4.1) and (4.2) the theoretical propulsion velocity U and angular velocity ω are found to be

$$U_{th} = \frac{W(1+\kappa^2)\left[2+\kappa^2 + \frac{4\pi\mu}{C_s}\left(\frac{b}{h}\right)^2\right]}{2C_s(1+\kappa^2)^2 + 4\pi\mu\left(\frac{b}{h}\right)^2(1+2\kappa^2)} \quad , \tag{4.3}$$

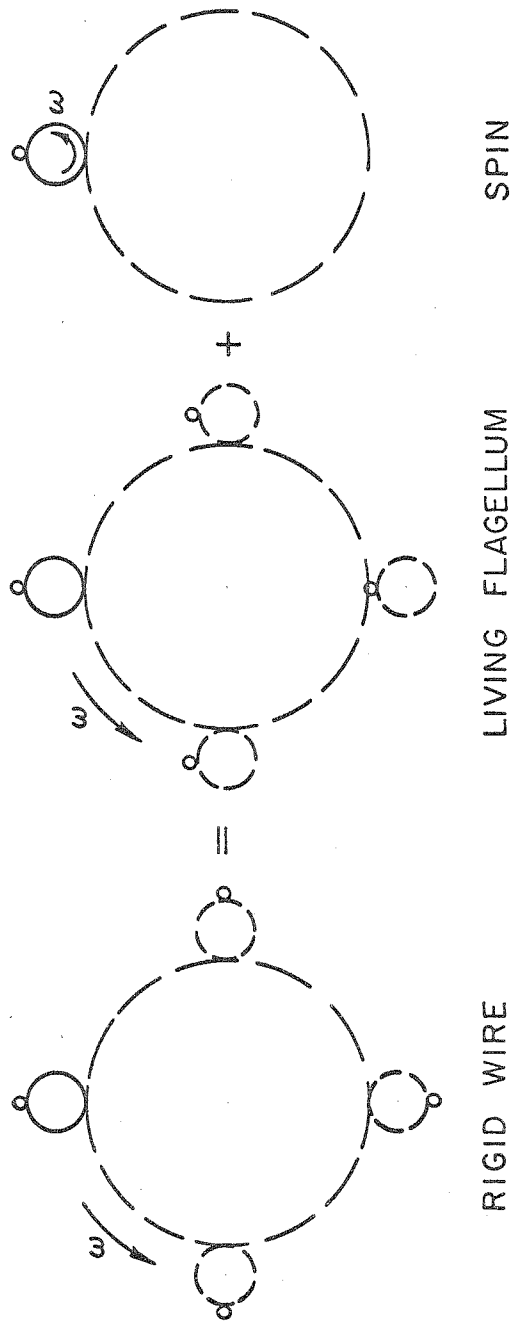

Fig. 17 The motion of a cross-section of a rigid helical wire.

$$\omega_{th} = \frac{kW(1+\kappa^2)}{2C_s(1+\kappa^2)^2 + 4\pi\mu\left(\frac{b}{h}\right)^2(1+2\kappa^2)} \quad . \qquad (4.4)$$

4.3 Data analysis

Let α_U be the ratio of the measured propulsion velocity U to the theoretical propulsion velocity U_{th} and α_ω be the ratio of the measured angular velocity ω to the theoretical counterpart ω_{th}. U_{th} and ω_{th} are given by (4.3) and (4.4) respectively. From the experiments, it is found that α_U and α_ω depend upon three parameters, namely kb, kh and n. In Fig. 18 and Fig. 19, α_U and α_ω are plotted versus the number of waves, n, for kb = 0.067 and kh = 0.98, 1.0, 1.4, 1.5, 2.3 and 3.1. From Fig. 18, we notice that for fixed values of kb and kh, α_U increases with the increase of n and it asymptotes to a certain value, which is different for different kb and kh, as n becomes very large. This is due to the fact that the end effect diminishes fairly rapidly with increasing length of the wire. For fixed kb and n, α_U increases as kh increases, which reflects the importance of the neighboring effect in the case when kh is fairly large. The influence of the neighboring effect on the angular velocity ω is shown in Fig. 19 in which we can see clearly that an increase of kh value is accompanied by an increase in α_ω for fixed kb and n. However, the end effect plays a less important role in affecting the angular velocity ω than its effect on the propulsion velocity U, for the experiments show that α_ω is relatively insensitive to the change of n. Comparing Fig. 18 with

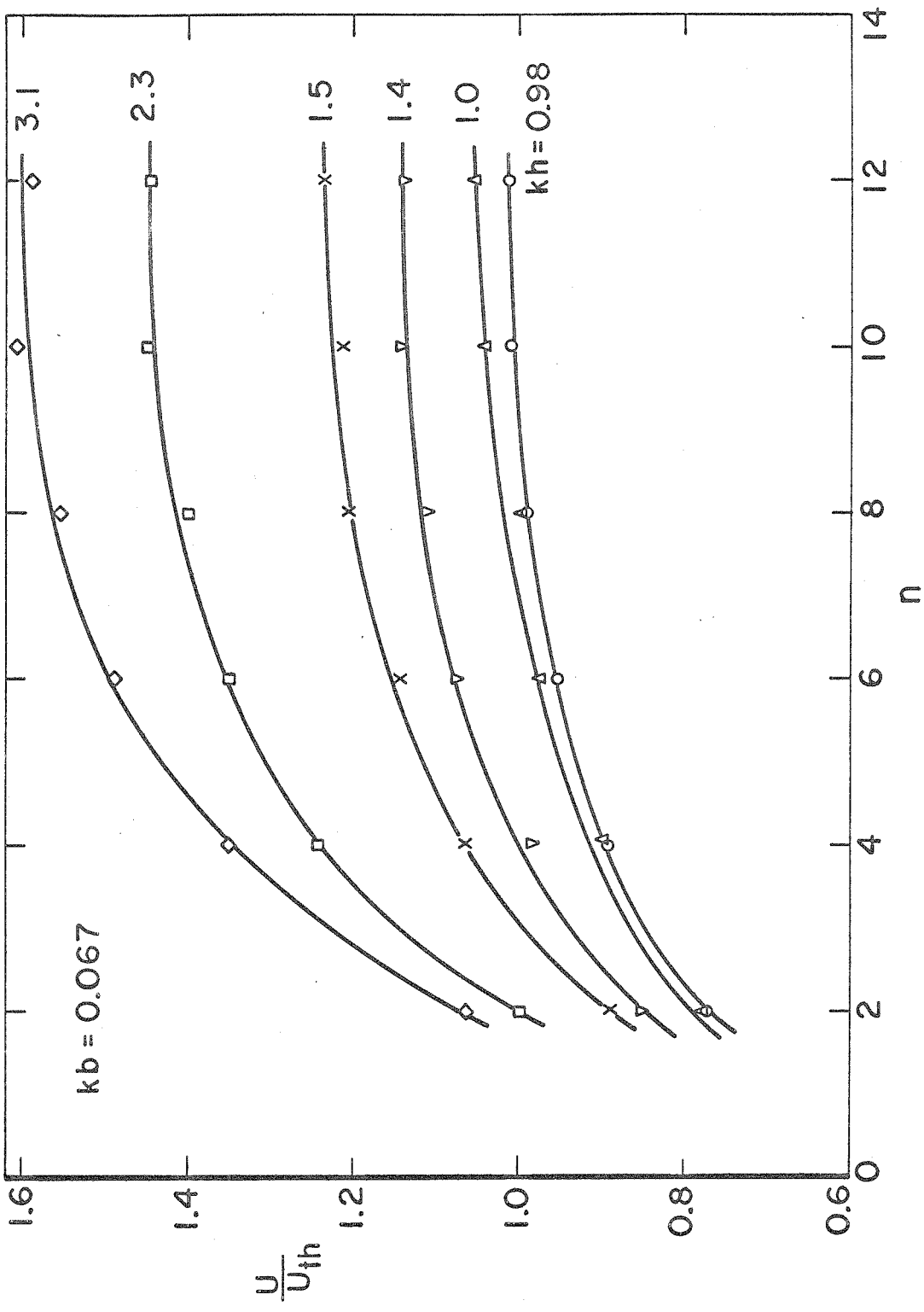

Fig. 18

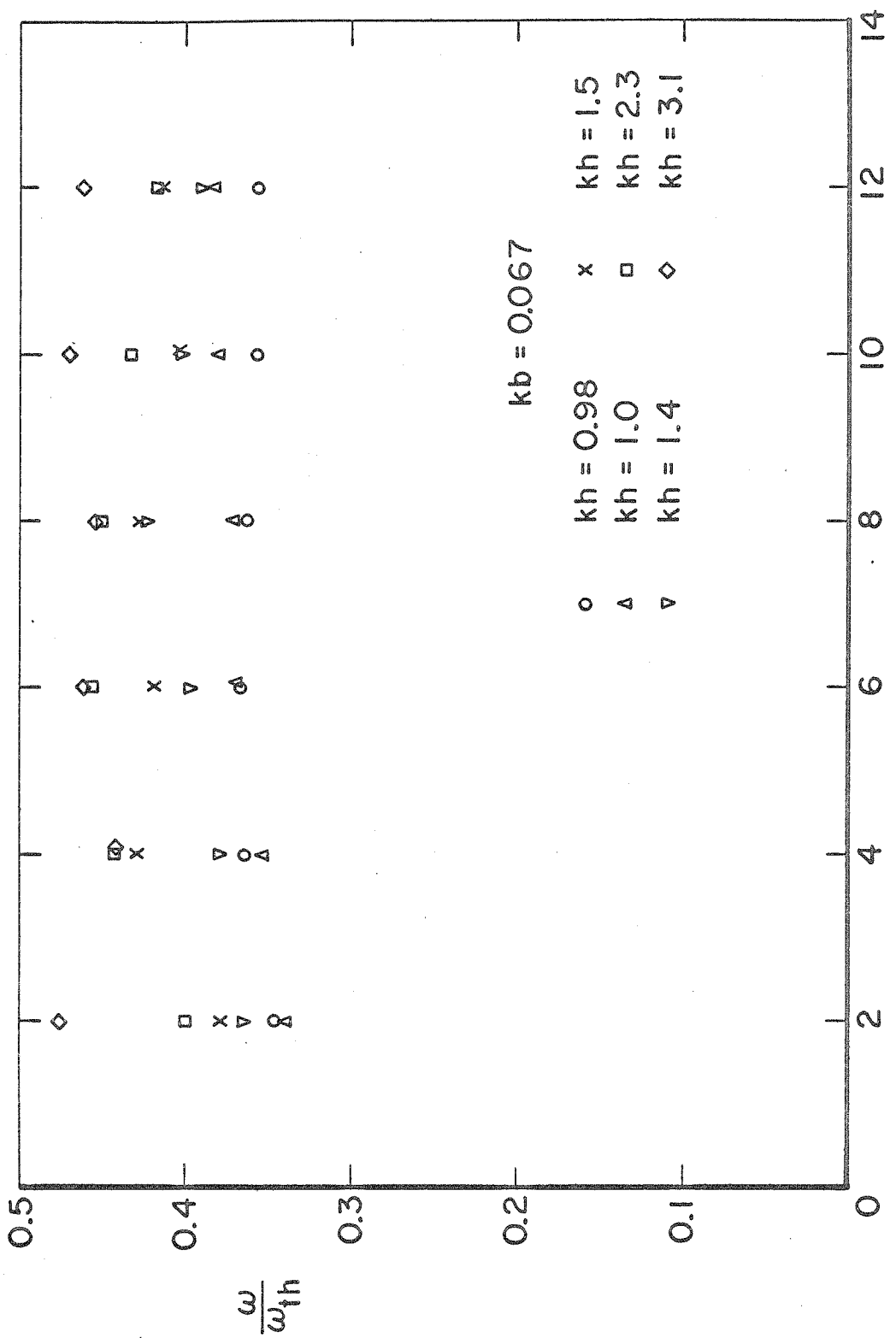
kb = 0.067
kh = 0.98
kh = 1.0
kh = 1.4
kh = 1.5
kh = 2.3
kh = 3.1
$\frac{\omega}{\omega_{th}}$
n
0.5
0.4
0.3
0.2
0.1
0
2
4
6
8
10
12
14

Fig. 19

Fig. 19, we further notice that the values of α_U are in a region around 1.0, yet the values of α_ω are about 0.4. This indicates that the theoretically predicted angular velocities are not in good agreement with the experimental ones, but the theoretically predicted propulsion velocities are. The same pattern appears in the case when kb = 0.053. In Fig. 20 and Fig. 21, α_U and α_ω are plotted versus the number of waves, n, for kb = 0.053 and kh = 1.0, 1.2 and 1.5. The dependence of α_U and α_ω on kh and n shown in these two figures is entirely similar to the previous case.

The influence of kb on the ratios of α_U and α_ω can be seen explicitly in Fig. 22 - 25. In the first two of these figures, kh is fixed at 1.2 and kb takes the value of 0.053, 0.067, 0.085 and 0.11. For fixed kh and n, α_U is seen to increase as kb increases (see Fig. 22). However, α_ω decreases with increasing value of kb as is revealed in Fig. 23. The above can be accounted for by the presence of the neighboring effect which becomes greater as the value of kb gets higher. Similar situation takes place in Fig. 24 and Fig. 25, except that kh is equal to 1.8 and kb changes from 0.080 to 0.16 in these two figures.

The data of the above experiments on uniform helical wires indicate that Eq. (3.8) together with the approximate formulae (3.1) and (3.2) provide a fairly good result for the propulsion velocity U, yet they do not accurately predict the angular velocity ω. However, if we replace U by U/α_U and ω by ω/α_ω in the equilibrium conditions (4.1) and (4.2), we would obtain a very accurate result for the propulsion velocity U and the angular velocity ω since the inclusion

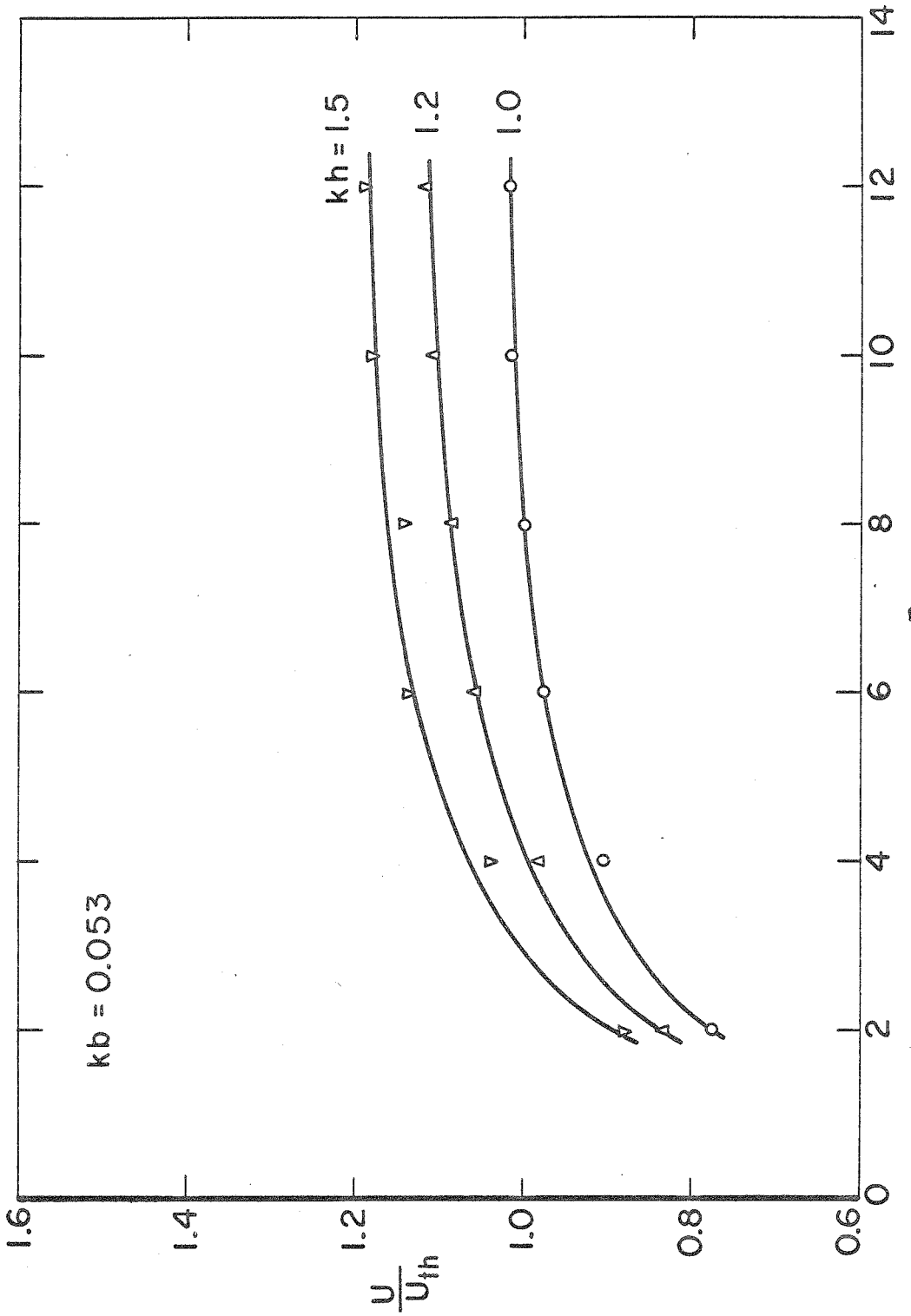

Fig. 20

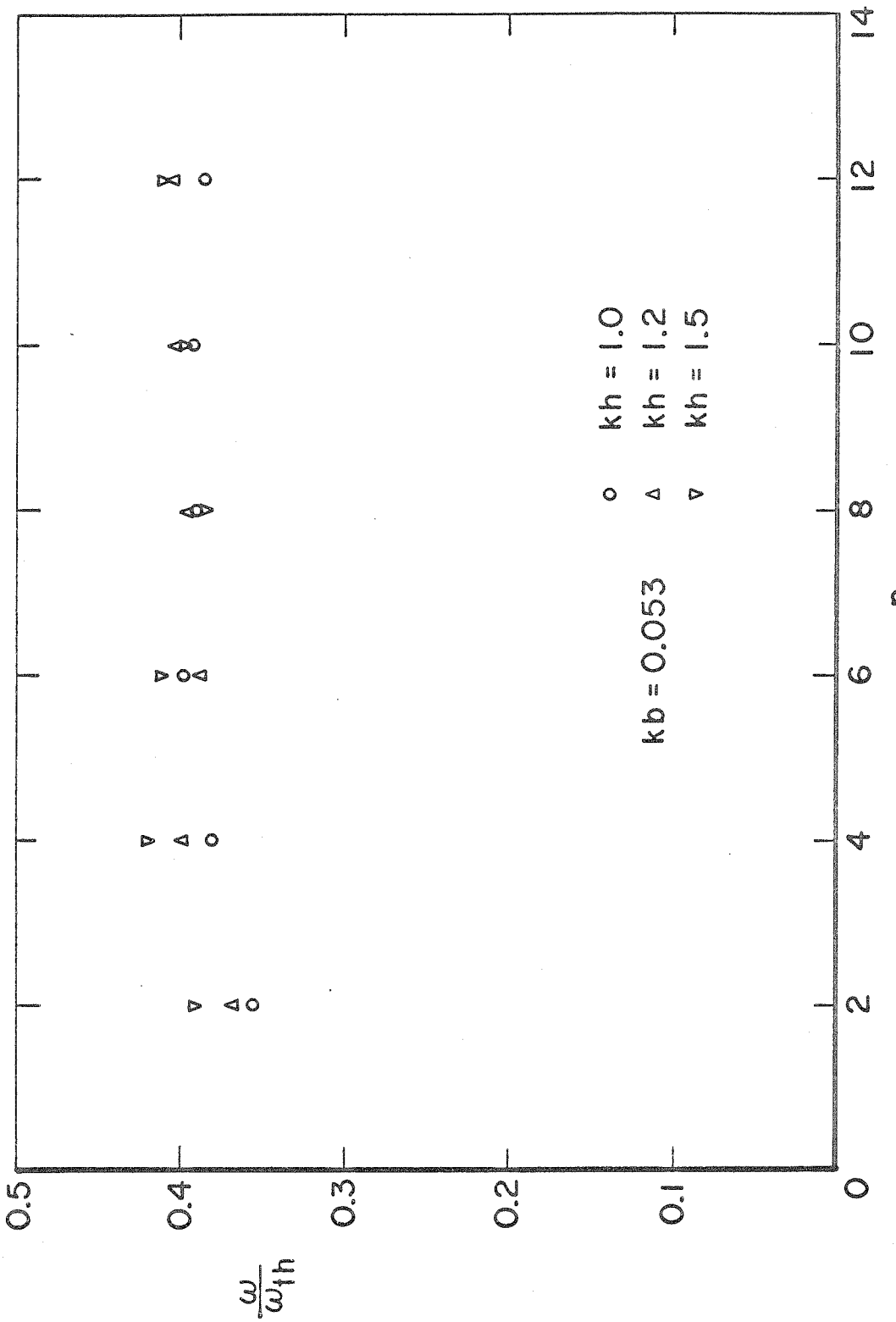
0.5
0.4
0.3
0.2
0.1
0
2
4
6
8
10
12
14
$\frac{\omega}{\omega_{th}}$
n
kb = 0.053
kh = 1.0
kh = 1.2
kh = 1.5

Fig. 21

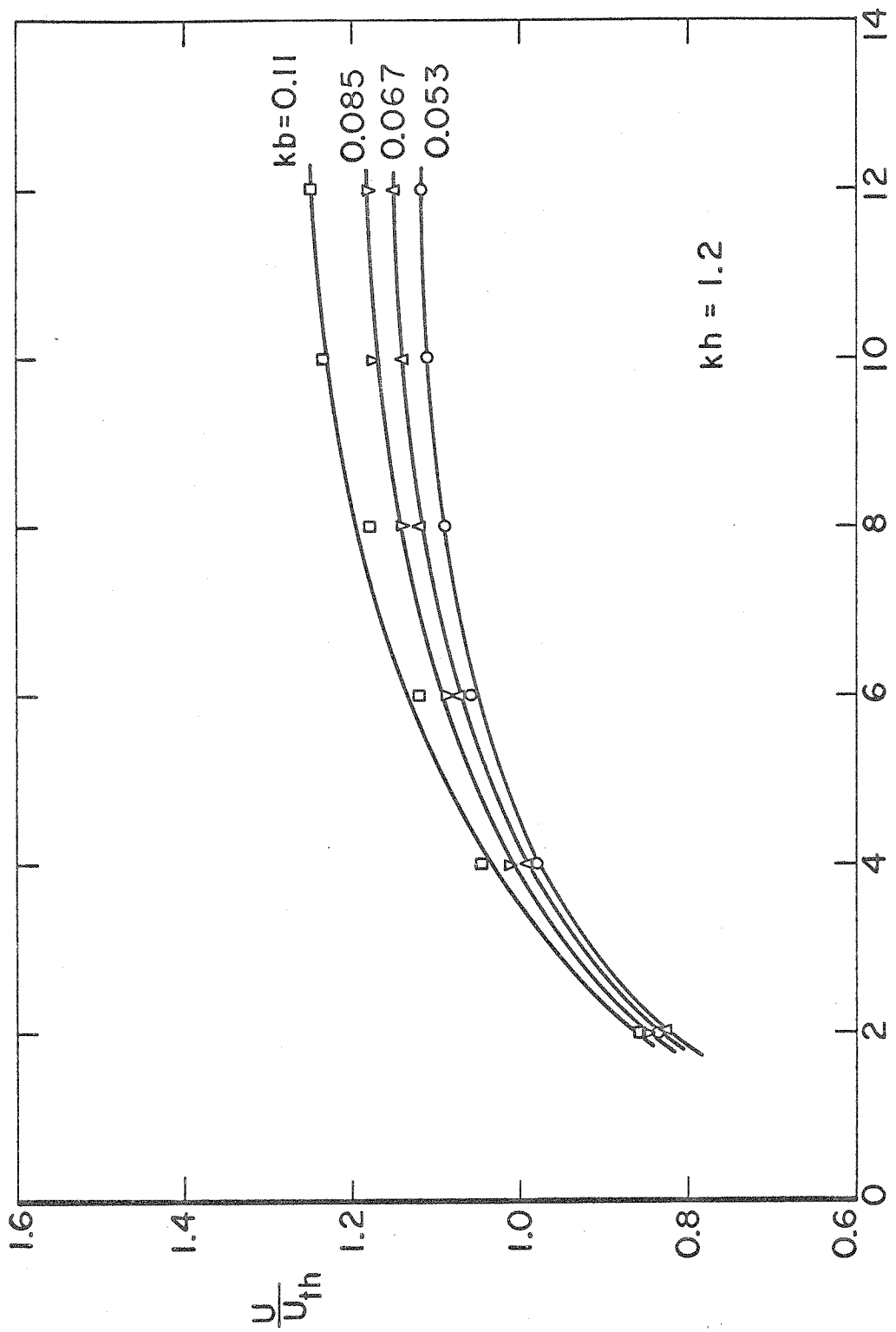

Fig. 22

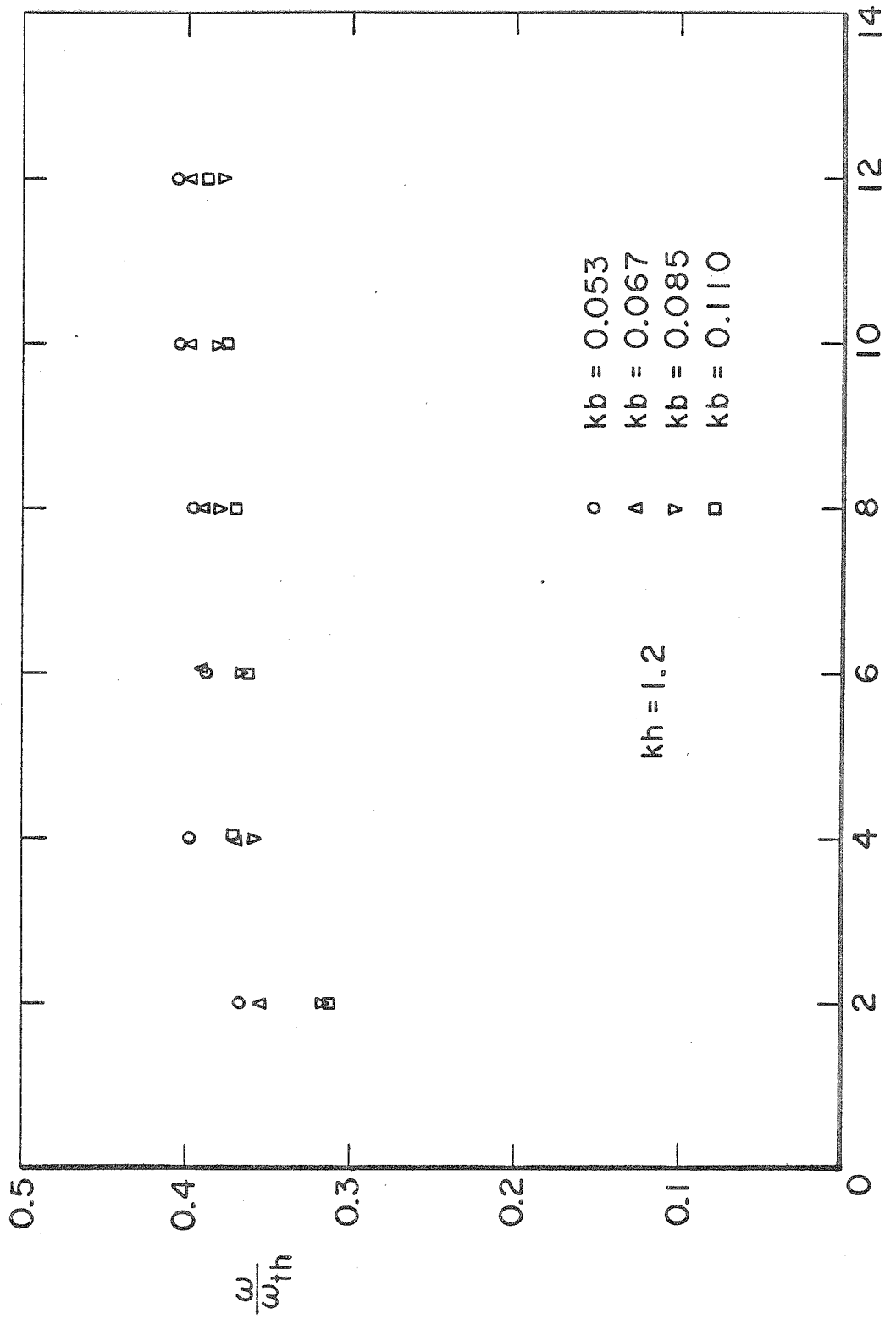
0.5
0.4
0.3
0.2
0.1
0
2
4
6
8
10
12
14
n
ω/ωth
kh = 1.2
o kb = 0.053
Δ kb = 0.067
▽ kb = 0.085
□ kb = 0.110

Fig. 23

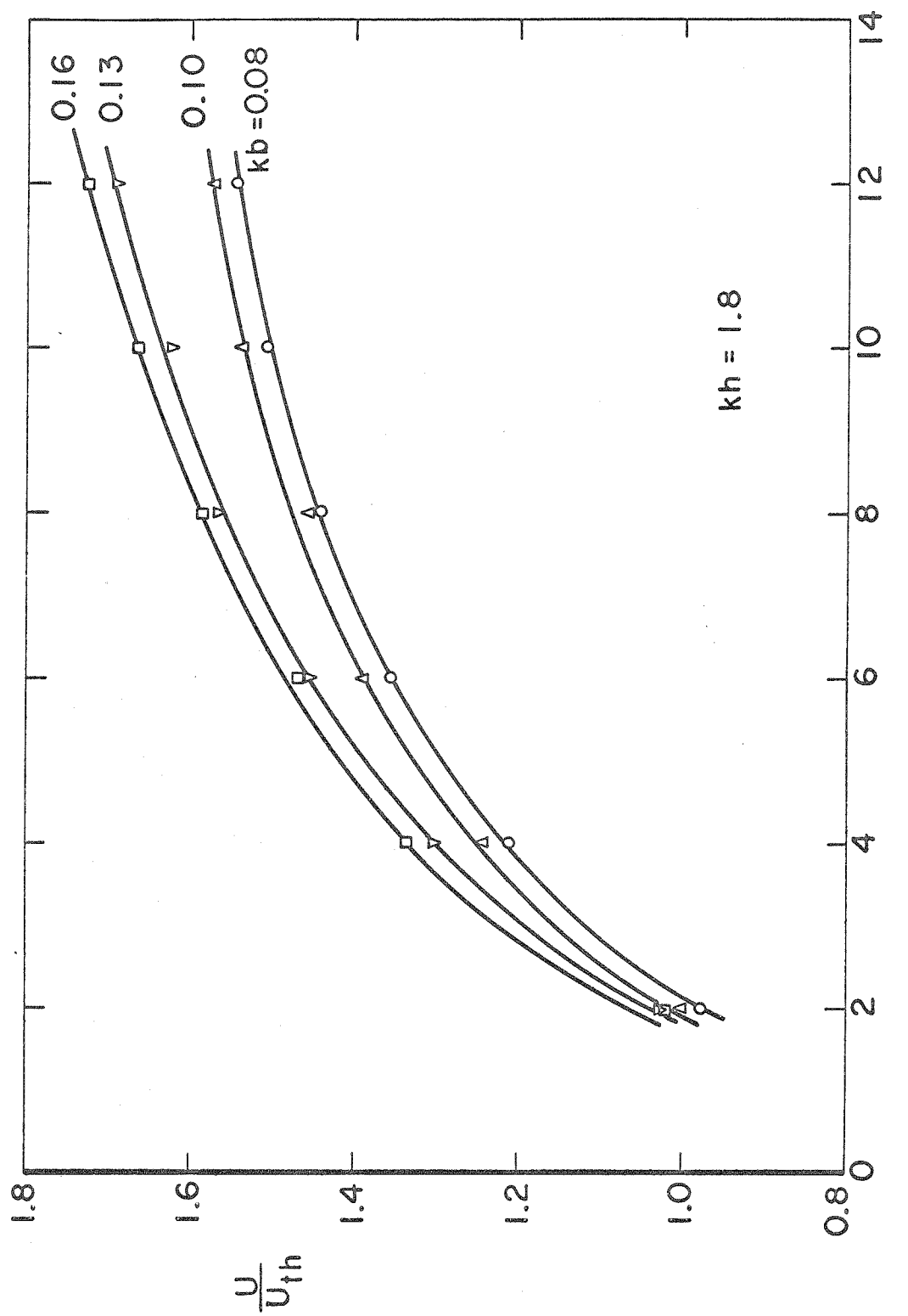

Fig. 24

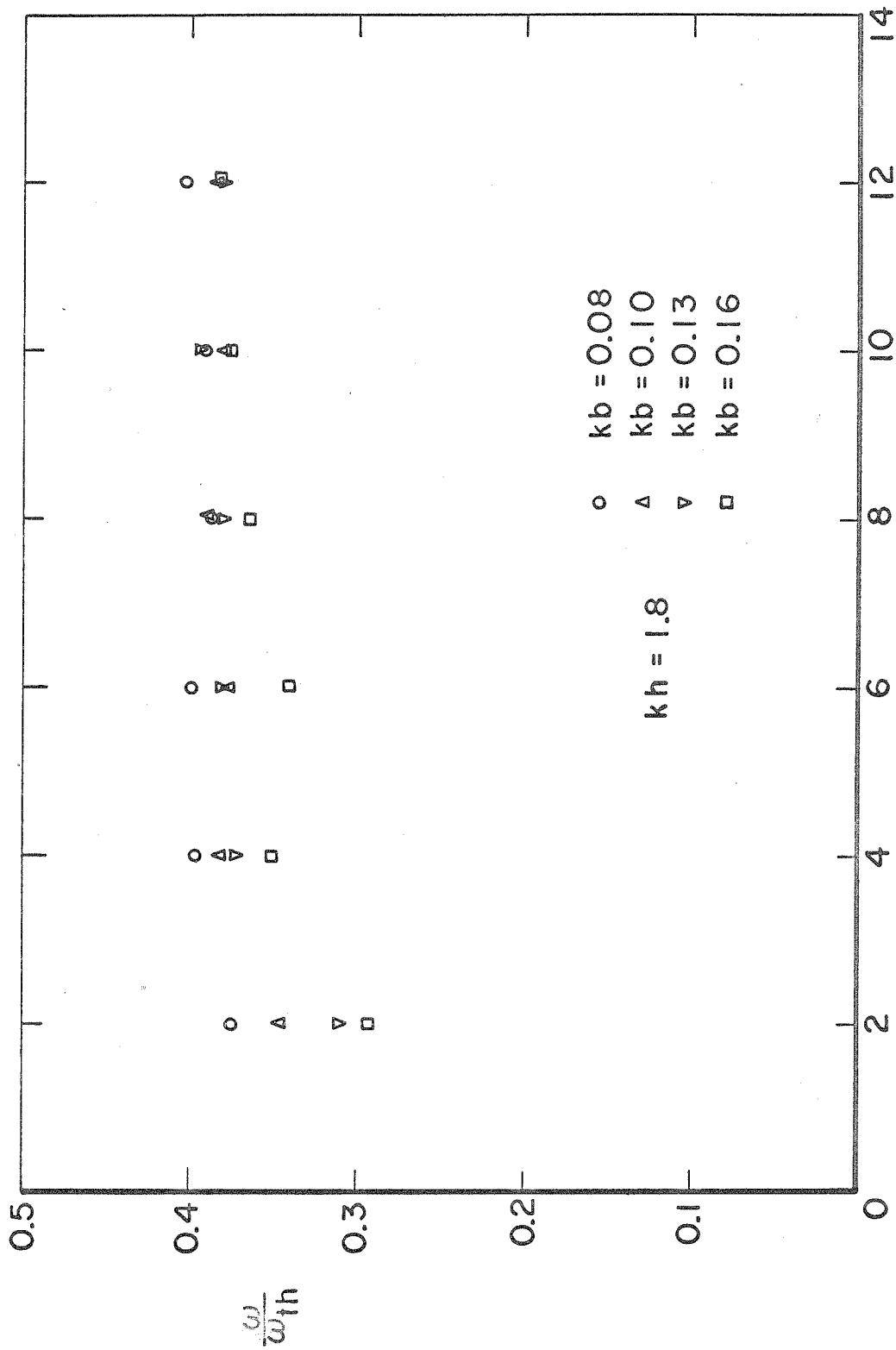
0.5
0.4
0.3
0.2
0.1
0
2
4
6
8
10
12
14
n
$\frac{\omega}{\omega_{th}}$
kb = 0.08
kb = 0.10
kb = 0.13
kb = 0.16
kh = 1.8

Fig. 25

of α_U and α_ω in those equations takes care of the so-called neighboring effect and the end effect. The values of α_U and α_ω for the values of kh, kb and n in the range of practical interest can be obtained from Fig. 18 - 25. Thus, for common practices, α_U varies from 0.7 to 1.7 and α_ω might be taken to be 0.4.

The above correction rule by replacing U and ω by U/α_U and ω/α_ω respectively is valid for motions produced by a uniform helical wire. But it does not quite apply to the actual flagellated-propelling microscopic organisms, because the presence of the head and a transition section between the head and the regular uniform helical flagellum also affects somewhat the motion of the remaining uniform helical flagellum. Nevertheless, when the head is small or the transition section is short, one might expect that the correction rule still holds.

V. CONCLUSIONS

In this thesis, the helical movements of flagellated-propelling microorganisms have been studied extensively. Stokes' equations are applied to analyze the helical wave motion produced by an infinitely long flagellum. It is convenient to solve these equations by expressing all the operators in terms of a helical coordinate system (r, ξ, x), while keeping the velocity components $u, v,$ and w in a cylindrical polar coordinate system (r, θ, x). In so doing, the boundary conditions, namely the no-slip condition on the flagellum surface and zero perturbation velocity at infinity, can be satisfied without due inconvenience, and the pressure and velocity distributions are determined. By a theorem proved in the thesis, the solutions can be made infinitely smooth in the entire flow region. As a result of the helical wave motion, an induced torque will exert on the flagellum about the direction of its motion by the surrounding fluid. This torque tends to rotate the flagellum in the direction opposite to that of the forward propulsion. Hence, in order to make the helical movement of flagellum possible, a constant torque of same magnitude but in the opposite direction of the induced torque must be applied on the flagellum. Formulae for calculating the induced torque in a wavelength and the energy required per wavelength of the flagellum to maintain it in helical motion are presented. In the limiting case when the radius of the flagellum b is much less than the wave amplitude h, by neglecting terms of second order $O(b/h)^2$ and higher orders in applying the boundary conditions, explicit formula for the propulsion velocity U

is obtained from a single-harmonic (in ξ) approximation.

For small values of kb and kh, a comparison is made between G.I. Taylor's, G. J. Hancock's and the present solutions. The propulsion velocity U predicted by the present approximation is proportional to $(kh)^4 \log kh$, a quantity which is smaller than that given by either Taylor or Hancock. It was reported by many biologists (e.g. Rikmenspoel, 1962) that the velocities predicted by Taylor (1952) or Hancock (1953) are too high, by a factor of 10 for the model of Taylor or a factor of 5 for that of Hancock. Hence the present solution is in a better agreement with the experimental data measured by biologists. Moreover, the present solution agrees quite well with the experimental result on a mechanical working model of swimming spermatozoan tested by G.I. Taylor (1952). All the above experimental evidences, biological or mechanical, suggest strongly that the present approximation is a satisfactory one.

The Gray and Hancock method (1955), which is originally devised to investigate the planar wave motion of minute creatures, is extended to incorporate the rotational movement of the flagellum. This modified and improved version of the Gray and Hancock method is then applied to evaluate the self-propulsion of a microorganism, in a viscous fluid, by sending helical waves down its flagellated tail. Under the equilibrium condition at a constant forward speed, both the net force and net torque acting on the organism are required to vanish, yielding two equations for the velocity of propulsion, U, and the induced angular velocity, Ω, of the organism. In order that this type of motion can be realized, it is necessary for the head of the

organism to exceed a certain critical size, and some amount of body rotation is inevitable. In fact, there exists an optimum head-tail ratio a/b at which the propulsion velocity U reaches a maximum, holding the other physical parameters fixed. The power required for propulsion by means of helical waves is determined, based on which a hydromechanical efficiency η is defined. When the head-tail ratio a/b assumes its optimum value and when b is very small compared with the wavelength λ, $\eta \simeq \Omega/\omega$ approximately. This η reaches a maximum at $kh \simeq 0.9$ throughout the range of kb covered, $0.01 < kb < 0.2$. In the neighborhood of $kh = 0.9$, the optimum head-tail ratio varies in the range $15 < a/b < 40$, the propulsion velocity in $0.08 < U/c < 0.2$, and the efficiency in $0.14 < \eta < 0.24$, as kb varies over $0.03 < kb < 0.2$, a range of practical interest. The above predicted values of optimum head-tail ratio a/b are very well supported by observational data.

The 'Spirochete paradox' is resolved upon application of the modified version of the Gray and Hancock method. It is discovered that a spirochete should keep its amplitude-wavelength ratio h/λ around 1:6 (or $kh \simeq 1$) in order to achieve a maximum propulsion velocity. At $kh = 1$, the propulsion velocity varies in the range $0 < U/c < 0.2$, and the induced angular velocity in $0.4 < \Omega/\omega < 1$, as the radius-amplitude ratio varies from 0 to 1.

A series of experiments have been carried out to determine the relative importance of the 'neighboring' effect and 'end' effect. Based on the data obtained, a simple correction rule that replacing U by U/α_U and ω by ω/α_ω in the equilibrium equations has been

suggested. The values of α_U and α_ω for rigid, uniform helical wires are found experimentally. For common practices, α_U varies between 0.7 and 1.7, and α_ω is about 0.4. This correction rule together with the experimental values of α_U and α_ω are not quite applicable to the actual flagellated-propulsion of microorganisms, because the presence of the head and a transition section between the head and the regular uniform helical flagellum also affects somewhat the motion of the remaining uniform helical flagellum. Hence further experiments, both mechanical and biological, are needed in order to refine the theory and enable us to make more accurate predictions of the helical movements of flagellated-propelling microorganisms.

References

Bishop, D.W. (1958) Motility of the sperm flagellum. Nature 182, 1638 - 1640.

Carlson, F.D. (1959) The motile power of a swimming spermatozoon. Proc. 1st Natl. Biophys. Conf., 443 - 449.

Childress, S. (1964) The slow motion of a sphere in a rotating, viscous fluid. J. Fluid Mech. 20, 305 - 314.

Drummond, J.E. (1966) Propulsion by oscillating sheets and tubes in a viscous fluid. J. Fluid Mech. 25, 787 - 793.

Gray, J. (1953) Undulatory propulsion. Quart. J. Microscop. Sci. 94, 551 - 578.

Gray J. and Hancock, G.J. (1955) The propulsion of sea-urchin spermatozoa. J. Exp. Biol. 32, 802 - 814.

Gray, J. (1958) The movement of the spermatozoa of the bull. J. Exp. Biol. 35, 96 - 108.

Gray, J. (1962) Introduction: Flagellar propulsion. Symposium on Sperm. Motility. Washington, D.C. Amer. Assoc. for the Advanc. of Sci. 1 - 12.

Hancock, G. J. (1953) The self-propulsion of microscopic organisms through liquids. Proc. Roy. Soc. A 217, 96 - 121.

Holwill, M.E.J. and Burge, R.E. (1963) A hydrodynamic study of the motility of flagellated bacteria. Archs. Biochem. Biophys. 101, 249 - 260.

Holwill, M.E.J. (1966) The motion of Euglena viridis: The role of flagella. J. Exp. Biol. 44, 578 - 588.

Jahn, T.L. and Landman, M.D. (1965) Locomotion of spirochetes. Trans. Amer. Micros. Soc. 84(3), 395 - 406.

Lamb, H. (1932) Hydrodynamics. Cambridge University Press.

Leifson, E. (1960) Atlas of bacterial flagellation. Academic Press.

Lowy, J. and Spencer, M. (1968) Structure and function of bacterial flagella, in "Aspects of Cell Motility". Symposia of the Soc. for Exper. Biology, No. XXII.

Rikmenspoel, R. (1962) Biophysical approaches to the measurement of sperm motility. Symp. on Sperm. Motility. Washington, D.C. Amer. Assoc. for the Advanc. of Sci. 31 - 54.

Rothschild, Lord (1961) Sperm energetics. An account of work in progress in "The cell and the organism" (Ramsay, J.E. and Wigglesworth, V.B. editors) 9 - 21. Cambridge University Press.

Rothschild, Lord (1962) Sperm movement: Problems and observations. Symp. on Sperm. Motility. Washington, D.C. Amer. Assoc. for the Advanc. of Sci. 13 - 29.

Taylor, G.I. (1952) The action of waving cylindrical tails in propelling microscopic organisms. Proc. Roy. Soc. A 211, 225 - 239.

Wu, T.Y. (1966) The mechanics of swimming, in "Biomechanics" (Fung, Y.C. editor). Proc. Symp. on Biomechanics, Amer. Soc. Mech. Engr. 187 - 204.